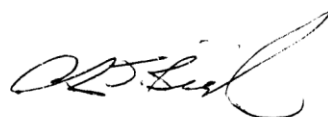


APPROVAL SHEET

Title of Dissertation: A substrate-guided approach for identification of pathways regulated by Pim kinases; new biomarkers and putative co-therapeutic strategies for cancer treatment

Name of Candidate: Tejashree Anant Joglekar
Doctor of Philosophy, 2017



Dissertation and Abstract Approved:

(*Signature of Supervising
Professor)

Dr. Charles J. Bieberich
Professor
Biological Sciences

Date Approved: 29 Nov 2017

ABSTRACT

Title of Document: A SUBSTRATE-GUIDED APPROACH FOR IDENTIFICATION OF PATHWAYS REGULATED BY PIM KINASES; NEW BIOMARKERS AND PUTATIVE CO-THERAPEUTIC STRATEGIES FOR CANCER TREATMENT

Tejashree Anant Joglekar
Doctor of Philosophy, 2017

Directed By: Professor. Charles J Bieberich, Biology

Kinase inhibition is a major strategy for therapeutic intervention as oncogenic kinase activity is a common feature shared by most cancers. Pim kinases are deregulated in certain solid tumors and hematopoietic cancers, notably in acute myeloid leukemia (AML). While cancer cells can become dependent on Pim kinase activity to sustain proliferation, these kinases appear to be dispensable in most normal adult tissues. These features make Pim kinases an attractive target for cancer therapy, however, their physiological roles have not been fully characterized. Pim kinases are considered a potential therapeutic target against AML as Pim kinase inhibitors can disrupt proliferation and survival of AML cell lines and primary patient cells *in vitro*. However, single agent Pim inhibition therapy may not be effective as resistance to Pim inhibitors is frequently observed in AML patients. Combination of Pim inhibition along with other inhibitors might

effectively overcome primary resistance and preemptively limit relapse by acquired resistance. Here, we describe a new approach to identify novel and effective synergistic combinations with kinase inhibitors in a substrate-guided fashion.

Research in our lab has identified ~570 Pim kinase substrates. In this work two Pim substrates- hnRNPA1 and rpS6 were validated as *in vivo* targets for Pim inhibitor-induced de-phosphorylation. Interestingly, a majority of novel Pim substrates were involved in mRNA splicing and rRNA processing pathways. Pharmacological inhibition of Pim kinases using AZD1208 led to large-scale changes in splicing patterns of cellular mRNAs, and induced several specific defects in rRNA processing. Further, we selected drug combinations based on the knowledge of these pathways regulated by Pim kinases, and demonstrate their synergistic potential against AML cell lines, irrespective of the response to single-agent Pim inhibition. Moreover, novel Pim substrates, Pim inhibitor-induced splicing changes, and rRNA processing changes can act as putative biomarkers for Pim activity and inhibitor responsiveness. Using Pim kinase as an example, we demonstrate a substrate-guided approach to biomarker identification and combination-therapy selection yielding drug synergy.

A SUBSTRATE-GUIDED APPROACH FOR IDENTIFICATION OF
PATHWAYS REGULATED BY PIM KINASES; NEW BIOMARKERS AND
PUTATIVE CO-THERAPEUTIC STRATEGIES FOR CANCER TREATMENT

By

Tejashree Anant Joglekar

Dissertation submitted to the Faculty of the Graduate School of the
University of Maryland, Baltimore County, in partial fulfillment
of the requirements for the degree of
Doctorate in Philosophy,
Biology
2017

© Copyright by
Tejashree Anant Joglekar
2017

Dedication

I dedicate this work to my family- my grandmother, parents, sister and my husband for their unconditional love and support.

Acknowledgements

During my PhD dissertation work, a number of people have helped and guided me and I wish to thank all of them. Firstly, I would like to convey my sincerest gratitude to my advisor Dr. Charles Bieberich. He has been a constant source of guidance and support at every step of the way and taught me how to be a researcher. I am really thankful to him for giving me the opportunity to work in his lab.

I would also like to thank my advisory committee, Dr. Phyllis Robinson, Dr. Stephen Miller, Dr. Michelle Starz-Gaiano and Dr. Terry Rogers for their guidance through all these years. I truly appreciate their valuable insights and feedback regarding my research and writing and also the support and encouragement that they all have given me.

Another person who I would like to convey my gratitude is Dr. Xiang Li. I have learnt a lot of techniques and skills from Xiang and he has been a mentor to me. He made the initial observations and identified the Pim substrates and shared his insights to shape the project and has contributed at all the stages with brainstorming and technical guidance for my experiments. I am really thankful to him for all the help and support.

I have been very fortunate to have a very supporting and upbeat lab environment due to very helpful lab mates. I want to thank the current lab

members Apruv, Mike and Shuaishuai who have kept the lab environment very happy. All of them are also very bright and have helped me with various experiments during our time together in the lab. All the lab members have also given useful insights for my presentation. I am thankful to all of them.

I would also like to thank previous lab members Yasaman Etminan and Arya Ashok for being wonderful labmates and friends. I really appreciate Yassie's encouragement during challenging times and I have found a good friend in her. I have also like to thank previous lab member Achuth Padmanabhan for helping me during my preliminary examination preparation and Gretchen Hubbard for teaching me the Northern blotting technique. I have enjoyed interacting in lab with many very bright undergraduate students. I would like to thank Azim Raja and Haneet Chaddha who have worked with me and helped me with this work. They have been very hard working and I have learned a lot while teaching them.

I am thankful to Dr. Marrikki Laiho for providing the BMH21 and to Dr. Thomas Webb for providing the Sudemycin D6 for our experiments. I would also like to thank Dr. Joseph Gera for his kind gift of hnRNPA1 phospho antibody, that was used in this study.

I would also like to thank my friends Afsoon, Sush, Nikhil and Ketaki who have been a constant source of encouragement and cheered me on

during the all times that I needed it during my PhD. I am very thankful to all the friends who have made my days at UMBC very memorable and fun.

I regard Dr. Avinash Upadhyay as my guru and he is a major reason that I am pursuing science. He has engendered the curiosity for science in me and introduced this field and his teaching and confidence in my abilities has steered my life towards research. I hold deep respect and gratitude in my heart for Upadhyay Sir and would have been on this path without his guidance.

My family has been my rock and have made me what I am today. My parents and my grandmother have been the biggest influence in my life. It is because of their hardwork and sacrifice and faith in me that I was able to achieve any success in life. I could never thank them enough for it, but I am so grateful to have such a supporting family. I want to thank my sister Shubhada for her support and her confidence in me. I have always tried to work hard to set a good example to my little sister and she has motivated me to be successful.

Lastly, one person whose support has been indispensable is my husband Anurag. He has been my mentor, friend and support throughout my PhD. He has helped, encouraged and guided me throughout my research and given valuable insights. I have learnt a lot from him regarding writing and

presentation skills. I am so thankful that I have him in my life. I could not have asked for a more supporting and loving partner and sincerely appreciate all his help for my success.

Table of Contents

Dedication	ii
Acknowledgements	iii
Table of Contents	vii
List of Tables	ix
List of Figures	x
List of Abbreviations	xiii
Chapter 1: Introduction	1
1.1 Kinase signaling in cancer	3
1.1.1 Kinases as cancer targets	4
1.1.2 Kinase inhibitors for cancer therapy	4
1.1.3 Successes and challenges with the use of kinase inhibitors as therapeutics.....	5
1.1.4 Combination cancer therapy using kinase inhibitors	7
1.2 Biology of Pim kinases	9
1.2.1 Upstream regulation of Pim kinases	10
1.2.2 Downstream targets of Pim kinases	11
1.2.3 Pim kinases in Cancer.....	13
1.2.4 Pim kinase inhibitors.....	15
1.2.5 Combination therapy with Pim kinase inhibitors	18
1.3 pre-mRNA splicing	22
1.3.1 Mechanism and regulation of pre-mRNA splicing.....	23
1.3.1.1 Generation of snRNPs	23
1.3.1.2 Spliceosome assembly	27
1.3.1.3 Alternative splicing	30
1.3.2 Phosphorylation-dependent regulation of constitutive and alternative splicing.....	31
1.3.3 Significance of mRNA splicing in cancer progression and treatment	34
1.4 rRNA processing.....	37
1.4.1 Mechanism of rRNA processing	39
1.4.2 Significance of protein phosphorylation in regulation of pre-rRNA processing.....	45
1.4.3 Significance of rRNA processing in cancer cells	46
Chapter 2: Substrate-guided identification of novel Pim kinase functions reveals potential therapeutic combinations for AML	51
2.1 Acute myeloid leukemia	52
2.1.1 Therapeutic regimen for AML: The choice of therapeutic regimen depends on individual prognosis	56
2.1.2 New therapeutic vulnerabilities of AML based on genetic mutations and over-expression	57
2.1.3 Kinase-substrate identification platforms	62
2.2 Results	68

2.2.1 Pim kinases regulate mRNA splicing in AML cells.....	71
2.2.2 Pim kinase inhibition does not affect SRPK activity.....	77
2.2.3 Pim inhibition by AZD1208 induces rRNA processing defects	78
2.2.4 Rational combination of Pim inhibitors with other molecular targeted drugs using a substrate-guided approach	86
2.3 Discussion.....	92
2.4 Materials and methods.....	104
Chapter 3: Identification and validation of novel Pim kinase substrates	
hnRNPA1 and rpS6 as potential Pim combination therapy biomarkers	114
Abstract	114
3.1 Introduction	115
3.1.1 hnRNPA1	116
3.1.2 Ribosomal protein S6 (rpS6)	118
3.2 Results	122
3.2.1 Pim1 phosphorylates hnRNPA1 in vitro.....	122
3.2.2 Confirmation of hnRNPA1 phosphorylation by Pim1 in vivo	124
3.2.3 Generation of stable cells expressing hnRNPA1 WT, S199A and S199E.....	126
3.2.4 Identification of rpS6 as a direct Pim kinase substrate	128
3.2.5 Dual inhibition of Pim kinases and p70S6K is required for effective inhibition of rpS6 phosphorylation in OCI-M1 cells	129
3.3 Discussion.....	130
3.4 Materials and methods.....	134
Chapter 4: Discussion and future directions	141
4.1 Pathways regulated by Pim kinases	142
4.2 Biomarkers for Pim kinase inhibitor responsiveness	147
4.3 Putative therapeutic drug combinations for AML treatment.....	149
References	152

List of Tables

Chapter 1

Table 2.1 The alternative splicing events observed in AZD1208-treated MOLM-16 and EOL-1 cells belonged to five categories depicted in the table.....	75
Table 2.2 KEGG pathway analysis for genes targeted by AZD1208-induced splicing changes.....	80
Table 2.3 Gene ontology (GO) analysis for genes targeted by AZD1208-induced splicing changes to identify enrichment of genes involved in specific biological processes.....	80
Table 2.4 Table 2.4 List of Pim substrates previously validated as rRNA processing factors.....	82
Table 2.5 Combination indices for Pim inhibitor combinations with pathway-based inhibitors calculated by CompuSyn synergy analysis software using the Chou-Talalay algorithm.....	91

Chapter 2

Table 3.1 List of antibodies used.....	138
--	-----

List of Figures

Chapter 1

Figure 1.1. Sequence homology of Pim kinases.....	10
Figure 1.2. Pathways regulated by Pim kinases.....	12
Figure 1.3. Schematic representation of snRNP assembly.....	25
Figure 1.4 Graphical representation of a typical splice site.....	27
Figure 1.5 Schematic representation of spliceosome assembly and the catalysis of splicing.....	28
Figure 1.6 Diagrammatic representation of a nucleolus.....	37
Figure 1.7 Diagrammatic representation of pre-rRNA cleavage sites in human cells.....	39
Figure 1.8. Schematic representation of stepwise pre-rRNA processing in human cells.....	43

Chapter 2

Figure 2.1. Microscopic images of acute myeloid leukemia blast cells.....	53
Figure 2.2. Schematic representation of 2D reverse in-gel kinase assay.....	64
Figure 2.3. Schematic representation of phosphorylation in RIKA.....	65
Figure 2.4. RIKA with stable isotope labelling.....	66
Figure 2.5. Schematic representation of modified Reverse in gel kinase assay (RIKA) following protein dephosphorylation with HF treatment.....	67
Figure 2.6 Putative Pim kinase substrates identified by RIKA.....	70

Figure 2.7 Schematic flowchart for microarray analysis for alternative splicing changes.....	71
Figure 2.8 Figure 2.8 Graphical representation of microarray data for AML cell lines.....	73
Figure 2.9 Validation of microarray results using RT-qPCR and RT-PCR analysis.....	76
Figure 2.10 Effect of AZD1208 on SRPK1 activity.....	79
Figure 2.11 Pim inhibition induced pre-rRNA processing defects.....	84
Figure 2.12 AZD1208-induced pre-rRNA processing defects are specific to Pim activity.....	85
Figure 2.13 Cytotoxicity assay on MOLM-16 cells treated with inhibitor combinations.....	88
Figure 2.14 Cytotoxicity assay on EOL-1 cells treated with inhibitor combinations.....	89
Figure 2.15 Cytotoxicity assay on OCI-M1 cells treated with inhibitor combinations as indicated.....	90
Figure 2.16 Comparison of Pim-induced splicing changes with published data from AML patients.....	97

Chapter 3

Figure 3.1 Validation of hnRNPA1 phosphorylation and identification of sites.....	122
Figure 3.2 Validation of hnRNPA1 phosphorylation in cells.....	125

Figure 3.3 Characterization of HA-hnRNPA1 WT and mutant expressing
stable cell lines.....127

Figure 3.4 Validation of rpS6 phosphorylation by Pim kinases.....129

Chapter 4

Figure 4.1 Novel and known pathways regulated by Pim kinases.....142

List of Abbreviations

- i. 4EBP1: Eukaryotic translation initiation factor 4E-binding protein 1
- ii. 5'-TOP: 5'-Terminal oligopyrimidine
- iii. ABL: Abelson murine leukemia viral oncogene homolog 1
- iv. AML: Acute myeloid leukemia
- v. APL: Acute promyelocytic leukemia
- vi. ASE: Alternative splicing event
- vii. ATP: Adenosine triphosphate
- viii. BAD: Bcl-2-associated death promoter
- ix. Bcl2: B-cell lymphoma 2
- x. BCR: breakpoint cluster region
- xi. BIN1: Bridging Integrator 1
- xii. cAMP: Cyclic adenosine monophosphate
- xiii. CDK: Cyclin dependent kinases
- xiv. CEBPA: CCAAT/Enhancer Binding Protein Alpha
- xv. CLK: Cyclin-dependent kinase like kinases
- xvi. CLL: Chronic lymphocytic leukemia
- xvii. CML: chronic myelogenous leukemia
- xviii. COG5: Conserved oligomeric golgi complex subunit 5
- xix. CR: Complete remission
- xx. CRISPR: Clustered regularly interspaced short palindromic repeat
- xxi. CRM1: Chromosomal maintenance 1

- xxii. DBA: Diamond blackfan anemia
- xxiii. DDX51: DEAD-box helicase 51
- xxiv. DEF: Digestive organ expansion factor
- xxv. DFS: Disease-free survival
- xxvi. DMSO: Dimethyl sulfoxide
- xxvii. EGFR: Epidermal growth factor receptor
- xxviii. eIF4E: Eukaryotic translation initiation factor 4E
- xxix. ER: Endoplasmic reticulum
- xxx. ERK: Extracellular signal–regulated kinase
- xxxi. ESE: Exon splicing enhancers
- xxxii. ESS: Exonic splicing suppressors
- xxxiii. EXOSC10: Exosome component 10
- xxxiv. FAB: French America British
- xxxv. FDA: Food and drug administration
- xxxvi. FGFR: Fibroblast growth factor receptor
- xxxvii. FLT3: Fms like tyrosine kinase 3
- xxxviii. gp: Glyco protein
- xxxix. Her2: Human epidermal growth factor receptor 2
- xl. HF: Hydrogen fluoride
- xli. hnRNPA1: Heterogeneous nuclear ribonucleoprotein A1
- xlii. HSCT: Hematopoietic stem cell therapy
- xliii. HSP90: Heat shock protein 90
- xliv. IC50: Half maximal inhibitory concentration

- xlv. IDH1: Isocitrate dehydrogenase 1
- xlvi. IFN α : interferon-alpha
- xlvii. IFN- γ : Interferon gamma
- xlviii. IGC: Interchromatin granule
- xlix. IL7: Interleukin 7
 - i. IPTG: Isopropyl β -D-1-thiogalactopyranoside
 - ii. ISE: Intronic splicing enhancers
 - iii. ITAF: IRES trans-acting factor
 - liii. ITD: Internal tandem duplication
 - liv. ITS: Internal transcribed spacer
 - lv. JAK: Janus kinase
 - lvi. KCl: Potassium chloride
 - lvii. kDa: Kilo dalton
 - lviii. KESTREL: Kinase substrate tracking and elucidation
 - lix. LC-MS: Liquid chromatography–mass spectrometry
 - lx. MAPK: Mitogen-activated protein kinase
 - lxi. MCL: Mantle cell lymphoma
 - lxii. MCL1: Myeloid cell leukemia sequence 1
 - lxiii. MDS: Myeloid dysplasia
 - lxiv. MEF: Mouse embryonic fibroblast
 - lxv. MEK: MAPK/ERK Kinase
 - lxvi. MPN: Myeloproliferative neoplastic
 - lxvii. MS: Mass spectrometry

- lxviii. mTOR: Mammalian target of rapamycin
- lxix. MuLV: Moloney murine leukemia virus
- lxx. NFYA: Nuclear transcription factor Y subunit alpha
- lxxi. NFkB: Nuclear factor kappa-light-chain-enhancer of activated B cells
- lxxii. NGDN: Neuroguidin
- lxxiii. NOR: Nucleolar organizer
- lxxiv. NPM: Nucleophosmin
- lxxv. NPM-ALK: Nucleophosmin-Anaplastic lymphoma kinase
- lxxvi. NSCLC: Non-small cell lung cancer
- lxxvii. NXF1: Nuclear RNA export factor 1
- lxxviii. PCa: Prostate cancer
- lxxix. PDX: Patient derived xenograft
- lxxx. PERK: Protein kinase RNA-like endoplasmic reticulum kinase
- lxxxi. PF: Perichromatin fibril
- lxxxii. PHAX: Phosphorylated adaptor for RNA export
- lxxxiii. PI3K: Phosphatidylinositide 3-kinase
- lxxxiv. PIM: Pro-viral insertion of murine Maloney leukemia virus
- lxxxv. Plk: Polo like kinase
- lxxxvi. PP1: Protein phosphatase 1
- lxxxvii. PRAS40: Proline-rich AKT substrate 40 kDa
- lxxxviii. PSE: Proximal sequence element
- lxxxix. PSR: Probe selection region
- xc. PTEN: Phosphatase and tensing homolog

- xc. RBC: Red blood cell
- xcii. RGG: Arg-Gly-Gly
- xciii. RIKA: Reverse in-gel kinase assay
- xciv. RPL31: Ribosomal protein L31
- xcv. RPS11: Ribosomal protein S11
- xcvi. RPS19: Ribosomal protein S19
- xcvii. RPS3: Ribosomal protein S3
- xcviii. RPS6: Ribosomal protein S6
- xcix. RRM: RNA recognition motif
 - c. rRNA: Ribosomal ribonucleic acid
 - ci. RRP17: Ribosomal RNA-processing protein 17
 - cii. RTK: Receptor tyrosine kinases
 - ciii. SD6: Sudemycin D6
 - civ. SDS-PAGE: Sodium dodecyl sulfate polyacrylamide gel electrophoresis
 - cv. SF3B: Splicing factor 3B
 - cvi. shRNA: small hairpin RNA
 - cvii. siRNA: small interfering RNA
 - cviii. SMN: Survival motor neuron
 - cix. snoRNA: small nucleolar RNA
 - cx. snRNA: small nuclear RNA
 - cx. snRNP: small nuclear ribonucleoprotein
 - cxii. SRPK: Serine arginine rich protein kinase

- cxiii. SRSF1: Serine Arginine rich splicing factor 1
- cxiv. SRSF2: Serine arginine rich splicing factor 2
- cxv. ss: splice site
- cxvi. SSU: Small ribosomal subunit
- cxvii. STAT: Signal transducer and activator of transcription
- cxviii. TAC: Transcriptome analysis console
- cxix. U2AF35: U2 small nuclear RNA auxiliary factor
- cxx. UPR: Unfolded protein response
- cxxi. UTR: Untranslated region
- cxxii. VEGFR: Vascular endothelial growth factor receptor
- cxxiii. WT: Wild type
- cxxiv. WT1: Wilms tumor 1
- cxxv. XBP1: X-box binding protein 1
- cxxvi. XRN1: 5'-3' Exoribonuclease 1
- cxxvii. ZRSR2: Zinc finger CCCH-type, RNA binding motif and serine/arginine rich 2

Chapter 1: Introduction

The American cancer society has projected an estimated 1,688,780 new cases of cancer to be diagnosed in the year 2017 and 600,920 deaths due to cancer. We are still fighting the age-old war on cancer, despite many successes along the way, as cancer has been affecting the lives of many, directly or indirectly. There has been enormous progress in gaining knowledge about normal cellular processes and deregulation of these processes leading to diseases. All cancer cells show a hallmark feature of uncontrolled growth through deregulation of the very same mechanisms that are in place to maintain a disease free normal state. Using this knowledge, researchers have been developing numerous drugs to target these processes in cancer cells (DeVita and Rosenberg, 2012). Despite the basic similarity that all types of cancers are a result of uncontrolled growth of cells, the tumor cells from different cell types depend on different sets of mutations or aberrations in cellular pathways and stimuli, to become malignant and to support their growth. Thus, a magic pill to cure all cancers is not plausible. In this research, we have used acute myeloid leukemia as a prototype to validate a platform for stratifying novel rational drug combinations for potential treatment.

Acute myeloid leukemia (AML) is a hematopoietic malignancy characterized by uncontrolled growth of undifferentiated myeloid precursor cells called blasts. Contrary to chronic myelogenous leukemia (CML), in

which 90-95% patients show the presence of reciprocal translocation between chromosomes 9 and 12 causing BCR-ABL fusion genes, over 50% of patients with AML do not show any recurrent genetic abnormalities and have a normal karyotype (Welch et al., 2012). The most recurrent mutations in AML patients are found in *FLT3*, *NPM1*, *KIT*, *CEBPA* and *TET2* genes. Two of these genes are protein kinases that regulate cell survival and proliferation of hematopoietic cells. Thus, these and other protein kinases that regulate proliferation and survival of myeloid blasts can be targeted for AML therapy. Pim kinases are viable contenders for this role as they are frequently over-expressed in AML and *in vivo* results with Pim kinase inhibitors have shown promising inhibition of AML growth. However, due to challenges like inherent and acquired resistance observed with all molecularly targeted drugs, monotherapy may not provide a lasting solution. Using a novel substrate identification platform, we have uncovered novel pathways regulated by Pim kinases and applied this knowledge to rationalize drug combination with inhibitors targeting these Pim regulated pathways. The following sections will discuss the importance of kinases as therapeutic targets in cancer and the role of Pim kinases in normal and cancer cells, and the success and failures of Pim kinase inhibitors at preclinical and clinical stages. These sections will be followed by an introduction to the novel pathways regulated by Pim kinases, namely, pre-mRNA splicing and pre-rRNA processing.

1.1 Kinase signaling in cancer

The human genome codes for 518 known protein kinases which phosphorylate serine, threonine or tyrosine residues on protein substrates. Protein kinases act as messengers that relay important cellular signals involved in regulation of cell proliferation, growth, metabolism and cell survival. All protein kinases are classified into about 20 families on the basis of sequence homology and cellular function (Manning, 2002). Based on the residues that they phosphorylate, kinases are divided into three groups; serine-threonine kinases, tyrosine kinases, and dual specificity kinases. Histidine, lysine, and arginine residues are phosphorylated much less frequently in eukaryotes as opposed to prokaryotes. Although genes coding for kinases constitute only 1.7% of all the human genes, they are indispensable to almost every key cellular processes and thus play a crucial role in etiology of diseases such as cancer (Manning, 2002). The neoplastic transformation is a result of perturbation of a fine balance between cell proliferation, growth and programmed cell death (Reed, 1999). Protein kinase signaling is the most widely used mechanism to regulate this balance. Thus, one cannot overstate the importance of protein kinases as targets for cancer therapy. Therefore, the knowledge of kinase function and substrate profiles is essential for realizing the best therapeutic response while reducing the risk of harmful side-effects.

1.1.1 Kinases as cancer targets

Three types of kinases are potential targets for cancer therapy based on their role in cancer development (Zhang et al., 2008). The first group contains the oncogenic kinases that can cause neoplastic transformation in normal cells when over-expressed or mutated. A well-known example is the oncogenic kinase expressed from BCR-ABL fusion gene that is known to play a pivotal role in chronic myelogenous leukemia (CML) (Daley et al., 1990). The second group of kinase targets includes kinases that are synthetic lethal when inhibited in combination with another non-lethal mutation present in the tumor cells. Cyclin-dependent kinases (CDKs) fall into this category as cancer cells require their signaling to sustain rapid cell division (Malumbres and Barbacid, 2007). These kinases open a therapeutic window, as their inhibition can specifically target the acute addiction to their signaling and selectively eradicate tumor cells. The third group of target kinases includes kinases that facilitate various steps in tumor progression. They are either expressed by the tumor cells, or by the tumor's microenvironment and aid in processes like metastasis or angiogenesis (Kerbel, 2008). Vascular endothelial growth factor receptor kinase (VEGFR) or fibroblast growth factor receptor (FGFR) among others belong to this category of targets (Kerbel, 2008).

1.1.2 Kinase inhibitors for cancer therapy

The US Food and Drug Administration (FDA) has approved 28 small-molecular kinase inhibitors for therapy and a majority of those are protein kinase inhibitors approved for treatment of malignancies (Wu et al., 2015).

The most abundant group of kinase inhibitors are reversible and bind to the ATP binding site of kinases precluding ATP binding and catalysis. Study of protein kinase crystal structure revealed a bi-lobed kinase domain connected by a hinge region (Knighton et al., 1991). The adenosine ring of ATP makes hydrogen bonds with the amino acids within the deep cleft of the hinge region. The competitive kinase inhibitors mimic this hydrogen bonding and inhibit kinase catalytic activity (Zhang et al., 2008). Despite high conservation in the hinge region, relatively specific inhibitors have been designed by using the slight amino acid differences and structural variation in this domain (Bain et al., 2007).

1.1.3 Successes and challenges with the use of kinase inhibitors as therapeutics

Gleevec (STI571) is the first approved small molecular kinase inhibitor for the treatment of CML patients with a translocation between the BCR gene locus on chromosome 22 and the coding region of ABL gene located on chromosome 9, forming an abnormality known as “Philadelphia chromosome”. This translocation results in expression of abnormal BCR-ABL protein kinase which drives CML disease phenotype. Initial results with Gleevec were astounding with patients reporting complete disease remission (Druker et al., 2006). Next success story comes from metastatic breast cancer patients treated with anti-HER2 monoclonal antibody inhibitor known as Trastuzumab (Cobleigh et al., 1999). In clinical trials, Trastuzumab caused

disease remission in ERBB2-positive patients previously non-responsive to conventional chemotherapy and untreated patients with metastatic breast cancer. It was approved for treatment of metastatic breast cancer (Cobleigh et al., 1999).

Numerous new and improved kinase inhibitors in the clinical pipeline are expected to substantially extend the list of approved kinase inhibitors as therapeutics. However, intrinsic or acquired drug resistance caused by drug efflux, mutations in target kinase and activating mutations in compensatory pathways limit the success of kinase inhibitors approved as therapeutics and curtail the duration of relapse (Holohan et al., 2013). As observed in CML patients, a single mutation at specific sites in the ABL kinase domain (T315) can render the mutant kinase resistant to inhibition by Gleevec/Imatinib (Shah et al., 2004). In case of ERBB2-positive breast cancer patients, Trastuzumab treatment is rendered ineffective by mutations causing PTEN loss or truncation in ERBB2 receptors or activating mutations in compensatory pathways like ERBB3 (Luque-Cabal et al., 2016). Tumors may harbor a small population of cells with resistant mutations or acquire them after the introduction of treatment. Thus, ironically, the inhibitors themselves could provide the selective pressure to advance drug refractory malignancies.

Rational combination of more than one therapeutic and development of predictive biomarkers that help to stratify patients will help to overcome the

challenges posed by drug resistance (Holohan et al., 2013). Identifying near complete kinase substrate profiles will aid a better understanding of the intricate kinase pathways and fuel the identification of these novel strategies to combat drug resistance.

1.1.4 Combination cancer therapy using kinase inhibitors

Relapse is very frequently observed in cancer patients since neither molecular targeted therapeutic agents (a majority of which are kinase inhibitors) nor chemotherapeutic agents are sufficient to achieve long-term successful cancer remission in most cancers (Miller et al., 2016). As described earlier, inherent and acquired resistance inevitably develops with monotherapy. Thus, combinations of two or more therapeutics have been tested in preclinical and clinical trials. These efforts have led to the first therapeutic combination of dabrafenib (BRAF kinase inhibitor) and trametinib (MEK inhibitor) for the treatment of metastatic melanoma patients harboring the BRAF V600K or V600E mutation (Flaherty et al., 2012). The use of this combination has increased the median progression-free survival of patients in Phase III clinical trial and also reduced the incidence of cutaneous squamous cell carcinoma observed as a result of MAPK activation after dabrafenib treatment (Flaherty et al., 2012). This combination has recently also been approved for treatment of non-small cell lung cancer (NSCLC). Mainly, two strategies are employed to design these combinations. The first method is co-administration of a molecular targeted agent with another approved

chemotherapeutic drug. VEGF/VEGFR anti-angiogenesis inhibitors (Bevacizumab) in combination with cytotoxic agents (Paclitaxel) have shown improved efficacy in clinical trials for metastatic breast cancer, and ovarian cancers (Aravantinos and Pectasides, 2014; Zhao et al., 2014). The second strategy involves co-inhibition with two molecular targeted agents as is the case with dabrafenib and trametinib co-therapy (Long et al., 2015).

Knowledge of pathways regulated by the target kinase and compensatory signaling pathways is key to combining kinase inhibitors with other molecular targeted therapeutics. Inhibitors could be co-administered to target two signaling molecules in one oncogenic pathway, resulting in complete blockade of the pathway, or parallel pathways could be targeted to avoid the adaptable cancer cells from activating compensatory mechanisms. In either situation, the expected result is a long-term disease-free survival of the patient. The synergistic combinations could also help in reducing the minimum effective dose of the individual drugs and incidentally reduce the side effects associated with chemotherapy. The inherent heterogeneity of tumor cells, coupled with their adaptability provided by compensatory signaling pathways are the biggest challenges to monotherapy, and thus long-term effective therapeutic response may only be achieved by combining drugs that work together to combat cancer cells.

1.2 Biology of Pim kinases

The name Pim stands for pro-viral insertion of murine Moloney leukemia virus since the gene was identified using forward genetics in a murine tumor model, from a frequent site for viral insertion (Cuypers et al., 1984). Sequence analysis of these genes showed the presence of consensus kinase domains. Homologous genes were identified in human cells (Nagarajan et al., 1986). The human Pim kinase family constitutes of Pim1, Pim2, and Pim3. Both Pim1 and Pim2 genes encode two transcripts, the second originating from an alternate start codon CUG. The Pim1 gene codes for two protein variants 33 kDa and 44 kDa (Saris et al., 1991). The 44 kDa isoform is encoded by mRNA expressed from CUG start site upstream of the AUG start site, leading to an isoform with extended N-terminus (Xie et al., 2005). Pim3 gene was first identified in rat-derived PC12 cell line and named *KID-1* (Feldman et al., 1998). It was subsequently identified as an oncogene and it encodes only one transcript (Deneen et al., 2003). Pim kinases are expressed in embryonic and adult hematopoietic tissues. Pim1 and Pim2 are mainly expressed in cells of hematopoietic origin and Pim1 and Pim3 are expressed in neuronal tissues (Hoover et al., 1997; Mikkers et al., 2004).

All three kinases share high similarity in the protein sequences. Pim1 and Pim3 have most similar amino acid sequences with 66% identity, while there is 55% identity between Pim1 and Pim2 and 61% identity between Pim2 and Pim3 (Figure 1.1) (Saurabh et al., 2014). They also share >60% gene

sequence homology. All three kinases contain a conserved kinase domain, however, there are no observed regulatory domains. Thus, it is generally accepted that these kinases are constitutively active, and the activity is proportional to the protein abundance. Transcription, translation and proteasomal degradation are major pathways for Pim kinase regulation.

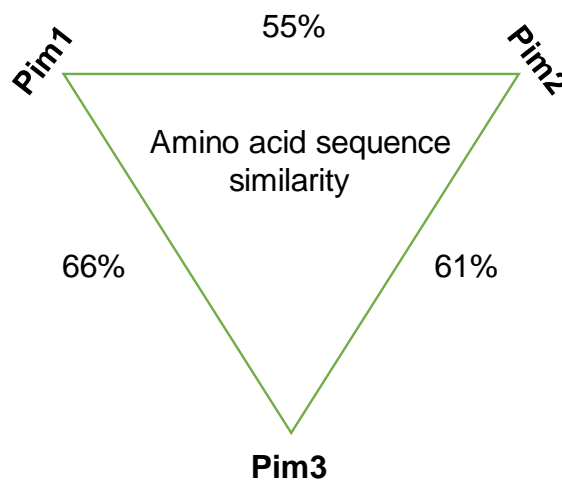


Figure 1.1. Sequence homology of Pim kinase isoforms (*adapted from* (Saurabh et al., 2014)). All the three Pim kinases have high similarity at the level of amino acid sequences. The percentage similarity between each pair is shown above the lines.

1.2.1 Upstream regulation of Pim kinases

JAK-STAT pathway is known to regulate transcription of Pim kinases. Transcription factors Stat 1,3 and 5 activated by cytokine interferon-alpha (IFN- α) signaling, are known to activate transcription of Pim1 (Matikainen et al., 1999) and NF- κ B acts as an activator of Pim2 transcription. Interferon-Gamma (IFN- γ) also regulates transcription of Pim kinases (Yip-Schneider et

al., 1995). The factor eIF-4E is known to bind to Pim mRNA and protect the mRNA from degradation (Hoover et al., 1997). The Pim kinase mRNA contains a long 5'-UTR (400bp) with highly structured domains that inhibit translation. This translational inhibition is relieved by the interaction between eIF-4E and Pim1 mRNA (Hoover et al., 1997). After translation, Pim1 protein is stabilized by a complex with heat shock protein 90 (HSP90) (Mizuno et al., 2001). Both HSP90 α and HSP90 β can interact with the Pim1 protein, but only HSP90 α is co-regulated by cytokine receptor gp180 signaling, in the same manner as Pim1. Inhibitor of HSP90 (geldanamycin) can induce degradation of Pim1 protein likely due to destabilization of the complex with HSP90 α (Mizuno et al., 2001).

1.2.2 Downstream targets of Pim kinases

Pim kinases share substrates and often phosphorylate the same sites. Pim kinases have a broad range of normal cellular functions including regulation of proliferation, protein translation, cell cycle progression and inhibition of apoptosis (Figure 1.2) (Chen et al., 2011). Few substrates have been identified for Pim1, including c-Myc as one of the important targets. Transcription factor c-Myc forms a heterodimer with Max and binds Enhancer (E-box) of more than >15% of promoters in cancer cells (Li et al., 2003). c-Myc is a classic oncogene and a very potent inducer of cellular proliferation (Dalla-Favera et al., 1982; Taub et al., 1982). Pim1 is known to phosphorylate c-Myc protein and increase its stability. Myc-Max dimers recruit Pim1 to RNA

pol 2-transcription initiation site through interaction between Pim1 and Myc. It is not known if this interaction is dependent on Myc phosphorylation. Thus, Pim1 phosphorylates its second known target; Serine 10 on Histone H3. Another important target of Pim kinases is the pro-apoptotic protein BAD which is an inhibitor of Bcl2 proteins (Aho et al., 2004). Pim1 phosphorylation of BAD causes its dissociation from anti-apoptotic Bcl-2 factors and thus helps in evading apoptosis (Aho et al., 2004). Pim2 can also phosphorylate BAD at the same residues, while Pim3 phosphorylates it at another residue (Macdonald et al., 2006; Popivanova et al., 2007).

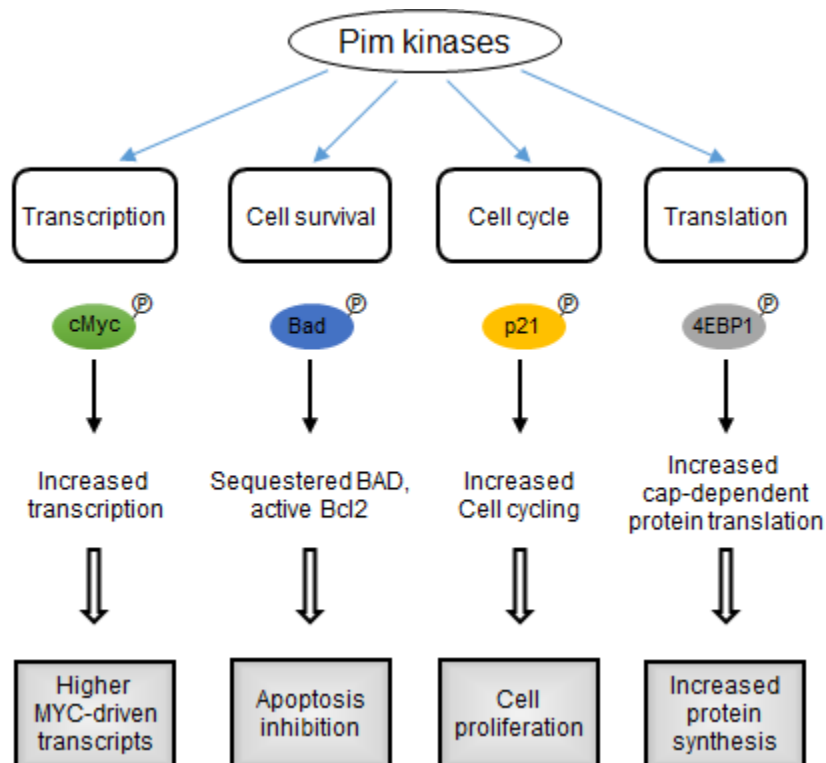


Figure 1.2. Pathways regulated by Pim kinases. Pim kinases phosphorylate various substrates and regulate important cellular pathways that support proliferation and survival. The figure depicts Pim kinase substrates involved in each pathway. Deregulation of Pim kinases observed in various cancers including AML leads to up-regulation of these pathways (*adapted from* (Chen et al., 2009)).

Pim1 also interacts with ribosomal small subunit protein 19 (RPS19) and co-sediments with active ribosomes (Chiocchetti et al., 2005). RPS19 mutations are mainly found in patients with diamond blackfan anemia (DBA) (Campagnoli et al., 2008). This interaction of Pim1 and RPS19 is also required for its role in inducing cap-independent translation of receptor tyrosine kinases (RTKs). Thus, Pim1 might have a more general role as a regulator of protein translation, at least in part through RPS19. There are two isoforms of Pim1, a shorter 33KDa protein present in the nucleus, and the cytoplasm, and a 44KDa form that localizes mainly to the plasma membrane but is also found in the cytoplasm. Interestingly, it is the 44KDa form of Pim1 that interacts with polysomes (active ribosomes) (Iadevaia et al., 2010).

1.2.3 Pim kinases in Cancer

Studies on cancer patient tumor samples have shown significant over-expression of Pim1 in hematopoietic cancers and certain solid tumors like prostate cancer at various stages suggesting their oncogenic potential (Chen et al., 2005; Nawijn et al., 2011). The oncogenic potential of Pim kinases has also been studied using transgenic mice. However, only 5-10% of the mice over-expressing Pim1 (E μ -Pim) showed an incidence of tumors. When these

mice were infected with Moloney murine leukemia virus (MuLV), they showed spontaneous tumors when the virus integrated at the Pim locus. This integration was almost always complemented by c-MYC overexpression, suggesting a key role of c-MYC in the tumor development. Further investigation showed that the transgenic combination of E μ -Pim1 and E μ -Myc was lethal. However, *in utero* inspection showed the development of lymphoma in the E μ -Myc E μ -Pim1 embryos (Verbeek et al., 1991). This finding underscores the importance of Pim1 and c-Myc collaboration in lymphomagenesis. However, transgenic mice with homozygous knockout of Pim1 are fertile and viable. Their development without showing any phenotypic abnormalities was attributed to the redundancy of Pim kinase isoforms. Interestingly, mice with homozygous deletion all the three Pim kinase isoforms are also viable and fertile, although, these triple knockout mice are smaller in size and have a reduced size of organs and have impaired hematopoiesis (Mikkers et al., 2004).

Pim kinases are over-expressed in a multitude of hematological cancers like acute myeloid leukemia (AML) (Keeton et al., 2014; Meja et al., 2014; Saurabh et al., 2014), mantle cell lymphoma (MCL) (Hogan et al., 2008), chronic lymphocytic leukemia (CLL) (Chen et al., 2009; Decker et al., 2014) and others. AML includes a heterogeneous group of malignant transformations that initiate in the myeloid blast cells of blood and bone marrow. Based on the two-hit model hypothesis, the genetic mutations that

lead to leukemogenesis are divided into two groups; mutations that lead to initial proliferation or survival of blast cells and mutations that confer self-renewability or block differentiation (Renneville et al., 2008). The first group includes molecules like FLT3-ITD, c-KIT which when expressed can provide a proliferative advantage to blast cells. FLT3-ITD is one of the most common mutations in AML patients (20.4%) (Thiede et al., 2002), caused by duplication in the juxta-membrane domain of FMS-like tyrosine kinase 3 (FLT-3). However, treatment by FLT-3 inhibitors is followed by a brief disease-free survival and relapse in most cases (Alvarado et al., 2014). Primary samples from patients with relapse showed increased Pim kinase expression. Co-inhibition of FLT-3 and Pim kinases eradicated primary AML cells in culture (Green et al., 2015). Therefore, Pim kinase inhibitors can be used alone or in combination with other kinase inhibitors to treat AML.

1.2.4 Pim kinase inhibitors

Several Pim kinase inhibitors have shown efficacy by inhibiting proliferation and/or inducing apoptosis in cancer cells in culture (Yang et al., 2014). Most notable effects are observed against hematopoietic cancers like AML (Chen et al., 2011; Keeton et al., 2014), MCL (Yang et al., 2012), CLL (Chen et al., 2009) and T-cell lymphoma (Lin et al., 2010b) and solid tumors like prostate cancer (Chen et al., 2005) and colon carcinoma (Popivanova et al., 2007; Weirauch et al., 2013). Small molecular Pim inhibitors have proven to be highly effective against AML cell lines and primary samples in preclinical

studies (Nawijn et al., 2011; Zhukova et al., 2011). While targeted cancer therapy is the ultimate purpose of kinase inhibitors, they can also be used to decipher the functions of the targeted kinases. A few inhibitors have been designed to inhibit specific Pim kinase isoforms (Pogacic et al., 2007). However, most small molecules are pan-inhibitors that target all three Pim isoforms albeit to varying potentials. The hinge region of all kinases contains residues that interact with ATP and form hydrogen bonds. Pim kinases contain a proline in this region and this results in an unusual hydrophobic pocket and hydrogen bonding (Qian et al., 2005). This peculiar structural difference has driven the development of highly specific small molecular inhibitors for Pim family kinases.

AZD1208: AZD1208 is a highly selective small molecular, ATP competitive, pan-Pim inhibitor (Keeton et al., 2014). AZD1208 inhibits all three Pim kinases with $IC_{50} < 5nM$ and inhibits BAD phosphorylation in cell-based assays with $IC_{50} < 150nM$. Keeton et. al investigated the effects of AZD1208 treatment on AML cell lines and primary cells from AML patients. AZD1208 strongly inhibited the growth of 5 out of 14 AML cell lines and showed promising activity against primary patient samples irrespective of their FLT3 status (Keeton et al., 2014). This and other preclinical studies suggested a potential for AZD1208 as a drug against AML, thus warranting clinical trials. A clinical trial for AZD1208 was conducted to study the efficacy in AML patients (NCT01410981). However, this study was terminated, following a lack of

therapeutic response in 19 of the 32 patients who received treatment (NTC01410981; additional information section). The best response observed in patients was a decrease in peripheral blasts in five patients and most modest reduction in bone marrow blast in two patients. Analysis of these trial data uncovered two caveats (Cortes et al., 2016); firstly, there was no correlation between peripheral blast reduction and extent of dephosphorylation of Pim substrates, and secondly, the AZD1208 activated CYP3A4 activity (Cytochrome P450 enzyme), which leads to a higher rate of its clearance and most likely resulted in low efficacy. As AZD1208 treatment was not effective as monotherapy, it warrants further investigations for identifying combinatorial approaches for therapy.

SGI1776: SGI1776 is a pan-Pim and Flt3 kinase inhibitor. SGI1776 induced cell cycle arrest and cell death in AML cell lines and patient samples. Pim inhibition also resulted in inhibition of transcription and protein translation (Chen et al., 2011). However, another study suggested that due to dual inhibition of Flt3 and Pim kinases, the exact contribution of Pim kinases in the survival of AML cells was undetermined (Hospital et al., 2012). Notably, SGI1776 was able to induce apoptosis in FLT3-WT and FLT3-ITD cell lines and primary samples alike (Chen et al., 2011). SGI1776 improved the efficacy of frontline AML chemotherapeutic drug cytarabine (Ara-C). Ara-C resistant HL-60 AML cells showed over-expression of Pim1 and Pim3 (Kelly et al., 2012). SGI1776 was the first Pim kinase inhibitor in a clinical trial. However,

the trial was terminated due to cardiac toxicity observed in patients (NCT00848601).

CX6258: CX6258 was derived from an oxinol-based parent compound as a pan-Pim kinase inhibitor. This inhibitor shows low nanomolar efficacy against all three Pim kinases (Haddach et al., 2012).

Among novel Pim kinase inhibitors that have been tested *in vitro* and *in vivo*, PIM447 and INCB053914, have entered clinical trials. INCB053914 showed efficacy against various AML cell lines and xenograft models of AML (Koblish et al., 2015). A clinical trial is ongoing with this Pim inhibitor for the treatment of advanced malignancies (NCT02587598).

Another approach to target Pim kinases is using monoclonal antibodies. Immunofluorescence staining for Pim1 44KDa isoform showed that it mainly localizes to cell membrane while 33KDa is present in cytosol and nucleus (Xie et al., 2005). Monoclonal antibody against Pim1 (P9) was able to bind Pim1 isoforms and induce apoptosis in prostate cancer and leukemia cell lines (Hu et al., 2009; Li et al., 2009).

1.2.5 Combination therapy with Pim kinase inhibitors

Pim kinases regulate transcription, protein translation, cell cycle progression, apoptosis and drug resistance (Yang et al., 2014). Thus, Pim kinases can

resist the effect of inhibitors that target aforementioned cellular functions of cancer cells. This compensation is likely mediated by upregulation of Pim kinases in the presence of inhibitors of important cellular pathways (Wozniak et al., 2010; Zemskova et al., 2008). Pim kinases also intersect various other signaling pathways and thus compensate for absence or inhibition of other kinases including AKT, mTOR or PI3K pathways. The shared substrates of these pathways may be the reason why Pim kinases can provide alternative signaling for cancer cells to escape the toxic effects of other kinase inhibitors (Yang et al., 2014). Finally, Pim kinases play a role in activating drug efflux transporters like ABCB1 and ABCG2, and their inhibition has shown promise in overcoming acquired drug resistance (Mumenthaler et al., 2009; Natarajan et al., 2013). Activation of kinase Etk by the 44KDa Pim1 protein is also involved in doxorubicin resistance in prostate cancer cells (Xie et al., 2005). Aligning with the role of Pim kinases in drug resistance, Pim kinase inhibitors show synergy when combined with the standard-of-care chemotherapeutics. Pim kinase inhibitors SGI1776 and LGB321 augment the AML standard-of-care drug Cytarabine (Ara-C) in preclinical testing (Garcia et al., 2014; Kelly et al., 2012). Pim Inhibitor CX6258 showed a synergistic effect in combination with frontline chemotherapeutics like doxorubicin and paclitaxel against prostate cancer cells (PCa) (Haddach et al., 2012). The following section reviews current literature for effective Pim kinase combinations with other targeted drugs based on a rational mechanism-based approach.

Combinations targeting parallel signaling pathways: The hypersensitivity of Pim1^{-/-}/ Pim2^{-/-} mouse T lymphocytes to rapamycin (mTOR inhibitor and immunosuppressant), demonstrates the role of Pim kinases in rapamycin-resistant survival (Fox et al., 2005). Indeed, Pim (AZD1208) and mTOR (AZD2014) inhibitors synergize against AML cell lines and primary AML patient cells by suppressing proliferation via heat shock factor-mediated suppression of protein synthesis (Harada et al., 2015). The JAK2 signaling pathway is similar to Pim kinase pathway as it plays an important role in hematopoiesis and is upregulated in cytokine-dependent cancers. In order to identify potential synergistic combination partners, Huang et al., performed an shRNA screen for 5000 gene targets in presence of JAK2 pharmacological inhibitor. They identified c-Myc as one of the most effective target shRNA and that partial inhibition of c-Myc function by Pim kinase inhibitors had a synergistic inhibitory effect on myeloproliferative neoplastic (MPN) cell line proliferation (Huang et al., 2014).

Combinations targeting survival pathways: The Pim and AKT pathways overlap partially and regulate of apoptosis through shared substrates. Pim1, Pim2, and AKT phosphorylate and inactivate protein inhibitor of BCL2, known as BAD (Macdonald et al., 2006; Warfel and Kraft, 2015). Pim1 and AKT also phosphorylate cot protein kinase, leading to upregulation of NFκB dependent transcription of survival genes (Amaravadi and Thompson, 2005). Combination of Pim kinase inhibitor (AZD2908) and AKT inhibitor (AZD5363)

showed strong synergy *in vitro* by reducing proliferation of AML cell line and AML patient samples. The combination treatment results in loss of RPS6 and 4EBP1 phosphorylation, suggesting deregulation of mTOR pathway. The combination also resulted in a decrease in MCL1 protein levels thus affecting the survival pathway (Meja et al., 2014). As Pim kinases regulate cell survival, the combination of Pim inhibitors with molecules targeting apoptotic inhibitors is a rational strategy. Combination of Pim kinase inhibitor SMI-4a and Bcl-2 inhibitor ABT-737 showed synergism and caused apoptosis in prostate cancer cells (Song and Kraft, 2012).

Combinations targeting protein synthesis: Expression of Pim1 is regulated by c-Myc. Pim kinases can also phosphorylate at Ser⁶² to activate c-Myc and together they can accelerate tumorigenesis. c-Myc is a major activator of ribosomal biogenesis and thus, Rebello et al., hypothesized that Pim inhibition would synergize with rRNA biogenesis inhibition to affect the growth of prostate cancer cells. CX6258 was used in combination with an RNA Polymerase-I inhibitor CX5461 and showed a synergistic inhibitory effect in genetically modified mouse models of prostate cancer [Hi-MYC (prostate specific Myc overexpression) or PTEN deficient model of PCa]. This dual combination was also more effective against patient-derived xenograft (PDX) models of MYC overexpressing PCa samples (Rebello et al., 2016).

Our work has identified that two novel important cellular pathways, pre-mRNA splicing and rRNA processing, are regulated by Pim kinases through substrate proteins that play a role in these pathways. The next sections will provide a composite review of relevant literature for pre-mRNA splicing and rRNA processing in normal and cancer cells, their regulation by protein phosphorylation, and their potential as cancer target pathways.

1.3 pre-mRNA splicing

Eukaryotic genes contain relatively shorter stretches of protein-coding sequences, known as exons, interspersed with long stretches of untranslated regions known as introns, that get cleaved out of the pre-mRNAs. Genes give rise to pre-mRNAs, from which introns are removed and exons are ligated to give rise to mature mRNAs. The process of removal of one or more introns and covalent joining of exons leading to the mature mRNA transcripts is known as pre-mRNA splicing. The phenomenon of pre-mRNA splicing radically changed the one gene-one protein hypothesis. It takes a lot of cellular energy to produce these mRNA fragments and then much more energy to excise them right after. Although at first sight, this process seems counterproductive for the cells, there are various advantages to having introns and that make alternative splicing a desirable adaptation, despite the unfavorable energy requirements for this process. Introns can regulate gene expression by harboring binding sites for transcription factors. Intron coding sequences are not junk DNA, instead, they can code for non-coding RNAs

like snoRNAs (small nucleolar RNAs) that help in rRNA processing. The intron density increases from a total 296 introns in yeast (5% genes) (Parenteau et al., 2008) to 207,344 total introns in humans, which amounts to an average of 8 introns per every gene (Sakharkar et al., 2004). By correlation, this could suggest a possibility for a selective advantage for having more introns. The following subsections describe the process of mRNA splicing, regulation of constitutive and alternative splicing, regulation of these processes by protein phosphorylation, and finally the significance of splicing regulation in cancer.

1.3.1 Mechanism and regulation of pre-mRNA splicing

The spliceosome is a specialized macromolecular complex that consists of the noncoding catalytic RNAs called snRNAs (small nuclear RNAs) and associated proteins. In addition to these core components, there are more than 100 ancillary components that are required for accurate pre-mRNA splicing. The common theme observed in splicing is that assembly of these ribonucleoprotein particles occurs in stages at different cellular locations culminating into the final assembly at the splice site (Matera and Wang, 2014).

1.3.1.1 Generation of snRNPs

The snRNAs are catalytic RNAs named as small nuclear RNAs. There are two classes of snRNAs, namely, the sm and sm-like snRNAs. The sm snRNA class consists of U1, U2, U4, U4atac, U5, U11, and U12. The sm-like

class contains U6 and U6atac. The snRNAs are classified on the basis of their sequence features and associated proteins. The sm-like snRNAs are transcribed by RNA pol III while sm snRNAs are transcribed by RNA pol II. Transcription of sm-class snRNAs is parallel to mRNA transcription in many ways. They are transcribed by RNA pol II from promoters which contain elements called proximal sequence elements (PSEs) (Hernandez, 2001) which are similar to TATA boxes, and the transcriptional termination requires integrator complex proteins that have sequence similarities with the proteins required for pre-mRNA 3'-end processing and polyadenylation. snRNAs are not polyadenylated, but contain a 5'-cap and require 3'-end processing. After transcription in the nucleus, snRNAs are transported into the Cajal bodies in the nucleus before being exported to the cytoplasm. The pre-snRNAs associate with the cap-binding complex proteins like PHAX and CRM1 that are exported out with the pre-snRNAs. PHAX and CRM1 concentrate in the Cajal bodies and inhibition of PHAX activity also cause pre-snRNAs to accumulate in the Cajal bodies. Thus, a model is proposed where Cajal bodies are the sites for assembly of the pre-snRNA export complex (Figure 1.3) (Matera and Wang, 2014).

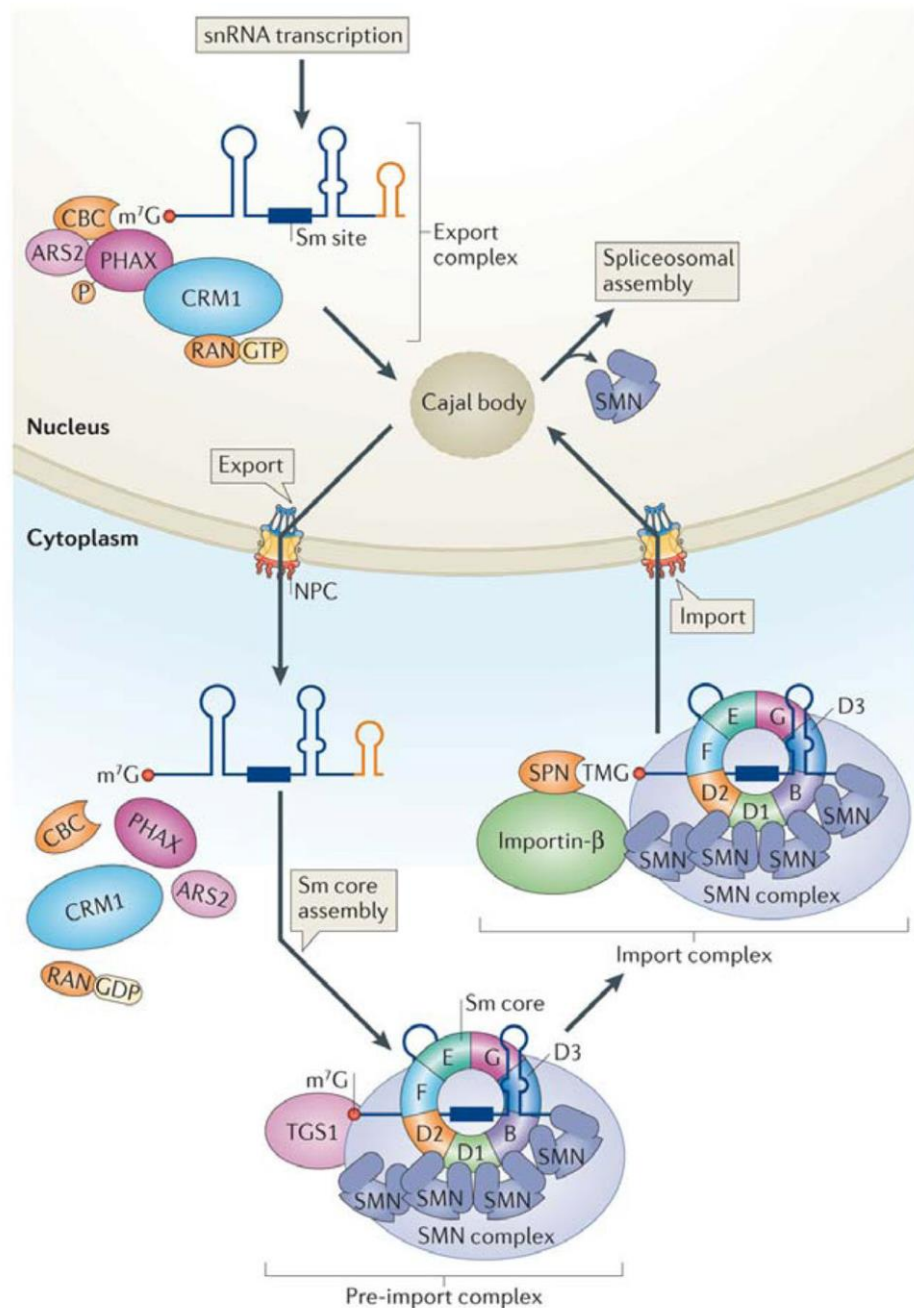


Figure 1.3 Schematic representation of snRNP assembly (from (Matera and Wang, 2014)) snRNP assembly begins with the transcription of snRNAs followed by their localization to Cajal bodies. snRNAs (with associated proteins) are exported to the cytoplasm, where they associate with sm core proteins to make the snRNP, after which these RNP complexes are imported into the nucleus. Finally, the pre-snRNPs reach the Cajal bodies, where the final maturation steps take place. After this step, mature snRNPs localize to nuclear speckles.

Once in the cytoplasm, the pre-snRNA export complex dissociates upon dephosphorylation of PHAX (Ohno et al., 2000) and snRNA is bound by proteins called GEMINs. One component of GEMIN complex is the survival motor neuron protein (SMN). The importance of proper pre-mRNA splicing is evident from the fact that reduced level of the SMN protein causes spinal muscular atrophy. SMN with Gemin2 and other proteins recruit the sm proteins onto the pre-snRNA. Sm-proteins form heterodimers and trimers which can bind to form the ring structure *in vitro* in purified form. In nuclear extracts, however, these proteins require the assembly factors like Gemin2 and SMN to form the intermediate horseshoe structure and finally a ring structure in complex with the pre-snRNA with six sm-proteins, namely, SmB, SmD1, SmD2, SmE, SmF and SmG (Matera and Wang, 2014). At this stage, the pre-snRNA is trimmed at the 3' end to its final length by endonucleases. This final complex is the core snRNP which gets imported to the nucleus. SMN factors dissociate from the snRNPs after nuclear import and localize to nuclear structures called Gems or Gemin bodies (Figure 1.3). Within the nucleus, the snRNPs revisit the Cajal bodies where final maturation steps like covalent modifications of snRNA and binding of associated proteins take place (Jády et al., 2003; Sleeman and Lamond, 1999). The mature snRNPs ultimately house in nuclear speckles which is their final storage place.

1.3.1.2 Spliceosome assembly

The next stage is the assembly of spliceosome complex. The spliceosome complex has been shown to be a 'protein directed metalloribozyme' (Shi, 2017). Various snRNPs and associated factors (SR proteins and others) associate and dissociate in a timely manner to orchestrate the feat of precisely cleaving an intron and joining the flanking exons. Figure 1.4 shows a schematic representation of a typical splice site (ss). A nascent mRNA might be bound by hnRNPs before being bound by the splicing machinery. This can encourage inclusion and exclusion of specific exons, thus providing an avenue for alternative splicing.

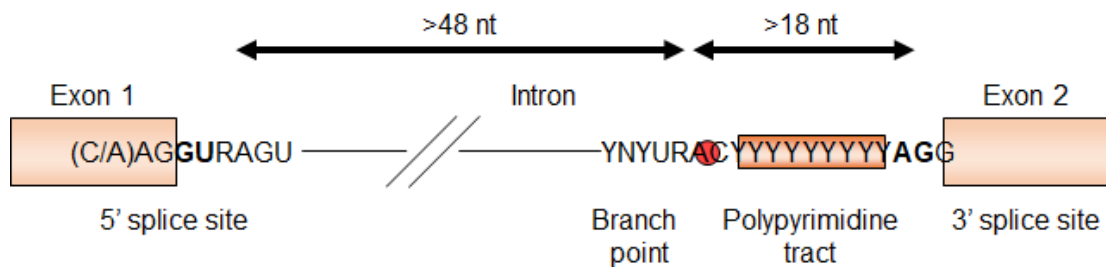


Figure 1.4 Graphical representation of a typical splice site (adapted from (Matlin et al., 2005)). This schematic shows the 3' splice site (ss), 5' ss, branch point and the pyrimidine track, which are all the consensus sequences that signal the binding of splicing factors required for pre-mRNA splicing.

The first step in spliceosome assembly entails recognition of all the consensus elements and exon splicing enhancers (ESEs) including U1 snRNP binding to the 5' splice site (ss), SF1/mBBP (splicing factor 1/mammalian branch-point binding protein) binding to the branch point and U2AF subunits (65 kDa and 35 kDa) interacting with the poly-pyrimidine tract

and 3' ss (Agrawal et al., 2016; Berglund et al., 1998; Zorio and Blumenthal, 1999). In the next step, U2 snRNP binds the branch point. This is the exon definition complex or complex E. The process of recognition of consensus elements in exons is called exon definition. All the steps require base pairing between the snRNAs and mRNA nucleotides. The E complex involves base pairing between U1 snRNA and 5' ss and also between U2 snRNA and 3' ss (Figure 1.5-(Krebs et al., 2014)).

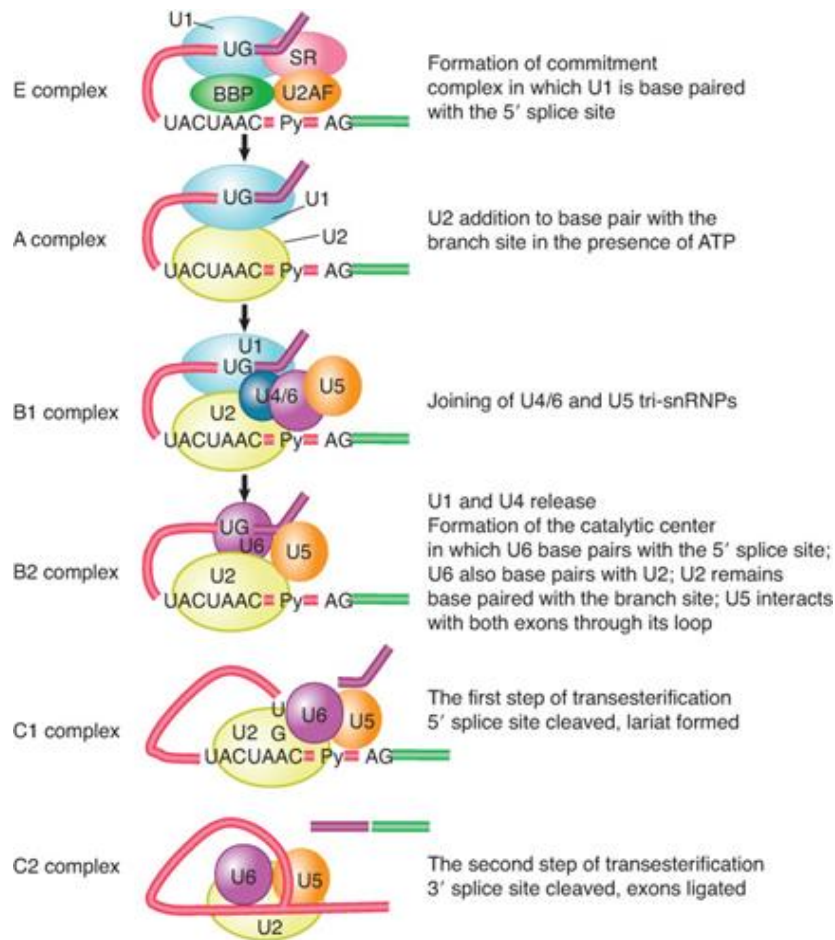


Figure 1.5 Schematic representation of spliceosome assembly and the catalysis of splicing (from *Chapter 21, Lewin's Gene XI* (Krebs et al., 2014)) The schematic shows various complexes formed during pre-mRNA splicing (see section 1.3.1.2 for more details).

The next complex is the intron-definition complex, which is formed by conformation changes using the energy of ATP hydrolysis to bring the two exons near each other, by folding the intron in a looped fashion (Figure 1.5- (Krebs et al., 2014)). This is known as the pre-spliceosome complex or A complex. The trio of preassembled snRNPs U4, U5 and U6 bind the A complex followed by another conformation change, converting it into active B* complex. Once activated, the U2 snRNA in complex B conformation interacts with U6 snRNA unwinding the interaction with U4 snRNA. U1 and U4 snRNPs leave the spliceosome at this point. The first cleavage occurs at the 5' splice site, creating a free 5' exon and lariat intron with the 3' exon. This is the first transesterification reaction caused by a nucleophilic attack by the 2'OH group of branch-point adenosine on the 5' splice site (Kornblihtt et al., 2013). This is complex C, which finally undergoes conformational changes and causes the second cleavage and transesterification reaction between 3'OH of the 5' splice site and the 3' splice site creating joined exons of mRNA and a cleaved lariat intron. All the steps including the last step are assisted by various helicases which help unwind the RNA interactions, finally releasing the snRNPs and intron (Matera and Wang, 2014).

All steps of splicing are reversible in a cell-free system. To test which steps are reversible, researchers created spliceosomes unable to release a joined exon and lariat intron. *In vitro* analysis with these spliceosomes showed that the catalytic steps are indeed reversible. By changing the KCl

concentration and removing ATP from the reaction these reactions could be reversed (Tseng and Cheng, 2008). However, it is still unknown if the catalytic steps are reversible *in vivo*. Once exon recognition takes place in early stages of spliceosome assembly, an intron-bridging complex needs to be formed. The coupling between the participating exons can occur up to the formation of B complex. Thus, all the three initial complexes can be the points for alternative splicing.

1.3.1.3 Alternative splicing

The discovery that humans contain only about 20,000 genes while even relatively simple invertebrate *C. elegans* has 19,000 genes was perplexing (Hodgkin, 2001). The obvious increase in complexity was not supported by the disproportional increase in gene number. One way that nature overcomes this shortage of genes is by the mechanism of alternative splicing, which increases the functional utility of the genetic real-estate and provides various permutations for creating gene products that could perform varying and tissue-specific functions. It is estimated that at least 74% of genes in the human genome have more than one mRNA isoforms created by alternative splicing (Johnson et al., 2003). Other studies have estimated that over 90% of all mRNAs are alternatively spliced (Wang et al., 2008). A single gene can give rise to one pre-mRNA which can, in turn, be spliced as several distinct mRNA transcripts. The more extreme example in *Drosophila* is the gene coding for cell surface marker protein *Dscam*, which produces up to

38,016 alternatively spliced transcripts (Matlin et al., 2005; Schmucker and Flanagan, 2004). The human gene similar to *Dscam* does not show alternative splicing similar to that observed in *Drosophilla*.

The decision of exon inclusion or exclusion depends on the strength of cis-regulatory regions on pre-mRNA and on the abundance of trans-regulatory splicing factors. The degree to which the actual splice sites overlap with the consensus splice sites denotes their 'strength'. Other cis-regulatory regions known as enhancers and suppressors play a major role in deciding the fate of the exon. There are four kinds of these regulatory regions- exonic splicing enhancer (ESE), exonic splicing suppressors (ESS), intronic splicing enhancers (ISE) and intronic splicing suppressors. Members of SR protein family are known to bind the ESEs and the members of the hnRNP family have been shown to bind ESSs and ISSs. Phosphorylation of SR proteins and hnRNP proteins plays a major role in the regulation of function or localization of these proteins, and thus leads to the regulation of alternative splicing (van der Houven van Oordt et al., 2000; Shen and Green).

1.3.2 Phosphorylation-dependent regulation of constitutive and alternative splicing

Pre-mRNA splicing begins co-transcriptionally and splicing factors physically interact with hyper-phosphorylated C-terminal domain of RNA polymerase II even in the absence of pre-mRNA (Kim et al., 1997). Most splicing factors

and snRNPs are localized to dense regions in the nucleus named as nuclear speckles (Huang and Spector, 1992; Misteli and Spector, 1997). These nuclear speckles, in turn, consist of interchromatin granules (IGCs) and perichromatin fibrils (PFs). Splicing factors are mainly located in the IGCs, however active transcription and splicing of transcripts, as identified by fluorescent labeling of nascent RNA, exclusively occurs in PFs (Wansink et al., 1993). Phosphorylation status of splicing factors was considered to be crucial determinant for their localization and function. Serine arginine-rich protein kinases (SRPKs) and cyclin-dependent kinase-like kinases (Clks) were among the kinases mainly devoted to the regulation of splicing factors. SRPKs phosphorylate within the RS domains in SR-protein and hnRNPs. The RS-domains contain serine and positively charged amino-acid arginine. Thus, the presence of negative charge due to phosphorylation of serine residues can change the nature of RNA and protein interactions involving these domains. Indeed, phosphorylation of SF2/ASF increases its binding to U1 snRNP (Xiao and Manley, 1997), but it is the hypophosphorylated SF2 that binds to RNA export factor NXF1 (Huang et al., 2004). Early studies showed that phosphorylation regulated the localization of these proteins. Addition of SRPK1 to permeabilized cells caused the redistribution of SR-proteins from nuclear speckles to a more diffused state. Similarly, over-expression of Clk also caused a more diffused distribution of SR-proteins. On the other hand, the addition of a phosphatase caused more confined localization of SR-proteins to speckles. Protein phosphatase 1 (PP1) was identified as the

phosphatase responsible for regulating SR proteins (Misteli and Spector, 1996). Since PP1 activity is regulated by the cyclic AMP (cAMP) signaling, alternative splicing is also in turn regulated by cAMP signaling. Another interesting finding was that in nuclear extracts where endogenous U1-snRNP was substituted with thio-phosphorylated U1-70K, this modified protein was able to bind the splice sites but was unable to complete splicing in presence of a constitutive negative charge in the RS-domain. This shows a need for phosphorylation for release and initial interaction of splicing factors into the spliceosome assembly and a need for dephosphorylation for successful completion and transport of splicing factors back into IGCs (Misteli and Spector, 1997).

A processive mechanism has been uncovered for SR protein phosphorylation. SRPKs phosphorylate RS domains in the cytosol and this causes nuclear localization of SR proteins (Lai et al., 2000), where they remain in the nuclear speckles. Clks (1-4), which also localize to nuclear speckles and contain RS domains, further phosphorylate SR proteins. Hyperphosphorylated SR proteins are recruited to the site of active splicing (Misteli et al., 1998). The phosphorylation of splicing factors by both the kinases can be regulated by cellular signaling pathways. Thus, phosphorylation plays an important role in the regulation of pre-mRNA splicing and alternative splicing.

1.3.3 Significance of mRNA splicing in cancer progression and treatment

Alternative splicing can be employed as a mechanism to alter protein function by addition of a novel protein domain due to the addition of alternate exon or by deletion of a functional domain due to skipping of an exon. Thus, defects in the accurate constitutive or alternative splicing can lead to dysfunctional proteins. Indeed, up to 50% of all mutations causing human diseases show defects in proper splicing (Wang and Cooper, 2007). Apoptotic regulator genes including *BCL-X*, *CASPASE 9* and *MCL1* encode multiple isoforms that perform opposite functions. *MCL1-L* (longer isoform) is anti-apoptotic protein while *MCL1-s* (short isoform) is proapoptotic. The short isoform lacks exon 2 which codes for the BH1, BH2, and transmembrane domains. Due to the lack of these domains, it can no longer interact with BCL-2 related protein and over-expression of *MCL1-s* induces apoptosis unlike survival by *MCL1-L* (Bae et al., 2000). Another example of isoforms with opposing functions comes from VEGF ligand proteins. VEGF-A encodes two spliced isoforms VEGF-A₁₆₅ and VEGF-A_{165b}. VEGF-A₁₆₅ is proangiogenic, while VEGF-A_{165b} is anti-angiogenic (Woolard et al., 2004). VEGF-A_{165b} is downregulated in colon cancer, prostate cancer, and melanoma while VEGF-A₁₆₅ is upregulated in tumors (Oltean and Bates, 2014). Thus, cancer cells can modulate these cellular processes by altering the splicing pattern of these targets. This splicing event is regulated by SRSF1, which, in turn, is regulated by SRPK1 mediated phosphorylation

(Amin et al., 2011). SRPK1 inhibitor SRPIN340 reverses VEGFA splicing to anti-angiogenic form VEGF-A_{165b} (Amin et al., 2011). SRPK1 inhibition by SRPIN340 or knockdown reduced the growth of melanoma *in vivo*.

Another insight into the significance of splicing in cancer comes from the identification of splice site mutations. 29 different splice site mutations were found in p53 from more than 12 different cancers. A mutated splice site cannot be identified by splicing factors, and therefore, causes exclusion of the exon resulting in a truncated protein. Analysis of tissue samples from acute myeloid leukemia patients uncovered that 29% of the total expressed gene products showed aberrant splicing in comparison to normal CD34+ bone marrow cells. The aberrantly spliced list of genes included 52 oncogenes and 50 tumor suppressors (Adamia et al., 2014). Thus, global aberrant splicing could affect numerous regulators and support tumor growth.

Mutation in splicing factor genes frequently occurs in hematopoietic malignancies and solid tumors. These mutations mainly were found to affect the members of the core spliceosome complex including U2AF1, SRSF2, SF3B1, and ZRSR2. These mutations were frequently observed in myeloid dysplasia (MDS) in 45-85% patient samples (Yoshida et al., 2011). Most of these mutations were mutually exclusive thus indicating they have a similar impact on the pathway. Other splicing factors like SRSF1 and hnRNPA1 are upregulated in various cancers (Karni et al., 2007; Roy et al., 2017). SRSF1

overexpression caused transformation of immortal rodent fibroblasts. SRSF1 was found to regulate alternative splicing of tumor suppressor BIN1 and pro-growth kinases MNK1 and S6K1. Over-expression of SRSF1 caused inclusion of an exon leading to an inactive tumor suppressor protein and induced formation of an unusual S6K1 isoform. Knockdown of this isoform was sufficient to reverse the transformation caused by SRSF1 over-expression. Therefore, SRSF1 is a proto-oncogene which can be targeted for cancer therapy (Karni et al., 2007).

Novel inhibitors that target the core spliceosome have been described in the literature. A number of these molecules affect the SF3B complex of the spliceosome. Preclinical studies with these inhibitors show promise as they inhibit cancer cells *in vitro* and *in vivo* (Crews et al., 2013; Wang et al., 2011a). Clinical trial with splicing inhibitor E7107 was terminated due to treatment dependent reversible blindness observed in 2 patients (Dehm, 2013; Eskens et al., 2013) (NCT00499499). This, suggests that inhibition of splicing complex may have deleterious side effects and may limit the maximum dose. A combination with another inhibitor may help to reduce the effective dose required for spliceosome inhibitors and could be a way to avoid the adverse effects.

1.4 rRNA processing

Ribosomal RNA is the most abundant form of noncoding RNA in the cell. The two mature rRNAs in eukaryotes, namely the 18S and 28S rRNAs, form visible bands when total RNA is resolved by agarose gel electrophoresis, due to their many fold higher abundance in the cell. rRNAs form an integral part of the ribosome and function in protein synthesis. The eukaryotic ribosomes are composed of two sub-units- 40S and 60S which join to form the 80S particles. 40S subunit contains 18S rRNA with 33 ribosomal proteins (RPs) and 60S subunit is composed of 5S, 5.8S and 25/28S rRNAs and 46 RPs.

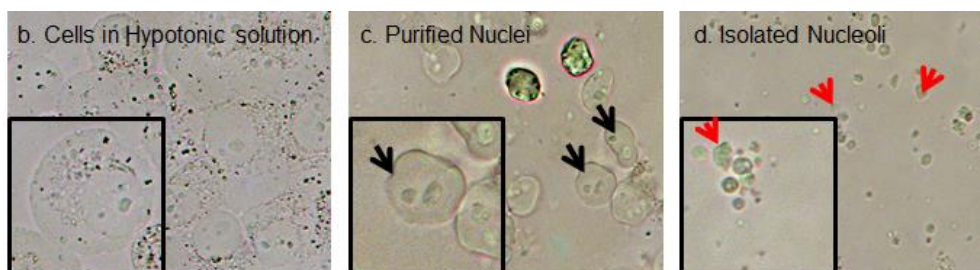
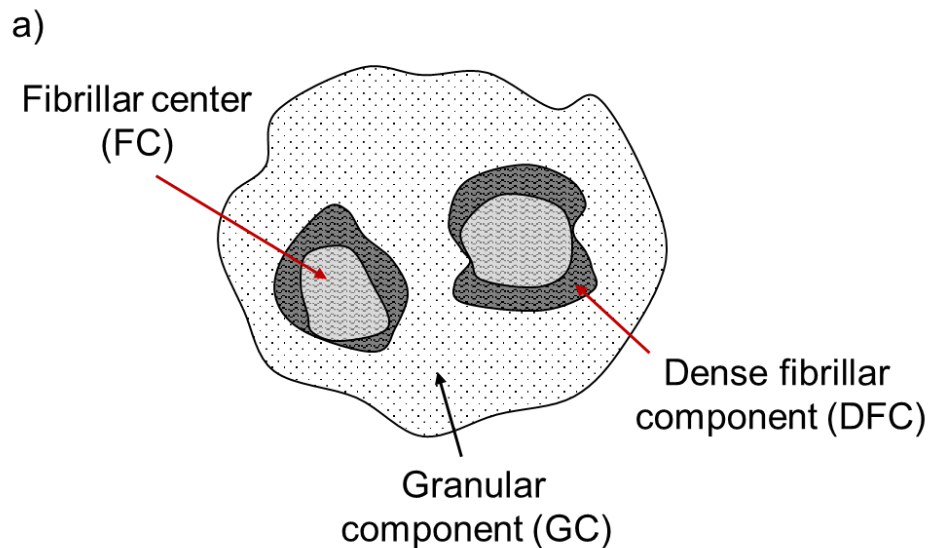


Figure 1.6 a) Diagrammatic representation of a nucleolus. There are three compartments in the nucleolus- the Fibrillar component (FC), the dense fibrillar component (DFC), and the granular component (GC). The rRNA processing begin in the nucleolus, continues into the nucleoplasm, and final rRNA maturation takes place in the cytoplasm. b) Swollen HeLa cells in hypotonic solution. c) The image shows nuclei purified from Hela cells (arrows show nuclei). d) The phase contrast image shows nucleoli isolated from HeLa cells (red arrows point to nucleoli).

The nucleoli, highly dynamic organelles inside the nucleus, lacking a membrane, are the hub for rRNA transcription. A single nucleus can contain several nucleoli that form around the rDNA loci (containing tandem repeats of rRNA genes) known as the nucleolar organizer regions (NORs). Figure 1.6a shows a diagram of the animal cell nucleolus. Figure 1.6b,c,d shows microscopic images of HeLa cells, HeLa cell nuclei, and nucleoli isolated from HeLa. Nucleoli are highly dense organelles and can be purified in the intact form using hypotonic lysis followed by sucrose gradient centrifugation. The proteomic analysis of purified nucleoli has increased our understanding of the complexity of the nucleolar functions (Andersen et al., 2005).

The steps in rRNA processing and ribosome assembly are highly coordinated and begin in the nucleolus. Both the processes begin with transcription of rRNA (47S precursor) from tandem repeats of rDNA genes by RNA polymerase I, as certain RPs and other rRNA processing factors bind the nascent rRNA molecules to create pre-ribosomal complexes. The pre-rRNA transcript is covalently modified and folded structurally during the ribosome assembly steps. The transcripts are also trimmed by endo and

exonucleases to remove the internal transcribed spacers (ITS1 and ITS2) and external transcribed spacers (5'-ETS and 3'-ETS). The composition of pre-ribosomal complexes changes through all the steps of ribosome assembly as RPs are added to the complex and associated processing factors bind and dissociate from the complexes. rRNA processing mainly occurs in the nucleolus, but ribosome assembly starts in the nucleolus, transitions into the nucleoplasm and the final maturation and ribosome assembly occur in the cytoplasm. 40S subunits are moved to the cytoplasm rather quickly while 60S subunit maturation mainly occurs in the nucleoplasm.

1.4.1 Mechanism of rRNA processing

The different steps in rRNA processing from the 47S precursors involve maturation of 18S maturation by 5' ETS processing and ITS1 processing, and 28S and 5.8S by ITS2 processing and 3' ETS processing. The following sections will briefly discuss the cleavages involved in each processing step beginning at the 5' end of rRNA precursor to the 3' end. Figure 1.7 shows the various cleavage sites in each region.

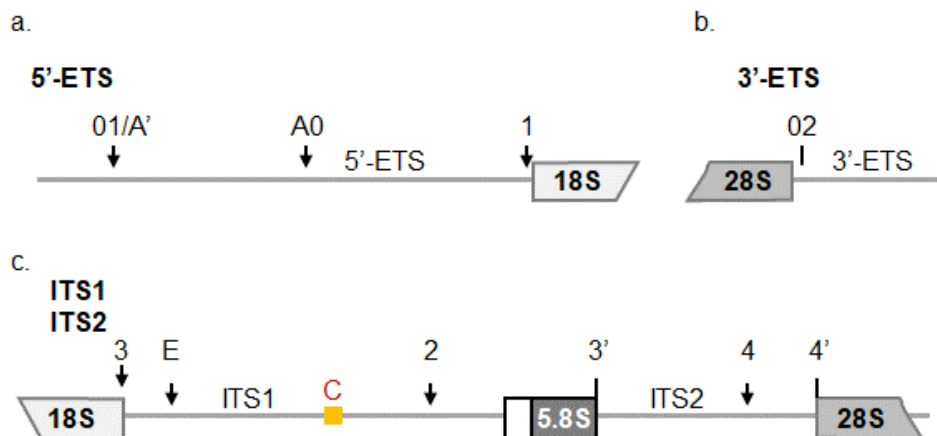


Figure 1.7 Diagrammatic representation of pre-rRNA cleavage sites in human cells (adapted from (Henras et al., 2015)) a) 5'-External transcribed spacer (5'-ETS), b) 3'-External transcribed spacer (3'-ETS), c) Internal transcribed spacer 1 and 2 (ITS1 and 2). The cleavage steps denoted by numbers and letters are explained in the text.

5' ETS processing: There are two cleavage sites in the 5'-ETS called A0 and 1 (Figure 1.7). Cleavage at these sites is usually coupled and occurs almost coincidentally. Any defect in coupling causes accumulation of 43S or 26S precursors. While the endonucleases responsible for these cleavages are still unknown, the small subunit (SSU) ribosomal processome including the U3 snoRNA, and numbers of RPSs are required for this step to happen (Ferreira-Cerca et al., 2005). In yeast U3 snoRNA was found to base pair with the 5'ETS of pre-18S rRNA and cause conformational changes. The fact that loss of this complementarity was lethal underscores the importance of proper folding of 18S rRNA (Dutca et al., 2011). Another additional step in metazoan 5'ETS processing is the cleavage at A' (Figure 1.7). Although it was shown that this step can be bypassed and does not affect the processing at A0 and 1 sites, it may be a quality control step (Sloan et al., 2014).

ITS1 processing: The ITS1 processing requires both endo and exonuclease activity in human cells. The cleavage steps occur at sites 2 and E, beginning with cleavage at site 2 approximately around nucleotide number 6470. However, another minor pathway was observed in HeLa cells where cleavage of the 45S rRNA at the E site happened first. This resulted in 36S

pre-rRNA (Prete et al., 2013). The cleavage at site E is about 78-81 nucleotides away from the 3' end of 18S rRNA and results in the formation of 18S-E precursor (Prete et al., 2013). 18S-E is the last precursor to the mature 18S rRNA. The 5'-3' exonucleases trim the remaining portion of 3' 18S-E precursor, which begins in the nucleus and continues during nuclear export (Prete et al., 2013). The processing at site 2 does not depend on processing at sites A0, 1 and E, however, processing at site E requires prior processing at sites A0 and 1. The absence of certain processing factors and RPs can cause defects in cleavage at site 2, leading to accumulation of 36S and 41S pre-rRNAs.

In the next steps, 5' end of 5.8S rRNA is created by two alternative pathways. In yeast, the major pathway creates a short precursor of 5.8S and involves trimming by at least three exonuclease activities of rat1p, xrn1 and Rrp17 (Henry et al., 1994; Oeffinger et al., 2009). The minor pathway creates a longer 5' end due to endonuclease cleavage. The ratio of 5.8 short to the long precursor in yeast is 80:20 while in HeLa cells is 60:40 (Schillewaert et al., 2012). Thus, both the pathways exist in mammalian cells.

ITS2 processing: The maturation of the 3' end of 5.8S rRNA involves cleavage in the ITS2 at site 4. Cleavage at site 4 creates two precursors, 12S and 28.5S. 12S is further shortened to 7S either by cleavage at site 4a (identified in mice) or by exonuclease dependent trimming. 7S is then

trimmed by 3'-5' exonuclease activity by the EXOSC10 and exosome cofactors and Las1. The 5' and 3' steps are coupled and both require the activities of Rat1/Xrn2 (Schillewaert et al., 2012). The final steps of pre-5.8S in yeast requires trimming of ~6 nucleotides, which occurs in the cytoplasm after nuclear export of the ribosome subunit (Thomson and Tollervey, 2010). The 28S rRNA is processed by cleavages in ITS2 and 3' ETS. Cleavage at site 4 creates two precursors 12S and 28.5S. The 5' end of 28.5S is trimmed by XRN2 exonuclease to form mature 28S rRNA.

3'ETS: The 3' ETS maturation occurs very early after rRNA 47S transcription and may drive the termination of transcription in human cells (Eichler and Craig, 1994). In vertebrates, this processing requires the activity of U8 snoRNA. The absence of U8 snoRNA causes accumulation of abnormal 28S precursor rRNA and interferes with the processing of 5.8S and 28S in *Xenopus* (Peculis, 1997; Peculis and Steitz, 1994).

Each pre-rRNA cleavage described above can happen in a stepwise order through one of two pathways in human cells. The stepwise processing pathways occurring in human cells are depicted in Figure 1.8. The first steps include the cleavages at 5' and 3' end leading to formation of 45S rRNA. The next steps can occur in two alternate pathways. The major pathway begins with processing at site 2 leading to the formation of the 30S and 32S. 30S is converted into 18S-E by processing at A0, 1, C and E as described before.

36S is processed into 5.8S and 28S by processing at 4a, 4b, 4' and 3'. The minor pathway involves processing at steps A0 and 1 in the beginning, leading to the formation of 41S, followed by cleavage at site 2 leading to 21S and 32S precursors. 32S is further processed into 12S and 28S. 32S is further processed into 12S and 28S.

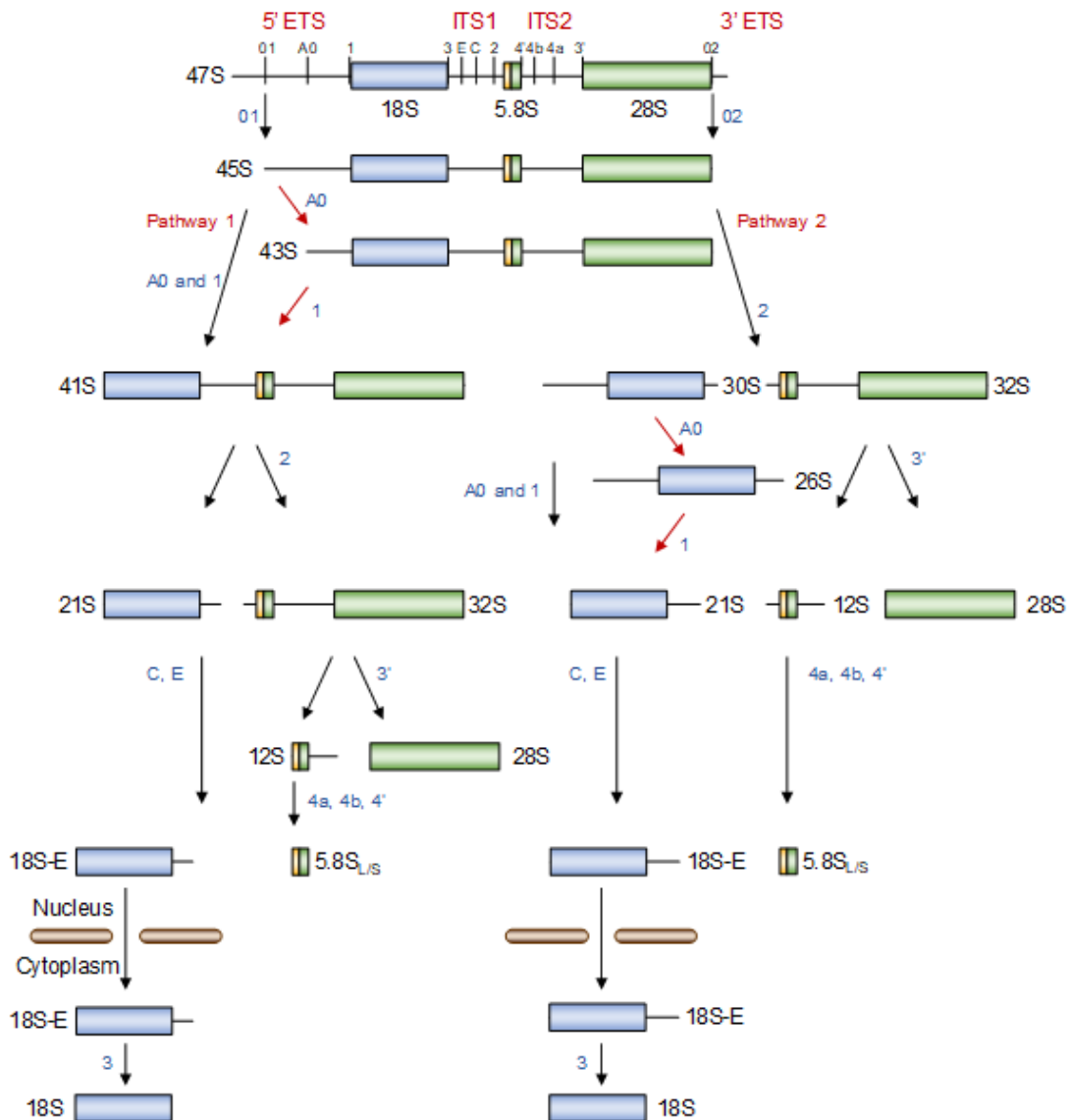


Figure 1.8 Schematic representation of stepwise pre-rRNA processing in human cells (adapted from (Lafontaine, 2015)). Two distinct pathways exist for processing of pre-rRNAs. Pathway 2 is the major pathway in human cells, while pathway 1 is the minor pathway, which has been observed to occur less frequently. Both pathways begin with the transcription of the 47S transcript, go through alternate intermediate cleavage steps, ultimately resulting in the formation of mature 18S, 28S, and 5.8S rRNAs.

Some small nucleolar RNAs (snoRNAs) are required for some of the processing steps to guide the nucleases at cleavage sites via base-pairing. Other snoRNAs function by modifying the rRNAs by 2'-O-methylation and pseudouridylation. Various steps of rRNA processing also required RNA helicases for proper refolding of rRNAs. One example is the RNA helicase-DEAD box protein Ddx51 which helps in displacing U8 snoRNA from the 3' ETS and allows processing in this region (Srivastava et al., 2010).

Recent studies have shed light on a much higher level of complexity in the regulation of human pre-rRNA processing. A meticulous study by Tafforeau et al., tested the function of 625 human nucleolar proteins and identified 286 of them as pre-rRNA processing factors (Tafforeau et al., 2013). Interestingly their findings suggest that at least 25% of these proteins have no homologs in yeast, 25% with yeast homologs that have different functions in humans and yeast, and 38% that are related to diseases.

1.4.2 Significance of protein phosphorylation in regulation of pre-rRNA processing

The role of protein phosphorylation in regulation of rRNA processing is not completely known. As phosphorylation is such an important regulator of pre-mRNA splicing and a heavily employed mechanism to control localization and function of splicing factors, it is not farfetched to speculate a role for protein phosphorylation in regulation of pre-rRNA processing factors. Protein kinases like mTOR, AKT, PERK and Pim have been very well established as regulators of protein synthesis and/or rRNA transcription (DuRose et al., 2009; James and Zomerdijk, 2004). However, to our best knowledge, few kinases have been linked to regulation of rRNA processing (Burger et al., 2013; Widmann et al., 2012).

An interesting example is the kinase family named hRIO (human RIO). These kinases were found to interact with the 40S ribosomal sub-unit and regulate the binding of rRNA processing factors to the ribosomal complex. Through its phosphorylation of the pre-rRNA processing factors, hRIO1 was found to regulate the cytoplasmic steps in 18S maturation from 18S-E (Widmann et al., 2012).

CDK9 is another kinase implicated in pre-rRNA processing regulation and the coupling between RNA pol II transcription (Burger et al., 2013). Pharmacological Inhibition of CDK9 induced specific rRNA processing defects

in the 3' ETS processing. CDK9 is a part of the RNA pol II complex, and its knockdown reduced Pol II-mediated U8 snoRNA transcription. Since U8 snoRNA is required for 3'-ETS processing (Peculis, 1997; Srivastava et al., 2010), CDK9 inhibition causes rRNA processing defects (Burger et al., 2013).

Another example of regulation of rRNA processing by a kinase is RPS3 phosphorylation by Hrr-25 kinase. The kinase Hrr-25 was found to phosphorylate RPS3 and 40S synthesis factor Enp1. The phosphorylation and subsequent dephosphorylation are required for maturation of the 40S subunit after allowing proper folding of 18S rRNA and tight binding of RPS3 (Schäfer et al., 2006). Therefore, the phosphorylation event affects proper folding of rRNA.

1.4.3 Significance of rRNA processing in cancer cells

The processes of rRNA transcription, pre-rRNA processing, ribosomal protein expression and ribosome assembly finally lead to ribosome biogenesis. A number of quality control measures are put in place in the cells to protect against making malfunctioning ribosomes. Thus, impairment of any of these individual processes affects ribosome biogenesis and regulation of other processes involved in ribosome biogenesis. Many diseases including Diamond Blackfan anemia (DBA) and T-cell acute lymphoblastic leukemia have been termed ribosomopathies as they are linked with abnormalities in ribosomal components or ribosome assembly factors leading to aberrant hematopoiesis and increased susceptibility to cancer.

Ribosomal proteins play a part in the regulation of rRNA processing. siRNA-mediated knockdown of specific ribosomal proteins caused impairment of steps in rRNA processing leading to signature pre-rRNA accumulation (O'Donohue et al., 2010). Cells from DBA patients show abnormalities in rRNA processing and maturation corresponding to the deficiency of ribosomal proteins. These aberrantly expressed pre-rRNA signatures in DBA patients have been used to identify RPL31 as the novel gene de-regulated in DBA (Farrar et al., 2014). Thus, lack of specific ribosomal proteins leads to inhibition of specific steps in rRNA processing.

In addition to ribosomal proteins, numerous other proteins act as rRNA processing factors. The study by Tafforeau et al., 2013 identified 286 pre-rRNA processing factors, of which 38% (109 proteins) were related to diseases. Out of the 109 processing factors, 89 were related to cancer including 54 factors that are over-expressed in cancers, 15 factors that are mutated in cancers, 12 factors that are downregulated in cancers, 5 factors that are related to the p53 pathway and 3 factors that are proto-oncogenes (Tafforeau et al., 2013). Thus, their function in rRNA processing might have significance in cancer.

Nucleophosmin (NPM1), an rRNA processing and transport factor protein, is frequently mutated in cases of AML. These mutations have been

found in the C-terminal domain of this nucleolar protein, and the mutant protein shows aberrant nuclear transport and stable localization to the cytoplasm. The NPM1 protein is involved in its binding to G-quadruplex structures through the C-terminal domain. G-quadruplexes are formed by four guanine nucleotides forming a non-canonical tetrad structure and are found in both DNA and RNA. The C-terminal domain mutations in NPM1 eradicate this G-quadruplex binding. Thus, a deregulated NPM1 and its role in pre-rRNA processing might play a part in AML tumorigenesis, as the C-terminal region is stipulated to bind the precursor rRNAs.

Tumor suppressor p19^{ARF} is frequently mutated in tumor cells. p19^{ARF} is induced in response to cellular stresses like aberrant c-Myc activation or oncogenic RAS activation (Serrano et al., 1997; Zindy et al., 1998). It was found to interact with NPM1 and resulted in delayed rRNA processing (Bertwistle et al., 2004). This function of p19^{ARF} may have implications to its role as a tumor suppressor and stress response gene.

Another pre-rRNA processing factor DEF is over-expressed in human neuroblastoma. Haploinsufficiency of *def* reduced the penetrance of MYCN-induced neuroblastoma in zebrafish, while over-expression accelerated the pathogenesis of the disease, and thus *def* was identified as the rate-limiting step in MYCN dependent pathogenesis (Tao et al., 2017). Def is a known component of the SSU processome and involved in pre-18S processing.

MYCN was found to regulate def transcription and leads to changes in pre-18S processing. Thus, it is plausible that def and other SSU processome factors increase rRNA processing and co-operate with MYCN to accelerate neuroblastoma.

Numerous regulators of ribosome biogenesis and protein synthesis have been linked to tumor progression and tumorigenesis. An important regulator of tumorigenesis, oncoprotein c-Myc, upregulates protein synthesis genes. Another example is the translation initiation factor eIF4E which controls the rate-limiting step in translation. Over-expression of eIF4E leads to upregulation of mRNA translation which can cause cellular transformation (Lazaris-Karatzas et al., 1990).

Targeting various steps in ribosome biogenesis and protein translation can be an effective therapeutic avenue for treatment of cancers. Specific inhibitors have been developed to block the transcription of rRNA by RNA pol I. Two small molecules, BMH21, and CX-5461 have been shown to target RNA Pol I activity and inhibit *de novo* transcription of rRNA (Drygin et al., 2011; Peltonen et al., 2014a). BMH21 was shown to target a number of cancer cells *in vitro* and inhibited *in vivo* tumor growth (Peltonen et al., 2014b).

Interestingly, rRNA transcription and processing has been a target for cancer treatment since the advent of chemotherapy. Several

chemotherapeutic drugs thought to affect DNA metabolism in fact inhibit rRNA biogenesis and processing. 36 conventional chemotherapeutic drugs were found to affect rRNA transcription and early or late rRNA maturation (Burger et al., 2010) at the therapeutically effective concentrations. Thus, the inhibition of pre-rRNA processing by these drugs could, albeit in part, play a role in efficacy against cancer cells.

In conclusion, both RNA processing pathways (pre-mRNA splicing and pre-rRNA processing) are important targets for therapeutic intervention in cancer. We have identified the oncogenic Pim Kinases as regulators of these processes in AML cells. The next chapters will discuss our findings in detail.

Chapter 2: Substrate-guided identification of novel Pim kinase functions reveals potential therapeutic combinations for AML

Contributions to the work

Dr. Xiang Li identified novel Pim2 substrates and validated a few using RIKA as described in Figure 2.6. Azim Raja contributed in the standardization of MTT assay protocol and performed experiments described in Figure 2.13c. All other experiments were performed by Tejashree Anant Joglekar.

Abstract

Kinase inhibition has emerged as a major strategy for targeted oncology therapy. Following the success of imatinib mesylate in chronic myelogenous leukemia (CML), intense scientific investigation has focused on identifying novel kinase inhibitors for cancer therapy. However, most targeted oncology therapies, including kinase inhibitors, fail at the clinical trial stage. To avoid this expensive and inefficient outcome, protein kinase inhibitors have to be vetted at two levels: 1) evidence should be provided for kinase pathway modulation leading to effectiveness against cancer models, and an effect on pharmacodynamic biomarkers in the cancer models should be demonstrated; 2) combinatorial therapies should be identified to combat inhibitor resistance. Regrettably, our current knowledge of kinase-substrate profiles is limited, which inhibits fulfillment of both criteria. To resolve this

issue, our lab has developed new approaches that utilize high-resolution mass spectrometry (MS) to allow rapid and comprehensive kinase- substrate profiling. Using PIM kinases in acute myeloid leukemia (AML) as a model, we demonstrate that broad knowledge of kinase substrates can guide identification of cellular pathways regulated by the kinase and provide proof of pathway-modulation in response to kinase inhibition. We successfully test a rational approach to select mechanism-based drug combinations with kinase inhibitors, which result in synergy against cancer cells. We demonstrate that Pim kinases regulate pre-mRNA splicing and pre-rRNA processing in AML cell lines. Pim inhibitors induce wide-spread modulation of these processes specifically in inhibitor-sensitive AML cell lines. The lack of modulation in inhibitor-resistant cells demonstrates the specificity of these effects to Pim activity.

Introduction

2.1 Acute myeloid leukemia

The term ‘acute myeloid leukemia’ covers a group of hematopoietic malignancies characterized by the unchecked growth of immature myeloid blast cells. In the bone marrow, multipotent stem cells give rise to all the cells of hematopoietic lineage. These cells can differentiate into myeloid stem cells (myeloid blasts) or lymphoid stem cells (lymphoid blasts). During normal hematopoiesis, myeloid blasts can differentiate into erythrocytes (red blood cells), monocytes, megakaryocytes or granulocytes, and lymphoblastic blasts

give rise to B or T lymphocytes. In AML, however, the myeloid blast cells fail to differentiate, are arrested in an immature state, divide rapidly and 'crowd out' the other healthy blood cells. This leads to a decrease in the count of RBCs (anemia) resulting in fatigue, reduction of platelet count (thrombocytopenia) resulting in bleeding or reduction in the number of neutrophils (neutropenia) resulting in infections (Lowenberg et al., 1999). This condition is termed 'acute' because the leukemic cells grow very quickly and the disease progresses very rapidly if left untreated. AML blast cells develop in bone marrow and eventually also enter the bloodstream increasing the white blood count of AML cells. Under a microscope, AML blasts appear to be much larger than other blood cells and have a large nucleus surrounded by a thin layer of cytoplasm (Figure 2.1a (Lowenberg et al., 1999)). A differentiating feature for AML is the exclusive presence of an enzyme called myeloperoxidase. This enzyme is also present as a crystalized aggregate structure termed an Auer rod (Figure 2.1b (Lowenberg et al., 1999)).

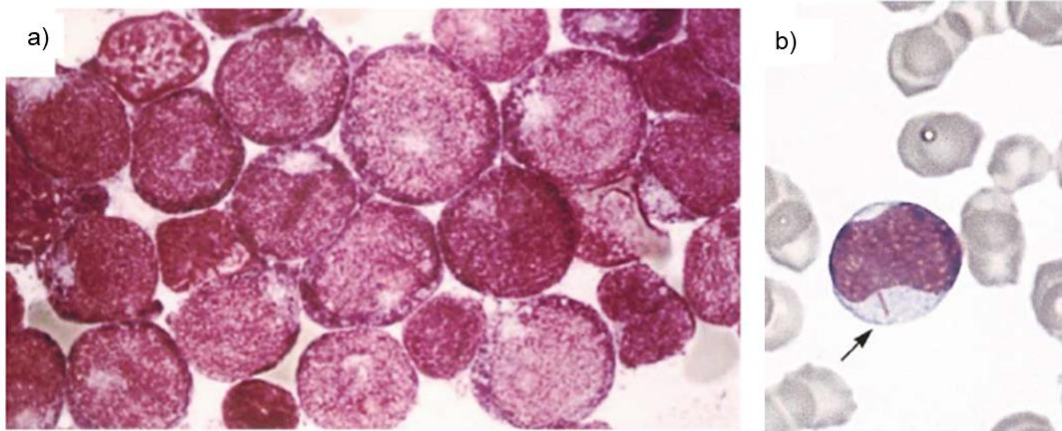


Figure 2.1 Microscopic images of acute myeloid leukemia blast cells. (This figure is from (Lowenberg et al., 1999). a) Acute myeloid leukemia blasts stained with May-Grünwald and Giemsa. b) AML blast cell stained with May-Grünwald and Giemsa. The arrow points to an Auer rod.

The American Cancer Society estimates that ~21,380 new cases of AML will be diagnosed in 2017, most of which will be adults over the age of 45. Although AML mostly afflicts older adults, acute leukemia (AML and ALL) are the most common cancers in children with the highest incidence in infants younger than 1 year. Based on the FAB (French- American-British) system, AML is classified into various subtypes from M0 to M7 depending on the type of the cells that AML develops. Patients with myelodysplastic syndrome (MDS) and Down syndrome (trisomy at chromosome 21) are at a higher risk of developing AML (Lowenberg et al., 1999). Secondary AML cases, which are caused by the progression of these complications, are classified in distinct categories. For example, AML in patients with MDS is referred to as MDS/AML. Roughly 30% of high-risk MDS cases progress to AML, and have been linked to a worse prognosis (Shukron et al., 2012; Wang et al., 2011b). Thus, it is important to classify the various subtypes of this disease.

Various features of AML have been used to predict the outcome of cancer treatment. Karyotype is considered as an important prognostic determinant. The world health organization classifies AML based on genetic alterations. A multivariate analysis showed that karyotype had the biggest prognostic value for the patient outcome (Grimwade and Hills, 2009). Notably,

patients suffering from the AML subtype termed acute promyelocytic leukemia (APL) have a translocation between chromosome 15 and 17 and have a better prognosis (Grimwade and Hills, 2009). Although these recurrent abnormalities have been identified for AML diagnosis and prognosis, about 50% of AML patients have a normal karyotype (Welch et al., 2012).

In recent years, recurrent genetic mutations observed in AML patients with a normal karyotype have been used as prognostic markers. AML blasts show recurrent mutations in various genes including NPM1, FLT3, c-KIT, CEBPA, WT1, and IDH1. Nucleophosmin (NPM1) is frequently mutated in primary AML patients and in about 50% of patients with a normal karyotype (Rau and Brown, 2009). Mutations are observed in the C-terminal domain of this nucleolar protein causing it to accumulate in the cytoplasm (Falini et al., 2005). However, NPM1 is associated with a better outcome in patients. Mutations in NPM1 frequently occurred with mutations in fms-like kinase 3 (FLT3) gene, suggesting a likely cooperation (Falini et al., 2005). A third of all AML patients have mutations in the FLT3 gene. The most common FLT3 mutations are caused by a duplication within the juxta-membrane domain of FLT3 known as FLT-ITD (internal tandem duplication) and to a lesser extent due to point mutations in the active site of the kinase. Mutations in tyrosine kinase FLT3 are linked to a worse prognosis and associate with higher initial blast counts. Age and initial blast counts are also independent prognostic markers (Röllig et al., 2011). Younger patients usually have a better

prognosis. Patients with primary disease (de novo AML) have a better outcome compared to secondary AML arising from a pre-existing condition like Myelodysplastic syndrome (MDS) (Sztokowski et al.).

2.1.1 Therapeutic regimen for AML: The choice of therapeutic regimen depends on individual prognosis

The following constitute the frontline treatment for patients: 1) Induction chemotherapy: The standard of care treatment for patients <60 years of age begins with treatment using Cytarabine and the anthracycline antibiotic daunorubicin. Complete remission (CR) is the desired outcome. In patients older than 60 years, a lower dose chemotherapy may be given to avoid treatment-related morbidity (Tallman et al., 2005). However, higher dose chemotherapy can be helpful in achieving CR in some older patients. Alternate chemotherapeutics are also used in place of Cytarabine.

2) Consolidation therapy: At this stage of therapy, high doses of chemotherapeutics are administered in rounds after the initial CR is achieved. Consolidation therapy was found to be especially helpful in younger adults (Bennett et al., 1997).

3) Hematopoietic stem cell therapy (HSCT): As a post-remission therapy, patients can also be given a round of very high dose of chemotherapy, with an injection of their own (autologous) or human leukocyte antigen-matched (allogenic) healthy hematopoietic stem cells. Patients treated with HSCT have shown better disease-free survival rates, but have a higher risk of treatment-related morbidity.

Recently, molecular targeted therapeutics have been approved and are being administered with the standard of care chemotherapy in selected patients. The most recent additions to approved AML therapeutics are FLT3-ITD inhibitor Midostaurin (April 2017) for patients with FLT3 mutations and isocitrate dehydrogenase (IDH2) inhibitor 'Idhifa' for AML patients with IDH2 mutations (August 2017). In Phase IIB clinical trial, Midostaurin induced over 50% blast reduction in 71% patients with FLT3 mutations (Fischer et al., 2010). Although these findings led to an approval for this drug for AML treatment, these results also show that 29% patients have an inherent resistance to these inhibitors. A recommendation to combine chemotherapeutics and other targeted agents was made, based on these results. Thus, new targets and combinations are needed for treatment of AML.

2.1.2 New therapeutic vulnerabilities of AML based on genetic mutations and over-expression

Complete remission (CR) is observed in almost 60-90% of patients younger than 60 years (Khwaja et al., 2016). Although some patients achieve long-term disease-free survival, relapse of a more aggressive disease is common (Verma et al., 2010). The effectiveness of standard therapy is much lower in older patients. Moreover, high chemotherapy regimens cannot be tolerated by older patients or weaker patients due to associated toxicities.

HSCT is also associated with risk of developing complications and can be fatal. Even for patients who show CR, the chemotherapy regimen comes with adverse side effects that have to be treated separately. Thus, improved therapeutics are needed to increase disease-free survival and improve patient quality of life.

Cooperation of at least two genetic mutations has been shown to be required for the development of AML in mouse models (Grisolano et al., 2003; Schessl et al., 2005). Various mutations are frequently observed in AML patients. Therefore, it is likely that several mutations may be involved in the pathogenesis of AML in humans. Similarly, treatment of AML may require inhibition of more than one deregulated cellular pathway. Based on recent discoveries, frequent genetic mutations in the spliceosome machinery, oncogenic signaling pathways and nucleophosmin (ribosome biogenesis pathway) among others, have been identified in AML subtypes. Therefore, targeting the deregulated functions of these pathways is a viable strategy for putative AML treatment.

The mRNA splicing machinery genes (U2AF35, SRSF2, ZRSR2, and SF3B1) were found mutated at high frequencies (45-85%) in diseases with myelodysplastic features. Approximately 84.9% cases of MDS and 25.8% cases of AML with features like myelodysplasia showed a presence of splicing factor mutations. Interestingly, de novo AML samples had these

mutations at much lower frequency (6.6%). Splicing factor mutations were initially linked to AML and MDS, but have since been detected in other cancers as well. Mutations in splicing factor SF3B1 were identified at a high frequency (15%) in chronic lymphocytic leukemia and cells with these mutations increased over time after chemotherapy (Landau et al., 2013; Wang et al., 2011a; Yoshida and Ogawa, 2014). Thus, these mutations can be drivers for drug resistance. SF3B1 mutations were also found in uveal melanoma (22 out of 105) patients (Harbour et al., 2013), and identified as frequently mutated in breast cancers (Koboldt et al., 2012) and pancreatic cancers (Biankin et al., 2012). Thus, spliceosome deregulation appears to be a general theme in many cancers and is a potential target for therapy. Novel SF3B1 inhibitors have been tested against AML have shown promise as a putative therapeutic (Crews et al., 2013). A study looked at genome-wide splicing in over 200 AML patient samples and found about a third of the expressed genes were differentially spliced in cancer patients versus healthy donors (Adamia et al., 2014). This study also showed that certain aberrant splice variants were only associated with a cancer phenotype (observed during diagnosis and relapse) and were absent in patient cells during remission (Adamia et al., 2014). Inhibitors of the spliceosome were identified from bacteria, and more effective inhibitors were later synthesized, based on the natural macrolides found in bacteria (Yokoi et al., 2011). These inhibitors have shown promise for prevention of relapse in AML patients (Crews et al., 2016).

Another feature of AML was identified as the frequent mutation of NPM1 in > 50% of patients with a normal karyotype (Rau and Brown, 2009). The nucleolar protein NPM1 is a multifunctional protein, that mainly regulates various aspects of ribosome biogenesis in the cell. Ribosome biogenesis and ribosome function have been identified as major targets in the treatment of cancers (Hein et al., 2017; Peltonen et al., 2014b). Thus, the deregulation of ribosomal function due to NPM1 mutations could be driving the AML pathogenesis. Heterozygous knockout (NPM1^{+/-}) mice developed disease with MDS-like characteristics. Animals with haploinsufficiency further develop hematopoietic malignancies, mainly of myeloid type (Sportoletti et al., 2008). Thus, deregulation of NPM1 function through loss or mutation leads to the development of AML. Therefore, targeting ribosome biogenesis or other pathways regulated by NPM1 can be a way to treat AML with NPM1 mutations. Indeed, an RNA Pol-I inhibitor CX-5461 was able to target the leukemia-initiating cell populations, in transgenic and patient-derived xenograft (PDX) models of AML, and these models showed better anti-tumor response with CX-5461 than conventional chemotherapy (Hein et al., 2017).

Multiple kinase signaling pathways are deregulated in AML cells, and several kinase genes, for example, FLT3 and c-Kit, are frequently mutated in AML patients. Apart from the approved FLT3 inhibitors, other kinase inhibitors that have shown promise against AML include Pim kinase inhibitors, Polo-like

kinases (Plk) inhibitors, and phospho inositol 3 kinase (PI3K) inhibitors. These inhibitors are being tested against AML in both preclinical and clinical studies.

Pim kinases are being tested as a therapeutic target for many cancers. Acute myeloid leukemia is one of these cancers, where Pim kinase inhibition shows promise to be a successful therapy. Pim kinases are frequently upregulated in AML patients and cell lines (Chen et al., 2011; Garcia et al., 2014; Meja et al., 2014). As Pim kinases play a role in normal hematopoiesis, it is conceivable that their deregulation could have a role in driving AML pathogenesis (Mikkers et al., 2004). Inhibitors of Pim kinases have shown promise against AML *in vivo* and *in vitro*. However, a clinical trial with Pim inhibitor AZD1208, showed an underwhelming response in AML patients, most likely due to inherent inhibitor resistance (Cortes et al., 2016). Thus, monotherapy with Pim inhibitors may be not as successful as previously anticipated. One way to approach this challenge is by combining other inhibitors to potentiate the effects of Pim inhibitors. Another important approach is identifying the patients who will benefit from using Pim inhibitors using pharmacodynamic biomarkers. Both the approaches mentioned above will benefit from knowing the complete Pim kinase substrate profile, which is currently lacking. Thus, the various functions played by Pim kinases (and other kinases) in cancer cells are still largely unknown. Kinase-substrate discovery platforms can be helpful in profiling Pim kinase substrates and

provide the basic functional information to design more effective ways to target Pim kinases in AML.

To that end, research in our lab has led to the invention of a kinase substrate discovery platform, which has been modified to address questions regarding biological functions of various kinases (Li et al., 2007, 2016). The next section will provide a review of the kinase substrate identification techniques including those developed in our lab.

2.1.3 Kinase-substrate identification platforms

Since the discovery of the first protein kinase, much research has focused on uncovering the kinase-substrate relationships. The last few decades have seen tremendous improvement in technologies for identification of phospho-proteins and detection of phosphorylation sites from complex biological extracts (Delom and Chevet, 2006; Lin et al., 2010a). Application of mass spectroscopy (MS) to biological analysis and efficient enrichment strategies for phospho-peptides have generated high throughput data for phosphorylation events in cells (Collins et al., 2007; Wilhelm et al., 2014). However, identification of the physiological upstream kinase responsible for substrate phosphorylation remains a challenge.

Most kinase substrates are identified by a candidate approach by *in vitro* kinase assays. But this approach is limited by the requirement for

purified recombinant proteins. One method for profiling of substrates from cell lysates is termed Kinase Substrate Tracking and Elucidation (KESTREL) (Cohen and Knebel, 2006). In this approach, cell lysates were incubated with recombinant kinase and $\gamma^{32}\text{P}$ -ATP. The labeled phospho-proteins were separated by gel electrophoresis and then identified by mass spectroscopy. However, this method is limited by high background and inefficiency of application for all kinases (Cohen and Knebel, 2006). Use of ATP analogs, coupled with genetically modified kinases that use these analogs in cultured cells, and detection of substrates carrying the phospho-analog can provide valuable information about the direct *in vivo* targets of kinases (Blethrow et al., 2008; Shah et al., 1997). The major challenge is that cells are impermeable to these ATP analogs and a very high concentration of cellular ATP makes it difficult to identify rare substrates. *In silico* analysis for identifying kinase-specific motifs to identify substrates is another approach for identifying direct upstream kinases (Lin et al., 2010a). This approach is complicated by the degeneracy and short length of kinase consensus sequences and multiple kinases in a family targeting similar sequences (Lin et al., 2010a).

A kinase substrate profiling technique developed in our lab addresses some of these existing problems and identifies direct substrates of kinases with high efficiency and a low false positive rate (Li et al., 2007). Use of radioisotope labeling and fractionated cellular extracts makes this method highly sensitive for identification of substrate in the picomolar range. This

method reverses the role of a kinase and its substrate, as seen in a traditional in-gel kinase reaction, and therefore, it is named as Reverse In-gel Kinase Assay (RIKA). In RIKA, the kinase is copolymerized in the SDS-PAGE gel, while the substrate proteins are separated first by isoelectric point (pI) and then by size on denaturing gels containing the polymerized kinase. The substrates and kinases are refolded to regain catalytic conformation followed

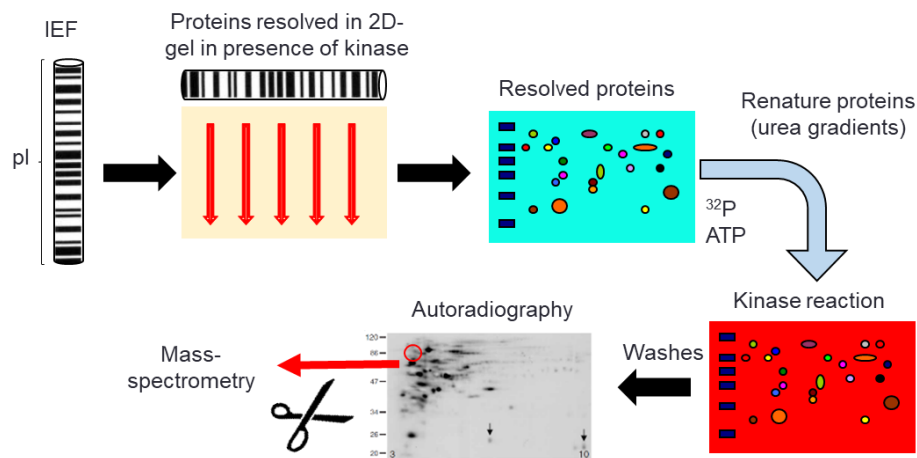


Figure 2.2 Schematic representation of 2D reverse in-gel kinase assay. The kinase is polymerized in denaturing gel. The proteins are separated by two-dimensional gel electrophoresis. The kinase and the separated proteins are refolded in the gel using a series of urea gradients. The kinase and separated proteins are incubated in radioactive gamma ^{32}P -ATP. This step labels the substrates for the kinase. Excess phosphate is washed away by multiple washes and gels are visualized by autoradiography (autoradiographic image from: (Li et al., 2007).

by an in-gel kinase reaction in presence of $\gamma^{32}\text{P}$ -ATP (Figure 2.2). The phosphorylated substrates can be visualized by autoradiography and identified by MS. This method has vast applications and subsequent modification of this technology has diversified its applications (Li et al., 2016).

It is important to note that only the unphosphorylated portion of any protein substrate gets phosphorylated and labeled in RIKA (Figure 2.3).

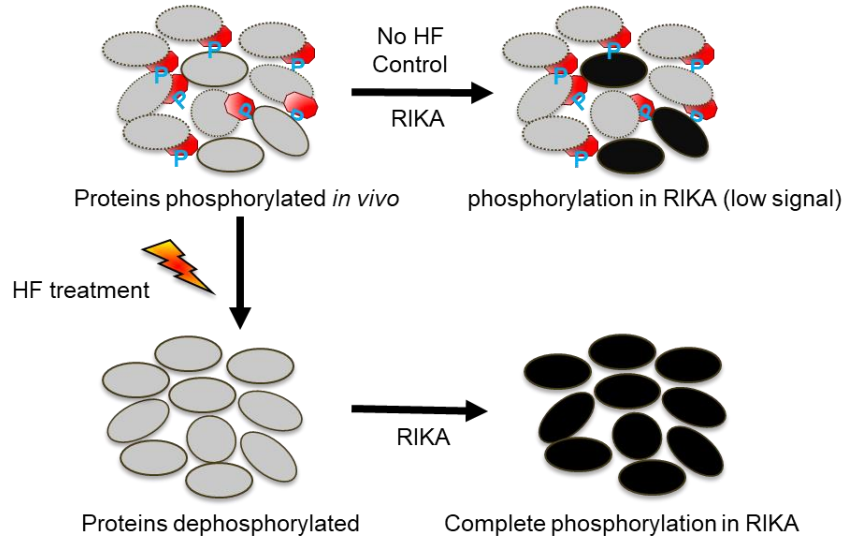


Figure 2.3 Schematic representation of phosphorylation in RIKA. RIKA detects the non-phosphorylated portion of the pool of substrates. A fraction of total proteins for any given substrate are phosphorylated *in vivo*. Thus, these molecules cannot be labelled in RIKA. Dephosphorylation by hydrogen fluoride (HF) treatment prior to RIKA removes the *in vivo* phosphorylation on substrates, and allows the kinase in gel to phosphorylate these proteins resulting in an increased signal intensity in RIKA.

Therefore, the signal in RIKA is inversely proportional to the phosphorylation stoichiometry of the substrate. This characteristic of the method was utilized in the next stage of development, to ask different biological questions. In addition to substrate identification, RIKA was diversified to study phosphorylation stoichiometry by the use of stable isotope labeled O^{18} -ATP instead of $\gamma^{32}P$ -ATP (Li et al., 2016). Using this technique, it is possible to distinguish between the fraction of proteins phosphorylated *in*

vivo and *in vitro*. The O^{16}/O^{18} ratio provides insights into the phosphorylation stoichiometry of a substrate (Figure 2.4 (Li et al., 2016)).

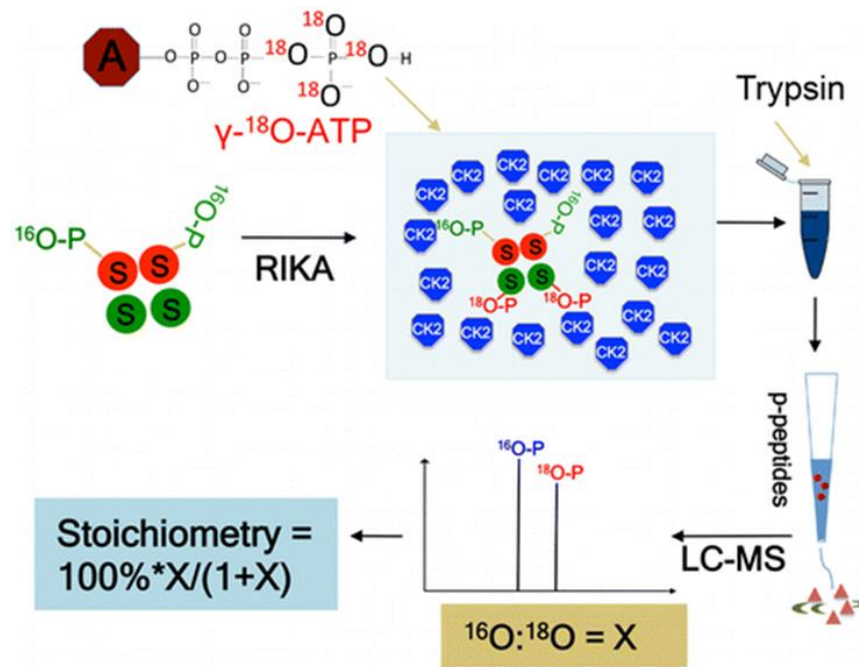


Figure 2.4 RIKA with stable isotope labeling (from (Li et al., 2016)). The RIKA technology was modified to incorporate use of stable isotope labeling using $^{18}\text{O}\text{-ATP}$. The schematic depicts a portion of substrate proteins phosphorylated inside the cells with ^{16}O -phosphate groups. Using RIKA, the non-phosphorylated portion of proteins is phosphorylated by heavy isotope ^{18}O -phosphate. Proteins are then fragmented into peptides by trypsin digestion followed by phospho-peptide enrichment using affinity chromatography. MS analysis for phospho-peptides is employed to obtain the $^{16}\text{O}:^{18}\text{O}$ ratio. Phosphorylation stoichiometry for substrates is calculated using this ratio.

Theoretically speaking, a substrate that is 100 percent phosphorylated *in vivo* will not be visualized through traditional RIKA (Figure 2.3). Since RIKA cannot ‘see’ substrates phosphorylated to completion, a dephosphorylation step was introduced prior to substrate profiling. An extremely efficient method

of dephosphorylation using hydrogen fluoride (HF) was applied to the RIKA technology by Dr. Xiang Li. Upon hydrogen fluoride treatment, proteins are dephosphorylated and deglycosylated (Greenberg et al., 1992). Through dephosphorylation, the substrates of the kinase that are hyperphosphorylated *in vivo* are revealed. Radioactive isotope labeling is no longer required, as the all the phosphorylation events detected by MS are a product of *in vitro* kinase reaction. Application of improved MS analysis has made RIKA a high throughput assay. Instead of analyzing each substrate from 2D-SDS PAGE, proteins can be resolved by 1D-SDS PAGE and the entire gel is cut into horizontal bands of about 1 cm and processed to extract peptides by trypsin digestion in the gel. The next step is phospho-peptide enrichment followed by mass-spectroscopy (Figure 2.5).

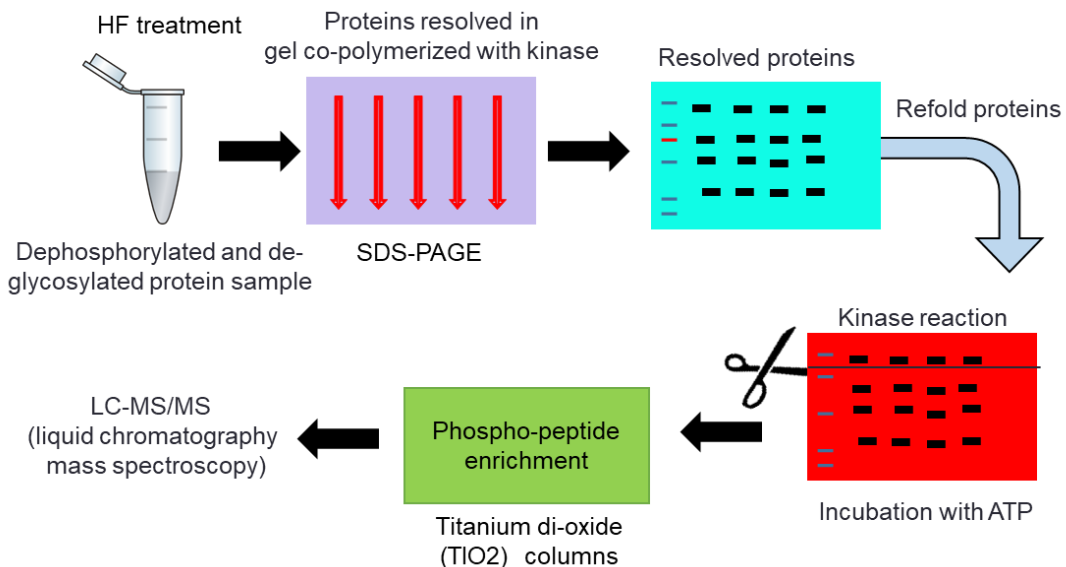


Figure 2.5 Schematic representation of modified Reverse in gel kinase assay (RIKA) following protein dephosphorylation with HF treatment. The kinase is polymerized in denaturing gel. The proteins are separated by SDS-PAGE. The kinase and separated proteins are refolded in the gel using a series of urea gradients. The kinase and separated proteins are incubated in non-radioactive ATP. This step phosphorylates the substrates by the kinase. In the next step, excess phosphate is washed away by multiple washes. The gel is cut into approximately 1cm bands and processed for trypsin digestion. Peptides are purified from gel and may be enriched for phospho-peptides using TiO₂ columns or other enrichment columns. This step is followed by substrate identification using high resolution mass spectroscopy.

Using this high-throughput RIKA analysis for identification of Pim kinase substrates, Dr. Xiang Li has identified over 570 substrates. In an attempt to decipher various functions of Pim kinases, we used the knowledge of novel substrates to identify pathways regulated by Pim kinases. Interestingly, a large number of Pim substrates were found to be proteins involved in RNA processing. We investigated the effect of Pim inhibition and identified a widespread regulation of pre-mRNA splicing and pre-rRNA processing by Pim kinases. Taking this substrate-guided approach, we rationalized co-targeting therapies and identified new synergistic drug combinations against AML.

2.2 Results

The aim of this study was to identify novel Pim kinase substrates to expand the knowledge about functions of these kinases. Using the reverse in-gel kinase assay (RIKA), Dr. Xiang Li has identified over 570 Pim kinase substrates. On further analysis we recognized that a majority of these substrates were RNA processing proteins including splicing factors, ribosomal

proteins, and rRNA processing factors. Figure 2.6a shows a schematic representation of the major subsets of proteins identified as putative Pim substrates. Several of these proteins were also validated by *in vitro* kinase assay of recombinant proteins (Xiang Li, unpublished data, Figure 2.6b,c). As multiple proteins belonging to each pathway seem to be under Pim regulation, we decided to use pan-Pim kinase inhibitor AZD1208 to validate the Pim activity-dependent effects on modulations of these RNA processing pathways.

Primary samples from AML patients and cell lines show upregulation of all the three Pim kinases to varying degrees (Meja et al., 2014). Sensitivity to Pim inhibition is also variable in AML cell lines, ranging from acute sensitivity to inherent resistance (Brunen et al., 2016; Tron et al., 2016). For this study, we used Pim inhibitor sensitive cell lines- MOLM-16 (AML M0) and EOL-1 (Eosinophilic AML) (Keeton et al., 2014). Sensitivity was defined by the effect on proliferation in presence of inhibitor AZD1208 (Keeton et al., 2014). As a negative control, we chose OCI-M1 (AML M6), known to be resistant to Pim kinase inhibition.

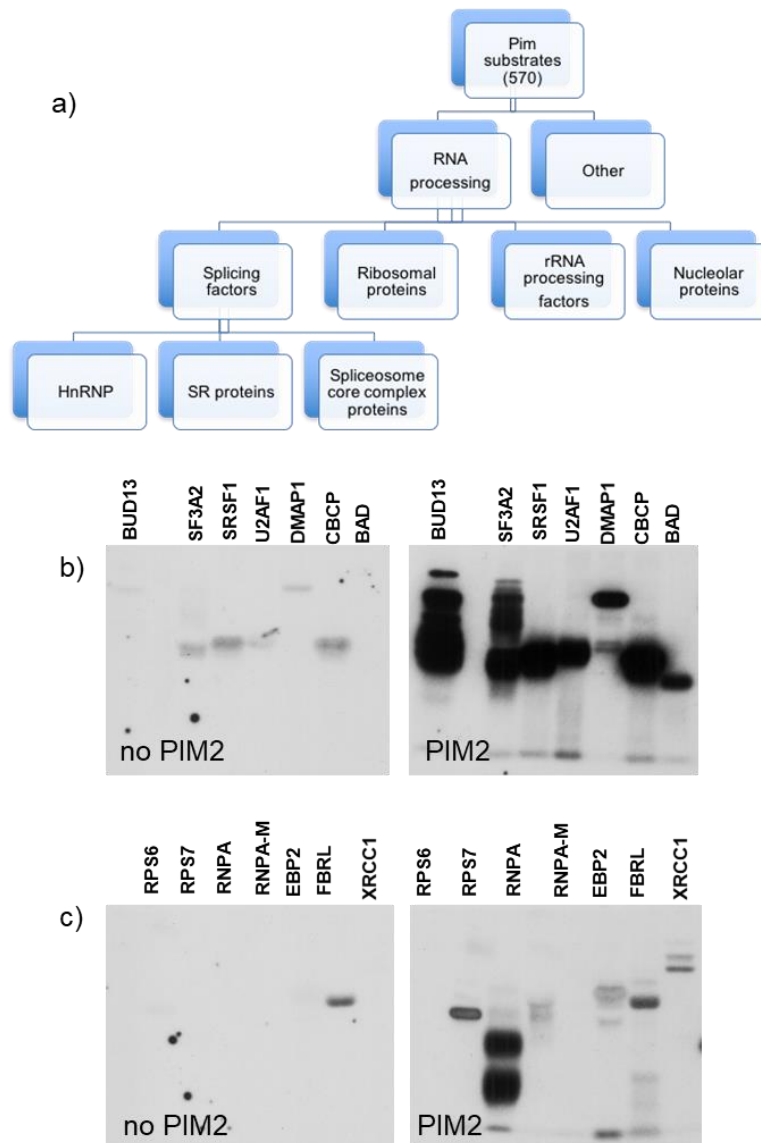


Figure 2.6 Putative Pim kinase substrates identified by RIKA. a) Schematic representation for various types of proteins identified as putative Pim substrates. Numerous proteins involved in RNA processing were observed in these substrate profiles including several splicing factors and rRNA processing factors. b,c) *In vitro* validation of Pim kinase substrates identified in HF-RIKA. BAD was used as a positive control substrate. b) Splicing factors validated as Pim2 substrates. The autoradiograph on left shows gel without Pim2 and on the right gel with Pim2. Purified recombinant proteins expressed from *E.coli* were loaded in each lane as denoted. c) Ribosomal proteins validated as Pim2 substrates. The autoradiograph on left shows gel without Pim2 and on right gel with Pim2 (Xiang Li, unpublished data).

2.2.1 Pim kinases regulate mRNA splicing in AML cells

To determine whether Pim kinases regulate alternative mRNA splicing, we tested the effect of Pim inhibition on global alternative splicing in AML cells lines. Based on the identification of over 28 splicing factors as Pim substrates in RIKA, we hypothesized that the inhibition of Pim activity would induce a change in splicing pattern of the genes regulated by these splicing factors. Thus, to validate regulation of mRNA splicing as a function of Pim kinases, we employed microarray analysis using Affymetrix array HTA 2.0 to identify global changes in alternative splicing. Figure 2.7 provides a schematic representation of the experimental strategy used for performing the analysis.

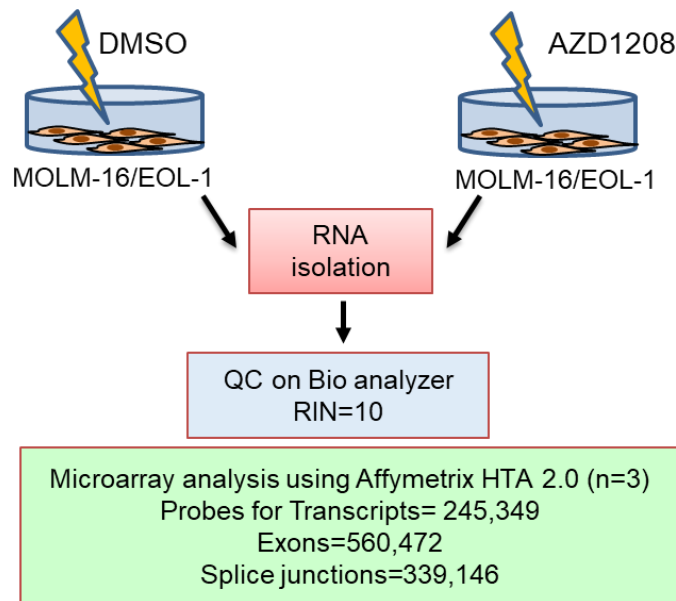


Figure 2.7 Schematic flowchart for microarray analysis for alternative splicing changes. Cells were treated with either DMSO or AZD1208 (1 μ M) for 6 hours. Total RNA was isolated from treated cells. RNA was treated with DNase 1 to remove gDNA contamination. RNA quality was analyzed using Bio-analyzer. HTA 2.0 array was used to quantify changes in alternative splicing after AZD1208 treatment of MOLM-16 and EOL-1 cells (n=3).

The transcriptome analysis console (TAC) software was used to identify the changes in splicing and calculate the splicing indices. HTA 2.0 array contains probes for 560,472 exons and 339,146 splice junctions. Probes within an exon (or part of a long exon) or the exon-exon junction are grouped together to generate a probe selection region (PSR). Normalized signal intensities are calculated for each PSR. Due to the presence of junction probes, the use of this microarray allows for quantification of the difference in inclusion and exclusion of exons. The magnitude of change in splicing is measured in terms of splicing index. A negative splicing index signifies decrease of relative exon intensity in a given condition or higher exon skipping, and a positive splicing index signifies an increase in relative exon intensity or higher exon inclusion. Thus, splicing index is calculated as the fraction of normalized signal estimates for condition 1 over the normalized signal estimates for condition 2. To calculate the normalized signal intensities in each condition, the exon level intensity is divided by gene level intensity. The TAC software was used to perform these calculations.

To test the effect of Pim inhibitor AZD1208, we used Pim inhibitor responsive MOLM-16 cells and EOL-1 cells. AZD1208 treatment induced transcriptome-wide splicing changes in MOLM-16 and EOL-1 cells. Upon AZD1208 treatment, MOLM-16 cells and EOL-1 cells showed >10000 exon level splicing changes in >5000 genes. On further analysis of these changes, we identified that >2400 splicing changes were common in the data sets for

both cell lines. Moreover, not only were most of these splicing changes in the same regions of mRNAs (identified by the unique PSR), they also exerted a similar effect on exon inclusion or exclusion among the two cell lines (denoted by the similar sign of splicing indices for the PSR in each cell line). Figure 2.8a shows the graphical representation of our findings. Each point on the graph corresponds to a single PSR region, and the X coordinate denotes the splicing index from EOL-1 cells, while the Y coordinate denotes the splicing index from MOLM-16 cells. The sign (+ or -) is also depicted using 4 quadrants. Thus, as observed in Figure 2.8a, most PSRs are positioned in the $-X -Y$ quadrant or the $+X+Y$ quadrants. Less than 40 PSRs showed splicing indices that had opposite signs between the two cell lines. (in $-X +Y$ or $+X -Y$ quadrants). Thus, in conclusion, we observed consistent and reproducible splicing changes after Pim inhibition in AML cell lines.

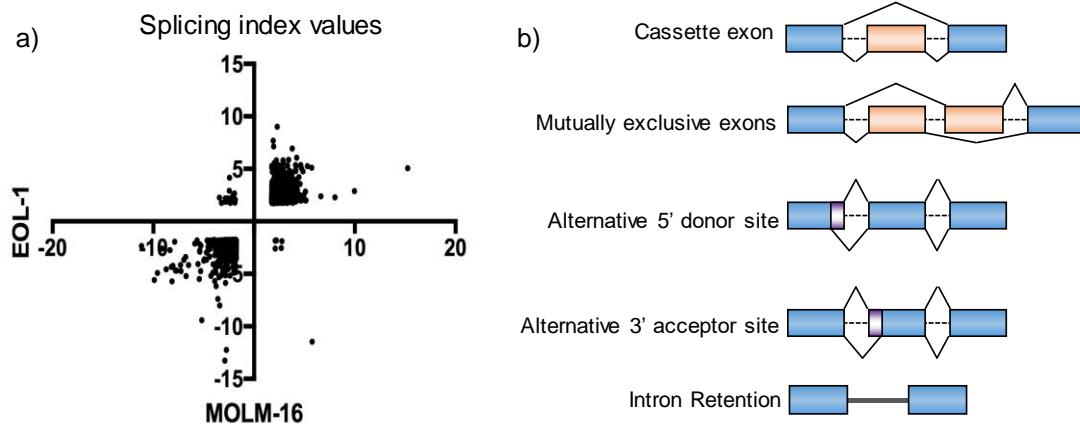


Figure 2.8 Graphical representation of microarray data for AML cell lines. a) Pim kinase inhibition by AZD1208 induces widespread changes in mRNA splicing. Splicing indices calculated from HTA2.0 microarray after 1 μ M AZD1208 treatment of MOLM-16 and EOL-1 cells for 6 hours were compared to identify >2400 common changes. b) Schematic representation of types of

alternative splicing events observed in MOLM-16 and EOL-1 cells treated AZD1208 (figure 2.8b adapted from (Wang et al., 2008))

TAC software analysis also provided insights into the type of alternative splicing events (ASEs) occurring in these cells. There are five categories of ASEs (Figure 2.8b) (Keren et al., 2010). The cassette exons are alternative exons that can be present in one isoform but absent from other isoforms (this type of ASE is also known as exon skipping). When two exons are never found in the same isoform, it leads to the second type of ASE termed mutually exclusive exons. The third and fourth type of splicing events involve the use of alternate 5' or 3' exon end known as alternative 5' acceptor site and alternative 3' donor site, respectively. The fifth type of ASE is known as intron retention, in which a portion of the intron is retained in the final mRNA transcript. The TAC software predicted the ASE category for a portion of the events that we observed. Table 2.1 shows the number of ASEs from each category observed in both the AML cell lines.

To validate AZD1208-induced splicing changes using an independent method, we performed RT-PCR analyses. We chose several targets from the microarray data whose splicing was affected by Pim inhibition. The selection was done by manual curation of data from TAC analysis, followed by searching the NCBI reference sequence database for availability of sequence information. Initially, we validated the changes in splice variants of a known apoptotic regulator, MCL1. The shorter isoform of MCL1 is pro-apoptotic

(MCL1-s), while the longer isoform has anti-apoptotic functions (MCL1-L) (Bae et al., 2000).

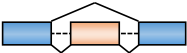
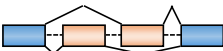
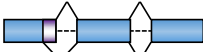
	MOLM-16		EOL-1		
	Genes	Exon rows	Genes	Exon rows	
	Cassette exons	851	1429	1098	1784
	Mutually exclusive exons	1	2	0	0
	Alternative 5' Donor	445	551	626	776
	Alternative 3' acceptor	457	560	606	759
	Intron retentions	163	251	222	365

Table 2.1 The alternative splicing events observed in AZD1208-treated MOLM-16 and EOL-1 cells belonged to the categories depicted in the table.

MCL1-s is created by exon 2 skipping, resulting in a shorter protein (Bae et al., 2000). After Pim inhibition, the MCL1-s specifically and significantly reduced as suggested by RT-qPCR using Taqman probes (Figure 2.9a,b). Although the general role of Pim kinases is anti-apoptotic, this regulation of MCL1 might act as a fail-safe mechanism against Pim over-expression. A significant regulation of MCL1 splicing was only observed in Pim sensitive MOLM-16 cells (Figure 2.9a $p < 0.001$). AZD1208 resistant OCI-M1 cells did not show any significant change in level of either splice variant (Figure 2.9c $p > 0.05$). In EOL-1 cells, the MCL1-L abundance increased while MCL1-s was reduced after Pim inhibition, albeit to a lesser extent than in MOLM-16 cells (Figure 2.9b $p < 0.001$). We also validated splicing changes in three other

targets: Glutathione-specific gamma-glutamylcyclotransferase 1 (CHAC1), Nuclear transcription factor Y subunit alpha (NFYA) and Conserved oligomeric Golgi complex subunit 5 (COG5) by RT-PCR in MOLM-16 cells and EOL-1 cells (Figure 2.9d). In all three examples, the changes measured by RT-PCR were concordant with the microarray data. As seen previously with MCL1 transcripts, OCI-M1 cells showed minimal changes in CHAC1 splicing, and no change in NFYA and COG5 transcripts (Figure 2.9d).

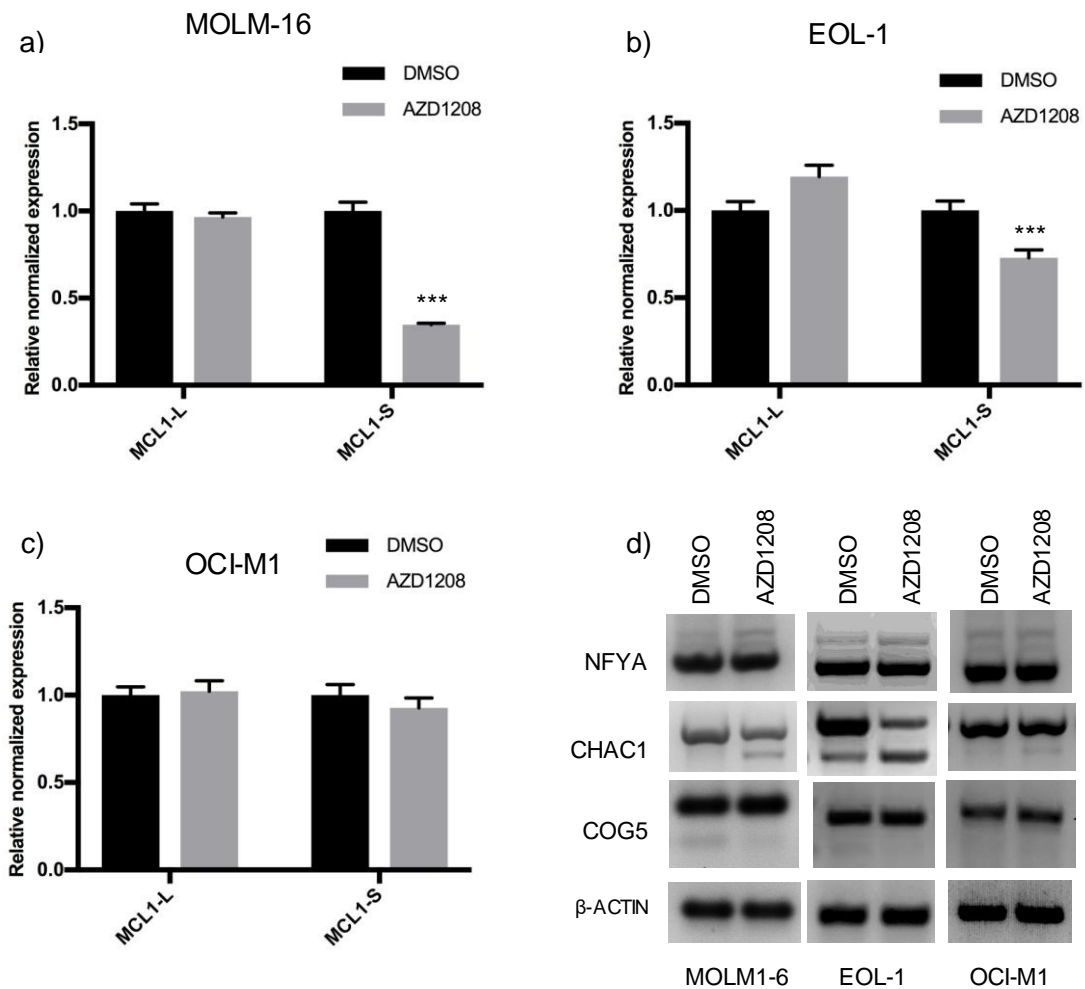


Figure 2.9 Validation of microarray results using RT-qPCR and RT-PCR analysis. a-c) AZD1208-induced splicing change observed in MCL1 splice variants was validated using Taqman probes against MCL1-L (Exon 2 included) and MCL1-S (Exon 2 skipped) in a) MOLM-16 ($p < 0.001$) and b) EOL-1 cells ($p < 0.001$), but not in c) OCI-M1 cells ($p > 0.05$) ($n = 3$). d) AZD1208-induced changes in splicing pattern of NFYA, CHAC1 and COG5 mRNAs were validated using RT-PCR ($n = 3$).

2.2.2 Pim kinase inhibition does not affect SRPK activity

Serine arginine-rich protein kinase (SRPK) 1 is a kinase known to phosphorylate SR proteins and hence regulate mRNA splicing (Colwill et al., 1996; Zhong et al., 2009). A previous study has shown that AKT regulates mRNA splicing indirectly by modulating SRPK1 activity (Zhou et al., 2012). Pim kinases and AKT have numerous shared protein substrates and regulate similar functions in the cells (Amaravadi and Thompson, 2005; Warfel and Kraft, 2015). Hence, we examined SRPK1 activity and the effect of Pim inhibition by AZD1208 on SR protein phosphorylation. The read-out was Western blotting for SR protein phosphorylation using a highly specific phospho-SR protein antibody (Zhou et al., 2012). Inhibition by AZD1208 did not induce changes in SR protein phosphorylation in MOLM-16 or EOL-1 cells, suggesting an unhindered SRPK activity (Figure 2.10a,d). To determine the consequences of SRPK1 inhibition, SRPIN340 a small molecular SRPK1 inhibitor (Fukuhara et al., 2006), was used to treat MOLM-16 and EOL-1 cells (Figure 2.10a,d). SRPIN340 treatment is known to reduce SR protein phosphorylation in cells (Fukuhara et al., 2006). Interestingly, SRPIN340 treatment reduced phosphorylation of SR proteins in EOL-1 cells, but not in

MOLM-16 cells (Figure 2.10a,d). We also tested the effects of SRPK1 inhibition by SRPIN340 on MCL1, CHAC1, NFYA and COG5 alternative splicing. SRPIN340 treatment induced splicing changes that were distinct to the splicing changes induced by Pim inhibitor AZD1208. (Figure 2.10b,e). In EOL-1 cells, SRPIN340 treatment induced reduction in SR protein phosphorylation and caused opposite changes in MCL1 transcript splicing compared to AZD1208 treatment (Figure 2.10c,f). Thus, Pim kinase activity-dependent splicing changes are not mediated by indirect SRPK1 inhibition. In MOLM-16 cells, SRPIN340 treatment caused opposite changes in CHAC1 splicing compared to AZD1208 treatment (Figure 2.10e). However, as the effect of SRPIN340 was not obvious on phospho-SR protein phosphorylation in MOLM-16 cells (Figure 2.10d), it remains unknown if the effect is mediated by loss of SRPK1 activity. In conclusion, AZD1208-induced splicing changes are not observed after SRPK1 inhibition, and AZD1208 does not induce a change in SRPK1 activity. Thus, the splicing changes observed after Pim inhibition are mediated in an SRPK1-independent fashion.

2.2.3 Pim inhibition by AZD1208 induces rRNA processing defects

Pim inhibition is known to alter protein translation by affecting phosphorylation of specific translational regulatory proteins but is not known to affect ribosome biogenesis (Yang et al., 2012). KEGG pathway analysis and GO analysis for biological processes enriched in the gene set targeted by Pim activity-dependent splicing changes pointed to ribosome biology as a major putative cellular target of Pim activity (Table 2.2 and 2.3).

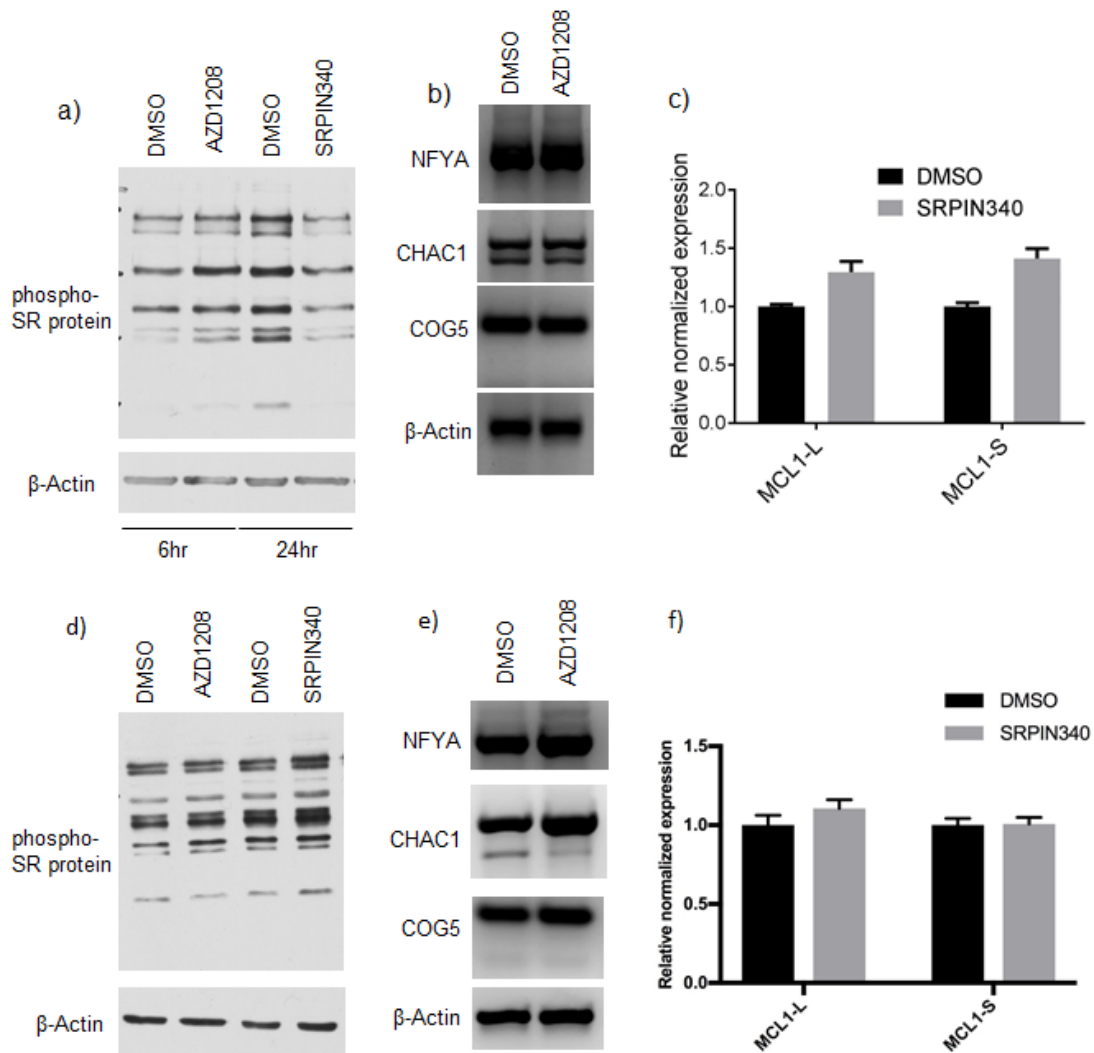


Figure 2.10 Effect of AZD1208 on SRPK1 activity. AZD1208 does not induce modulation of SRPK1 activity and AZD1208-induced splicing changes are independent of SRPK1 activity. a) Western blotting for phospho-SR protein antibody for EOL-1 cell lysates after respective treatments. b) RT-PCR analysis for Pim inhibitor splicing targets after SRPIN340 treatment (20 μ M 24 hours) in EOL-1 cells. c) qRT-PCR analysis for MCL1 splice variants after SRPIN340 treatment (20 μ M 24 hours) in EOL-1 cells (n=1) d) Western blotting for phospho-SR protein antibody for MOLM-16 cell lysates after respective treatments. e) RT-PCR analysis for Pim inhibitor splicing targets after SRPIN340 treatment (20 μ M 24 hours) in MOLM-16 cells. qRT-PCR analysis for MCL1 splice variants after SRPIN340 treatment (20 μ M 24 hours) in MOLM-16 cells (n=3) (p>0.05).

	Gene Set Name	# Genes in Gene Set (K)	# Genes in Overlap (k)	p-value
1	KEGG_RIBOSOME	88	39	4.16E-41
2	KEGG_SPLICEOSOME	128	29	2.65E-21
3	KEGG_RNA_DEGRADATION	59	13	3.73E-10
4	KEGG_PYRIMIDINE_METABOLISM	98	15	3.66E-09
5	KEGG_RNA_POLYMERASE	29	9	7.27E-09
6	KEGG_P53_SIGNALING_PATHWAY	69	12	3.05E-08
7	KEGG_PROTEASOME	48	10	7.17E-08
8	KEGG_PURINE_METABOLISM	159	17	8.46E-08
9	KEGG_AMINOACYL_TRNA_BIOSYNTHESIS	41	9	2.01E-07
10	KEGG_ANTIGEN_PROCESSING_AND_PRESENTATION	89	10	2.49E-05

Table 2.2 KEGG pathway analysis for genes targeted by AZD1208-induced splicing changes. Genes of ribosome and spliceosome pathways were enriched among genes effected by Pim dependent splicing changes.

	Gene Set Name	# Genes in Gene Set (K)	# Genes in Overlap (k)	p-value
1	GO_RNA_PROCESSING	835	163	2.60E-105
2	GO_RIBONUCLEOPROTEIN_COMPLEX_BIOGENESIS	440	123	3.28E-99
3	GO_NCRNA_METABOLIC_PROCESS	533	123	3.47E-88
4	GO_RIBOSOME_BIOGENESIS	308	100	7.96E-88
5	GO_NCRNA_PROCESSING	386	101	3.58E-78
6	GO_MRNA_METABOLIC_PROCESS	611	119	3.04E-76
7	GO_RRNA_METABOLIC_PROCESS	255	84	2.19E-74
8	GO_PEPTIDE_METABOLIC_PROCESS	571	105	1.40E-64
9	GO_AMIDE_BIOSYNTHETIC_PROCESS	507	99	1.80E-63
10	GO_CELLULAR_AMIDE_METABOLIC_PROCESS	727	114	1.99E-62

Table 2.3 Gene ontology (GO) analysis for genes targeted by AZD1208-induced splicing changes to identify enrichment of genes involved in specific biological processes. Genes involved in rRNA processing and ribosome biogenesis were enriched in these splicing targets.

Furthermore, manual curation of the list of newly identified Pim substrates revealed an abundance of ribosomal RNA processing proteins. To systematically identify the number of rRNA processing factors which are also Pim substrates, we compared the list of substrates with 286 known rRNA processing factors. These 286 factors were identified by a previous study using siRNA that targeted these factors (Tafforeau et al., 2013). We found that 25 Pim protein substrates were rRNA processing factors, which were previously shown to be required for rRNA processing. (Table 2.4) (Tafforeau et al., 2013). In addition to processing factors, depletion of ribosomal proteins is also known to affect rRNA processing (O'Donohue et al., 2010). The list of Pim substrates identified in RIKA contained both small and large subunit ribosomal proteins. These observations suggested a possible role for Pim kinases in the regulation of pre-rRNA processing.

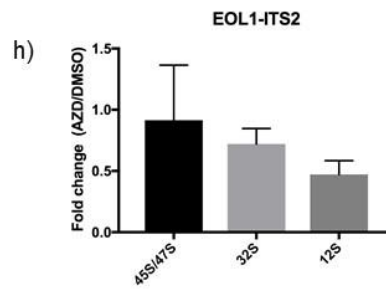
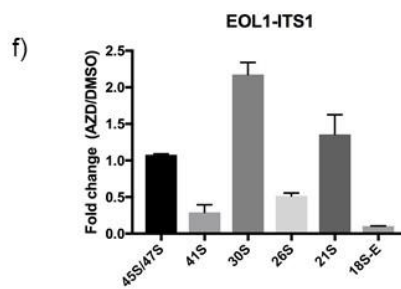
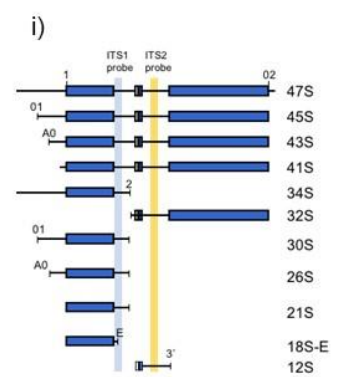
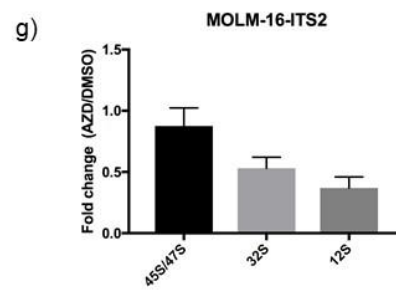
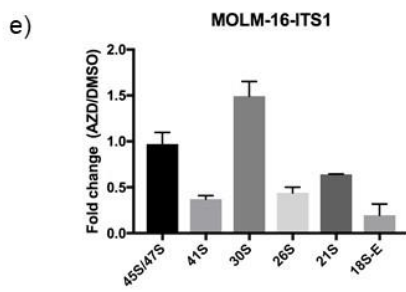
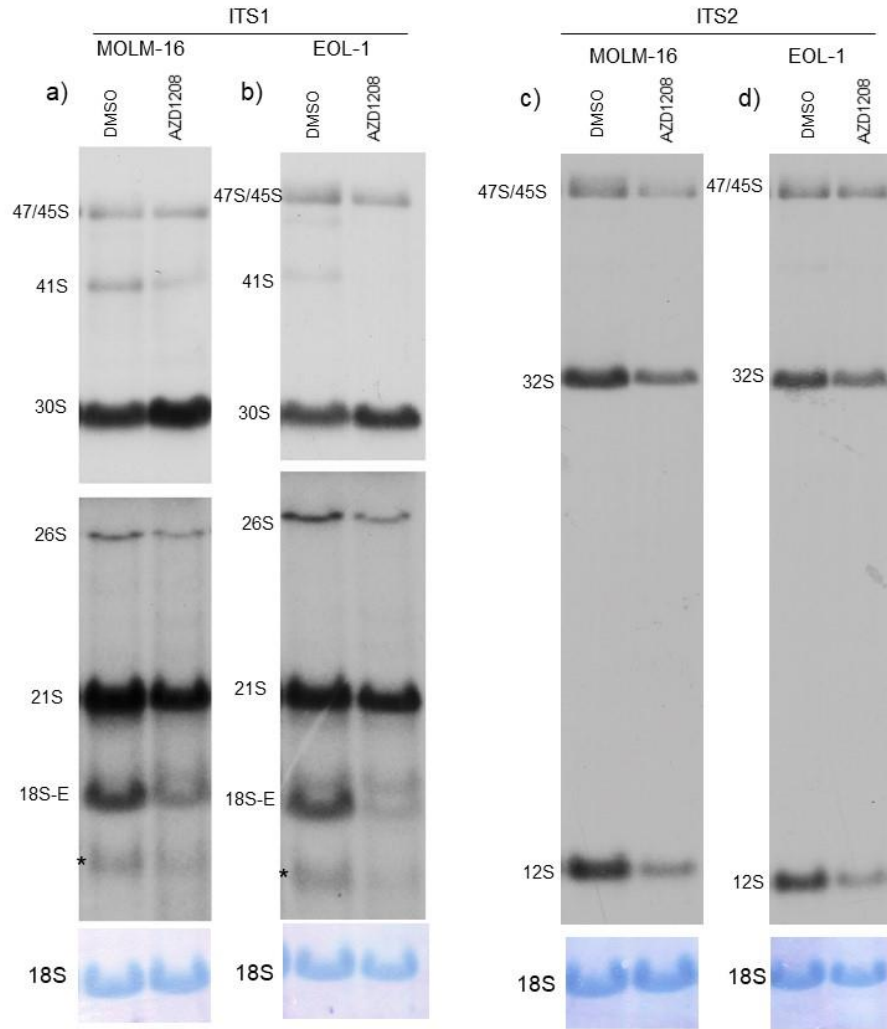
Pre-rRNA processing in eukaryotes initiates in the nucleolus co-transcriptionally during rDNA transcription and is completed in the cytoplasm in concert with ribosome assembly (Granneman and Baserga, 2005; Preti et al., 2013; Thomson and Tollervey, 2010). To observe changes in rRNA processing, Northern blot analysis was employed to quantify pre-rRNA abundance (Figure 2.11). During rRNA processing, the stepwise removal of internal (ITS1 and ITS2) and external spacers (3'-ETS and 5'-ETS) gives rise to a previously defined set of pre-rRNAs (Henras et al., 2015).

Pim kinase substrates with known functions as pre-rRNA processing factors		
	Pim substrates	Knockdown-induced Pre rRNA processing phenotype
1	DDX54	41S up, 32S up
2	DEK	21S up
3	DKC1	34S up, 30S down, 26S up, 21S up
4	FLNA	41S up
5	MBD3	all precursors down
6	NGDN	41S down, 34S up, 32S down, 30S up, 21S down
7	NOB1	45S & 41S up, 30S up, 26S up, 21S & 18S-E up
8	NOL7	47S up, 34S up, 21S down
9	NOP56	47S & 45S up, 34S up, 30S up, 21S & 18S-E down
10	NPM3	47S & 41S down, 30S down, 26S down, 18S-E down
11	PCNA	30S down, 21S down
12	PHF6	45S & 41S down
13	PNO1	41S down, 34S up, 30S down, 26S up, 21S & 18S-E down
14	RBM34	32S down, 30S down, 26S down
15	RPP38	47S up, 30S up, 18S-E down, 12S down
16	RRP12	41S up, 21S up, 18S-E down
17	RRP15	41S up, 30S down, 21S down, 12S down
18	RRS1	47S up, 34S up
19	SEN3	47S & 45S & 41S down, 32S down, 12S down
20	SEPT2	47S & 45S down, 18S-E down
21	TOP2A	47S & 45S down, 26S down
22	UTP20	47S up, 34S up, 30S up, 21S & 18S-E down
23	WDR43	45S & 41S down, 34S up, 32S down, 21S & 18S-E down, 12S down
24	WDR74	41S up, 30S down, 26S up
Processing factors from other studies		
25	RRP36	45S up, 41S down, 30S up, 21S/18SE down
26	WDR43	34S up
27	NOB1	45S/43S up, 26S up, 18S-E up

Table 2.4 List of Pim substrates previously validated as rRNA processing factors (Tafforeau et al., 2013). A list of previously known pre-rRNA processing factors were compared to the list of Pim substrates to identify these overlapping targets.

These pre-rRNAs are far lower in abundance than mature rRNAs, and are typically enumerated by Northern blotting using specific probes designed to recognize the internal transcribed spacers ITS1 and ITS2 (Tafforeau et al., 2013). Figure 2.11e shows a schematic representation of the major pre-rRNAs recognized by these probes. Pim kinase inhibition using AZD1208 in MOLM-16 and EOL-1 cells perturbed rRNA processing, resulting in accumulation of 30S pre-rRNA, reduction of 26S, 21S and 18S-E pre-rRNAs (Figure 2.11a,b). Appearance of an rRNA intermediate larger than the 18S-E pre-rRNA compared to the DMSO-treated control was observed in MOLM-16 cells (Figure 2.11a,b). We also observed a reduction in 47S/45S, 32S, and 12S abundance in AZD1208-treated MOLM-16 and EOL-1 cells as shown by ITS2 Northern blots (Figure 2.11c,d). The Northern blots (n=2) were quantified and relative fold change of pre-rRNAs in AZD1208/DMSO treated cells is presented (Figure 2.11e-h). Values <1 denote reduction and values >1 denote accumulation of respective pre-rRNAs after AZD1208-treatment.

Figure 2.11 Pim inhibition induced pre-rRNA processing defects. a) Northern blot analysis for AZD1208-treated MOLM-16 (a,c) and EOL-1 (b,d) cells using probes recognizing the pre-rRNA (a,b) ITS1 and (c,d) ITS2. For ITS1 top and bottom panels are presented at different exposures to observe low abundance rRNA intermediates (n=3). 18S rRNA abundance was analyzed by methylene blue staining on Northern membrane and presented as loading control for each Northern blot. The fast migrating band denoted by * may be a possible artefact. e-h) Quantitation of Northern blot bands for e) MOLM-16-ITS1, f) EOL1-ITS1 g) MOLM-16-ITS2 h) EOL1-ITS2 (results are averages from 2 independent experiments). Results show relative fold change of pre-rRNAs in AZD1208 treated cells to DMSO treated cells. i) Schematic representation of the major precursor rRNAs detected by either ITS1 (light blue) or ITS2 (yellow) probes (adapted from (Tafforeau et al., 2013)). The mature rRNA sequences within the precursors are depicted as blue rectangular boxes, while the spacers are shown as black lines.



In contrast, Pim inhibition of AZD1208-resistant OCI-M1 cells failed to induce detectable rRNA processing changes (Figure 2.12a,b). These data demonstrate that the modulation of rRNA processing is a consequence of modulation of Pim activity and not an off-target effect of AZD1208.

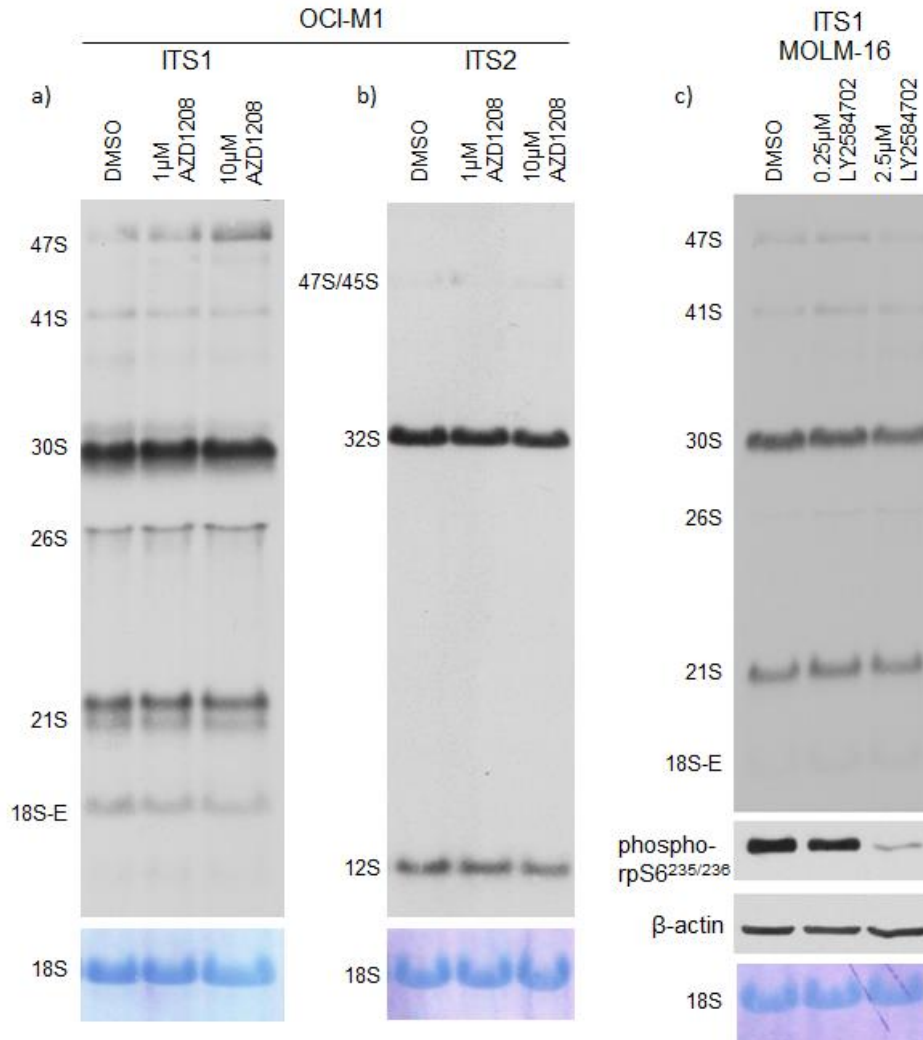


Figure 2.12 AZD1208-induced pre-rRNA processing defects are specific to Pim activity. a,b) Northern blots for ITS1 and ITS2 probes after AZD1208 treatment in OCI-M1 cells. c) Upper panel- Northern blot analysis of LY2584702-treated MOLM-16 cell samples using ITS1 probes. Lower panel- Western blotting analysis for phospho-rpS6^{235/236} antibodies for LY2584702-treated in MOLM-16 cell lysates. 18S rRNA abundance was analyzed by methylene blue staining on Northern membrane and presented as loading control.

Next, we sought to determine whether this pre-rRNA processing regulation was specific to Pim activity or an indirect effect of inhibition of protein synthesis downstream of Pim inhibition (Beharry et al., 2011; Yang et al., 2012).

The specificity of AZD1208-induced changes in rRNA processing was revealed when we inhibited p70S6 kinase, a known regulator of protein synthesis that phosphorylates rpS6 (Kawasome et al., 1998). p70S6 kinase inhibition with small molecular inhibitor LY2584702 (Tolcher et al., 2014a) in MOLM-16 cells did not induce rRNA processing changes, despite a clear decrease in phospho-rpS6-S²³⁵⁻²³⁶ (Figure 2.12c upper and lower panels). Thus, we demonstrate the modulation of pre-rRNA processing after Pim inhibition.

2.2.4 Rational combination of Pim inhibitors with other molecular targeted drugs using a substrate-guided approach

The success of protein kinase inhibitors as cancer monotherapy has been undermined by the emergence of acquired resistance after long-term inhibitor treatment (Green et al., 2015; Holohan et al., 2013). Evidence from Pim kinase inhibitors in clinical trials has also shown intrinsic inhibitor resistance in patients (Cortes et al., 2016). Effective synergistic drug combinations can help in circumventing the drug resistance, improve the

overall treatment efficacy, reduce toxicity by improving dose-reduction indices for each drug, and ultimately extend the patient's survival (Flaherty et al., 2012).

Since Pim kinase inhibition affects pre-mRNA splicing and pre-rRNA processing, we saw a potential for the therapeutic combination of Pim kinase inhibitors with inhibitors of splicing and ribosome biosynthesis. The spliceosome and ribosome have been identified as therapeutic targets for AML (Crews et al., 2016; Hein et al., 2017). Co-inhibition of a key signaling pathway using multiple inhibitors is a widely accepted strategy for drug combinations and has shown therapeutic promise (Baselga et al., 2012; Yap et al., 2013). We hypothesized that Pim kinase inhibition would synergize in combination with inhibitors of pre-mRNA splicing or inhibitors affecting ribosome biogenesis or function. To inhibit spliceosome function, we employed two different inhibitors: Pladienolide B and Sudemycin D6. Both drugs inhibit the SF3B complex of the spliceosome (Lagisetti et al., 2013; Yokoi et al., 2011). The rRNA pol I inhibitor BMH21, was used to inhibit rRNA biogenesis (Peltonen et al., 2014b), which will result in inhibition of ribosome biogenesis. To inhibit ribosome function, we used LY2584702, the inhibitor of p70S6 kinase (Tolcher et al., 2014a). Another rationale to combine these inhibitors was based on the finding that rpS6, which is a known p70S6K substrate, is also Pim substrate, thus, suggesting a possible cooperation of these kinases in AML (Discussed in Chapter 3).

MTT assays were performed to determine the type of interaction between the combined inhibitors. MTT assay is widely used to measure cytotoxicity of treatment. The colorimetric change due formation of a purple product is directly proportional to the number of active cells. Each inhibitor and combination were serially diluted and tested at 48 hours of treatment in 96-well plates. Upon colorimetric analysis, each inhibitor demonstrated varying degrees of cytotoxicity across cell lines (Figure 2.13). The Figure 2.13 presents the panel of cytotoxicity data from each synergistic drug combination for MOLM-16 cells. At each concentration, the combination treatment showed higher cytotoxicity than the individual inhibitor treatments.

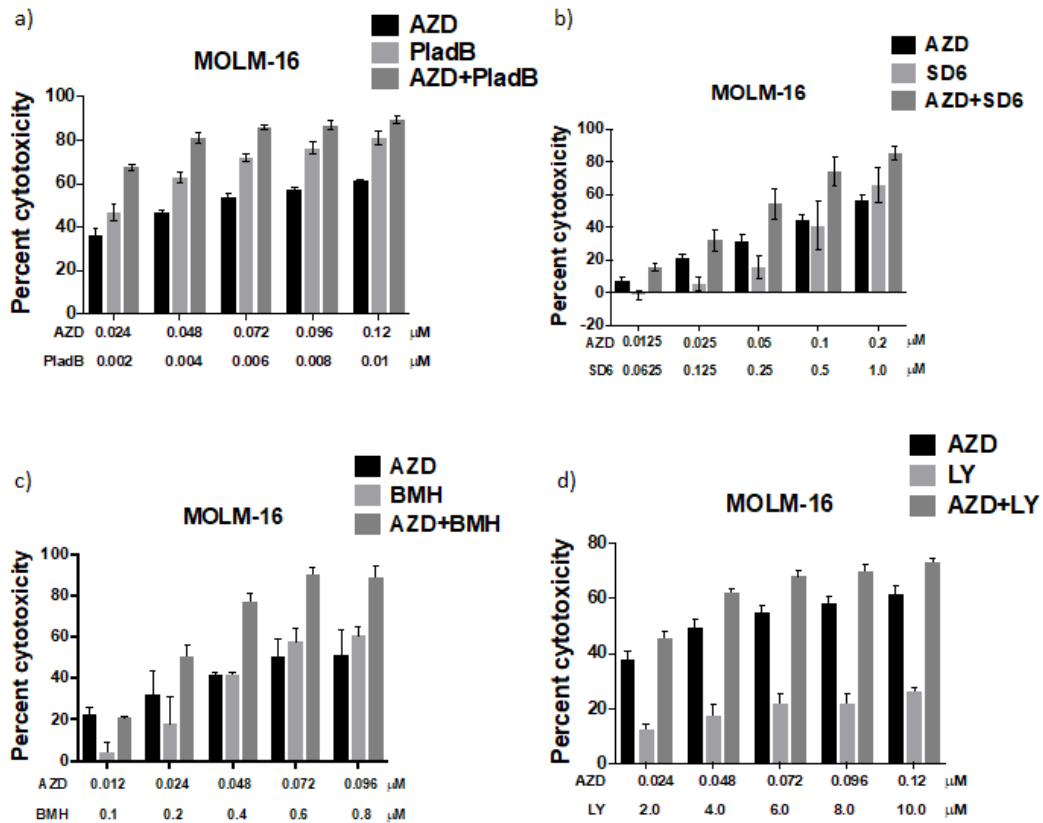


Figure 2.13 Cytotoxicity assay on MOLM-16 cells treated with inhibitor combinations. Graphs show percent cytotoxicity 48 hours after treatment with various drug-combinations as assessed by MTT assay. AZD1208 was combined with a) Pladienolide B, b) Sudemycin D6, c) BMH21, and d) LY2584702. (AZD is AZD1208, BMH is BMH21, LY is LY2584702, SD6 is Sudemycin D6 and PB is Pladienolide B).

Similarly, Figure 2.14 presents the panel for cytotoxicity data for inhibitor combinations in EOL-1 cells and Figure 2.15 shows the cytotoxicity data for treatment of OCI-M1 cells with inhibitor combinations. Similar to MOLM-16 cells, at each concentration, the combination treatment showed higher cytotoxicity to the individual inhibitor treatments.

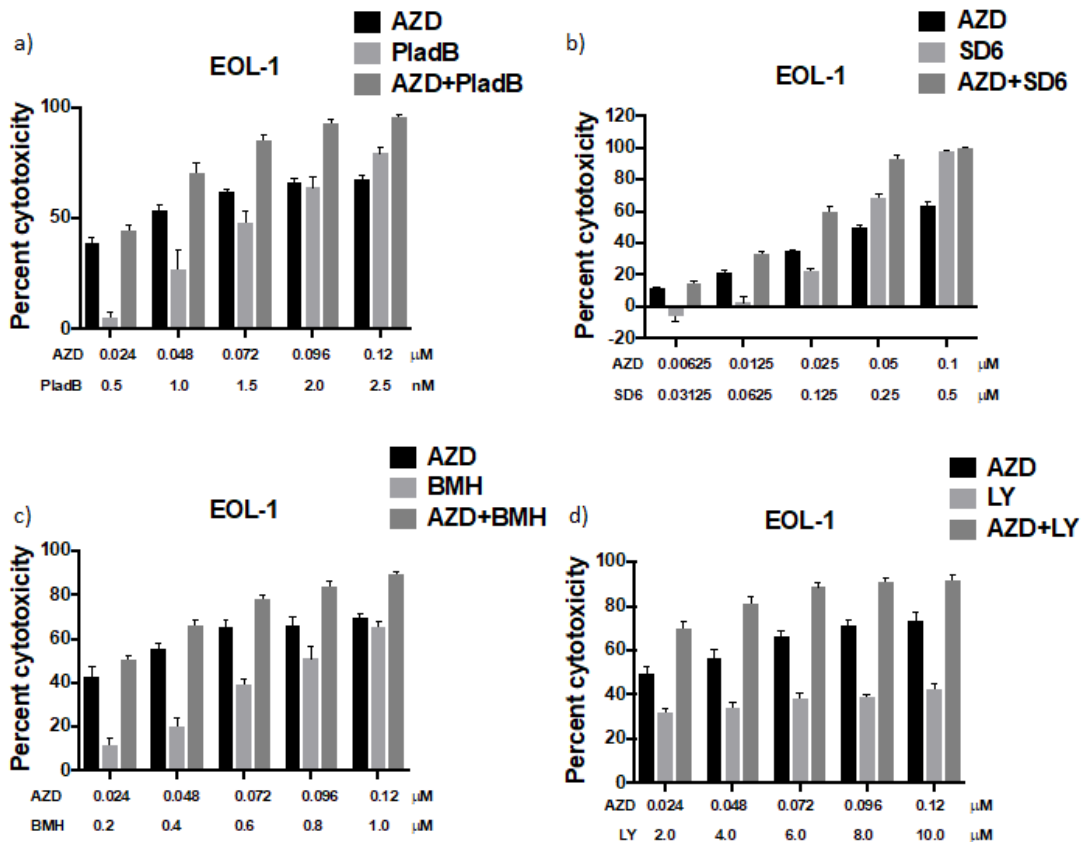


Figure 2.14 Cytotoxicity assay on EOL-1 cells treated with inhibitor combinations. Graphs show percent cytotoxicity 48 hours after treatment with various drug-combinations as assessed by MTT assay. AZD1208 was combined with a) Pladienolide B, b) Sudemycin D6, c) BMH21, and d) LY2584702.

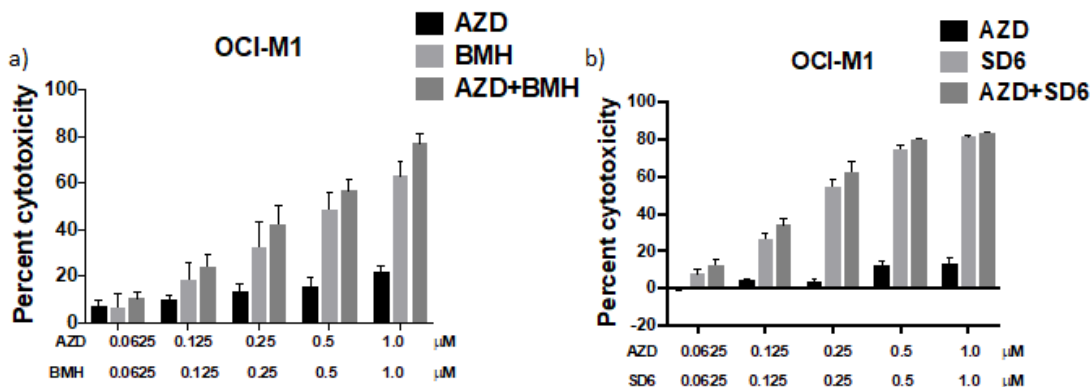


Figure 2.15 Cytotoxicity assay on OCI-M1 cells treated with inhibitor combinations as indicated.

Combination indices (CI values) calculated using the Chou-Talalay algorithm (Chou, 2010) for combinations of splicing inhibitors (Pladienolide B or Sudemycin D6) or RNA pol I inhibitor (BMH21) or p70S6 kinase inhibitor (LY2584702) with AZD1208, showed synergistic effects against MOLM-16 and EOL-1 cells (Table 2.5a). CI values represent the interaction between the drugs- $CI > 1$ shows antagonism, $CI = 1$ shows additive effect, $CI < 1$ shows synergy. A lower CI value shows stronger synergy. Notably, the combination of Pim inhibitor and p70S6K inhibitor shows strong synergism in MOLM-16 cells (ED95 CI-0.302) and very strong synergism in EOL-1 cells (ED95 CI-0.082). We also observed potentiation by the combination of AZD1208 with BMH21 or SD6 against OCI-M1 cells (Table 2.5b). The average CI values calculated from three independent experiments are presented in the tables.

a)

Cell line	MOLM-16				EOL-1			
	AZD:BMH 0.12:1	AZD:LY 0.12:10	AZD:PB 0.12:0.01	AZD:SD6 0.2:1	AZD:BMH 0.12:0.1	AZD:LY 0.12:10	AZD:PB 0.12:0.0025	AZD:SD6 0.1:0.5
ED50	1.172	0.614	0.507	0.678	1.070	0.439	1.170	0.753
ED75	0.804	0.452	0.504	0.664	0.714	0.220	0.682	0.642
ED90	0.575	0.350	0.532	0.691	0.609	0.120	0.536	0.621
ED95	0.468	0.302	0.566	0.732	0.609	0.082	0.511	0.635
Average	0.755	0.430	0.527	0.691	0.750	0.215	0.724	0.663

b)

Cell line	OCI-M1	
Ratio	AZD:BMH 10:1	AZD:SD6 1:1
ED50	0.729	0.853
ED75	0.623	0.854
ED90	0.548	0.868
ED95	0.507	0.855
Average	0.601	0.858

Table 2.5 Combination indices for Pim inhibitor combinations with pathway-based inhibitors calculated by CompuSyn synergy analysis software using the Chou-Talalay algorithm. a) Four combinations with AZD1208 show synergistic cytotoxicity against MOLM-16 and EOL-1 cells. b) In Pim-resistant OCI-M1 cells AZD1208 potentiates BMH and SD6. AZD is AZD1208, BMH is BMH21, LY is LY2584702, SD6 is Sudemycin D6 and PB is Pladienolide B. CI values represent the interaction between the drugs- CI>1 shows antagonism, CI=1 shows additive effect, CI<1 shows synergy. A lower CI value shows the stronger synergy.

Data from AML cell lines showed differing sensitivity to each combination and different strengths of synergism (Table 2.5). These observations underscore the significance of testing multiple drug combinations for putative therapy.

2.3 Discussion

One of the impediments in a successful cancer therapy is disease relapse, mainly owing to the development of drug-resistance. In some cases, inhibition of a particular pathway might result in cancer cells adapting an alternate pathway for survival and proliferation. A logical solution in this scenario is to identify new combinations of drugs to overcome these challenges (Banerji and Workman, 2016). To that end, we have leveraged the knowledge of novel Pim substrates identified using RIKA, to predict drug combinations that may be effective against AML. These drug combinations were based on the evidence of target pathway modulation by Pim kinase inhibitors and thus provide a rational approach that can be applied to other kinases for selection of putative co-targeting strategies. We demonstrate the modulation of pre-mRNA splicing and pre-rRNA processing in the cells treated with Pim inhibitors.

Post-translational modification by phosphorylation is known to regulate the function and localization of several splicing factors (Gammons et al., 2014; Misteli and Spector, 1996; Misteli et al., 1998; Zhong et al., 2009).

Since 28 known splicing factors were identified as *in vitro* Pim kinase substrates, we hypothesized that phosphorylation regulates the function of these factors, and indirectly regulates the splicing of target mRNAs. Indeed, inhibition of Pim kinases using small molecular inhibitor caused widespread changes in mRNA splicing. Thus, we have demonstrated that Pim kinases play a global role in the regulation of alternative splicing. Despite causing a large-scale change in mRNA splicing (>5000 transcripts), Pim inhibition induced fewer changes in total gene expression (>2-fold in <450 genes and only 62 genes with >4-fold change in MOLM-16 cells). Thus, alternative splicing appears to be a major target of Pim-dependent regulation, but gene expression does not appear to be extensively affected.

A majority of splicing changes that we observed after AZD1208 treatment resulted in abnormal isoforms that have not been reported in NCBI reference sequence database (RefSeq). Additionally, there were a few intron retentions that were also detected in each cell line. Thus, it is possible that Pim inhibition affects the general splicing machinery and causes a global change in splicing. Pim-substrate splicing factors SRSF1, U2AF1, and SF3B1 are important components of the spliceosome. Thus, their hypophosphorylation could result in widespread effects on pre-mRNA splicing. Guided by the knowledge of substrates generated by RIKA, we demonstrate modulation of the splicing pathway as a result of Pim kinase inhibition. Future investigation is required for a mechanistic understanding of the specific sets

of splicing factors involved in each splicing change caused by Pim kinase inhibition.

The alternative splicing changes observed after AZD1208 treatment in MCL1, CHAC1, NFYA, and COG5 were validated in two AML cell lines. The changes in alternative splicing could manifest as Pim kinase-dependent changes in the respective cellular functions controlled by these proteins. Such a switch in function is known for MCL1 isoforms (Bae et al., 2000): MCL1-L is an anti-apoptotic protein, while MCL1-s has pro-apoptotic functions. Interestingly, Pim kinases are generally known as pro-survival kinases (Aho et al., 2004; Decker et al., 2014), however, we observed a decrease in the pro-apoptotic MCL1 isoform, MCL1-s after Pim inhibition in MOLM-16 and EOL-1 cells (Figure 2.9 a,b). Thus, ironically, regulation of MCL1 alternative splicing could act as a mechanism to avoid aberrant pro-survival signaling through Pim kinase upregulation.

Pim kinase inhibitors have been previously shown to induce activation the unfolded protein response (UPR) pathway in prostate cancer cells (Song and Kraft, 2012). CHAC1 is also known to be involved in the UPR pathway (Mungrue et al., 2008). The UPR pathway is activated due to the presence of misfolded proteins, or due to over-burdening of endoplasmic reticulum (ER) (Wang and Kaufman, 2014). Multiple arms of UPR activation exist in the cells, which help to alleviate ER-stress by regulating translation and enhancing

protein-folding (Wang and Kaufman, 2014). Although UPR initially acts as a pro-survival pathway, continued UPR activation can result in apoptosis (Osowski and Urano, 2010). This dual nature of the UPR pathway may be exploited by cancer cells to overcome the ER-stress associated with tumor progression. One arm of the UPR pathway includes activation of the inositol-requiring enzyme 1 (IRE1), leading to a switch in XBP1 splicing (Back et al., 2005). Pim kinases are known to induce this switch in XBP1 splicing in prostate cancer cells (Song and Kraft, 2012). This switch in XBP1 splicing was also observed in microarray results from AZD1208 treated MOLM-16 cells, but not in EOL-1 cells. Thus, change in CHAC1 splicing upon Pim kinase inhibition might contribute to further activation of UPR in MOLM-16 cells (Figure 2.9d), and compensate for the absence of the switch in XBP1 splicing in EOL-1 cells. Although CHAC1 is known to promote induction of apoptosis, CHAC1 isoforms are upregulated in breast and ovarian cancers and correlate with poor outcome for patients (Goebel et al., 2012). Pim inhibitor dependent splicing changes in CHAC1 may trigger the pro-apoptotic components known to be regulated by CHAC1 signaling (Mungrue et al., 2008). However, the specific functional differences in CHAC1 isoforms are unknown, and future investigation may shed light on their specific functions, and reveal the significance of the switch in splicing. Notably, the robust and reproducible response to Pim inhibition observed in CHAC1 splicing of MOLM-16 and EOL-1 cells (Figure 2.9d) provides support for the use of CHAC1 as a putative biomarker for Pim kinase activity.

Splicing factors known as SR proteins have regions of multiple serine-arginine dipeptide sequences called 'RS domains'. Several serine residues in these RS-domains of SR proteins are phosphorylated by SRPK1 (Colwill et al., 1996). SRPK1 is normally localized to the cytoplasm but locates to the nucleus in response to stress signals (Zhong et al., 2009). A study demonstrated that phosphorylation of SRPK1 and its activity is regulated through AKT, which is regulated by EGFR signaling (Zhou et al., 2012). As AKT and Pim kinases share several substrates and have intersecting regulatory pathways (Warfel and Kraft, 2015), we asked if Pim kinases could regulate the SRPK1 signaling by modulating SRPK1 activity. To answer this question, we tested the effect of Pim inhibition on SR protein phosphorylation using phospho-SR protein antibodies (Figure 2.10a,c). Inhibition of SRPK1 activity by SRPIN340 treatment of cells caused a reduction in phospho-SR protein antibody signal in EOL-1 cell lysates (Figure 2.10a). However, Pim inhibition by AZD1208 does not induce a reduction in phospho-SR protein antibody signal in EOL-1 or MOLM-16 cells (Figure 2.10a,b). Thus, Pim kinases do not cause phosphorylation of these RS domains directly or indirectly through SRPK1. To validate these observations further, we tested the effect of SRPIN340 on Pim kinase-dependent splicing changes. As expected SRPIN340 treatment did not induce the splicing patterns similar to those observed after Pim inhibition. Thus, the effects on target mRNA splicing are not mediated by Pim kinase-induced SRPK1 modulation.

To further evaluate the significance of our findings, we compared our data to the existing information regarding aberrant splicing in AML patient samples. A study identified aberrant splicing events in samples from AML patients in comparison to normal donors (Adamia et al., 2014). They also provided a list of 52 oncogenes and 50 tumor suppressors which were aberrantly spliced in patient samples but not in normal donors. We compared this list of aberrantly spliced genes to the AZD1208-responsive splicing target genes in MOLM-16 cells. 12 oncogenes and 9 tumor suppressors, aberrantly spliced in primary AML patient cells were also affected by Pim inhibition dependent splicing changes. Figure 2.16 shows a schematic representation of these findings. Thus, it is possible that Pim kinases regulate splicing events in these 12 oncogenes and 9 tumor suppressors, and aberrant Pim over-expression observed in AML patients could be driving these aberrant splicing changes in patient samples.

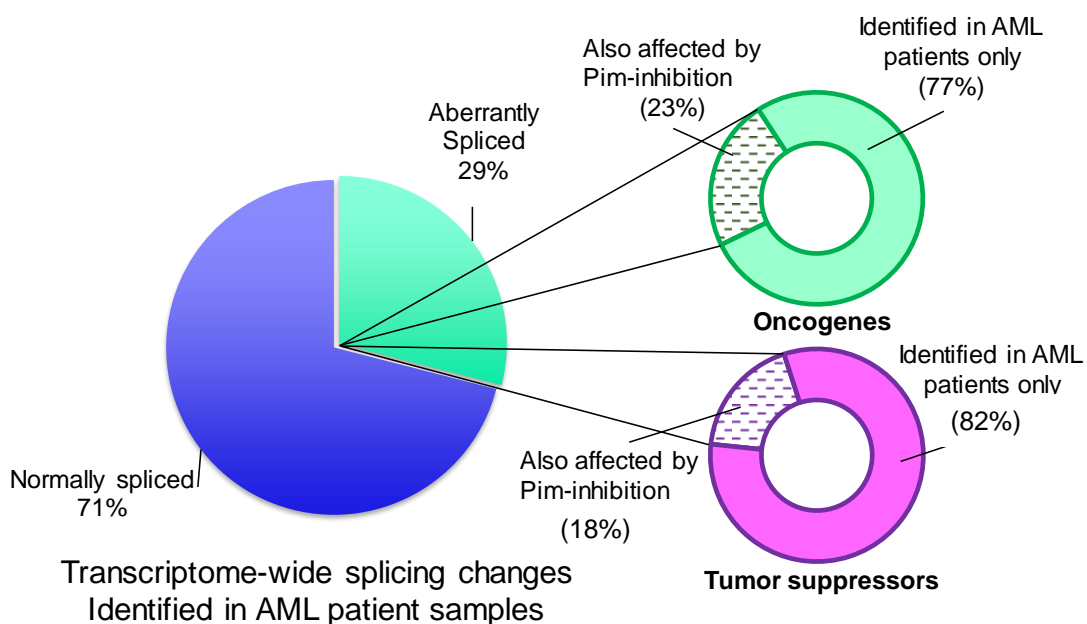


Figure 2.16 Comparison of Pim-induced splicing changes with published data from AML patients (Adamia et al., 2014). The authors showed that 29% of total mRNAs are aberrantly spliced in AML patient samples (green sector). When we compared our results with a set of 52 oncogenes (green doughnut) and 50 tumor suppressors (pink doughnut) from this dataset, we found 12 oncogenes (23%) and 9 tumor suppressors (18%) changed after Pim inhibition.

In addition to the splicing factors, a number of rRNA processing factors and ribosomal proteins were identified as Pim kinase substrates. Thus, we hypothesized that phosphorylation of these factors would regulate their functions in pre-rRNA processing. Various steps in pre-rRNA processing give rise to precursor rRNAs of varying lengths, that contain different portions of the spacer regions of rRNA, which are progressively removed during rRNA maturation (Eichler and Craig, 1994). Thus, accumulation of a specific precursor can be traced back to the deregulation of specific processing steps. The precursor rRNA abundance in cells treated with AZD1208 was compared to DMSO-treated cells, using Northern blot analysis for probes directed towards ITS1 and ITS2. Using Northern blot analysis, we demonstrated the modulation of pre-rRNA processing, after Pim kinase inhibition by AZD1208 (Figure 2.11a-d). Based on the ITS1 Northern blot analysis (Figure 2.11a,b), we observed accumulation of the 30S pre-rRNA, which suggests lack of processing at A0 and 1 (O'Donohue et al., 2010). As a result of 30S accumulation, all the following precursors show reciprocal reduced abundance.

Interestingly, we did not observe the 21S-C intermediate pre-rRNA in the AML cell lines used for this study. 21S-C intermediates were also previously reported to be absent in HeLa cells but appeared after siRNA mediated knockdown of processing factors (Tafforeau et al., 2013). It is likely that the processing steps occur almost instantaneously. Therefore, when 21S gets processed into 21S-C intermediate, which is quickly converted to 18S-E by cleavage at site E (Figure 2.11a,b).

Another deregulated step in AZD1208-treated cells appears to be at the level of 18S-E processing in MOLM-16 cells. The creation of 18S-E from precursor 21S requires both exonucleolytic and endonucleolytic processing. A slow migrating 18S-E intermediate accumulated after AZD1208 treatment in MOLM-16 cells and appeared to be slightly larger than the more abundant 18S-E pre-rRNA (Figure 2.11a,b). However, it is possible that this intermediate is not an aberrant precursor but the full-length 18S-E precursor. A lower abundance of longer 18S-E intermediates was observed in HeLa cells, through experiments aimed at mapping this region on 18S-E (Preti et al., 2013). Thus, the 18S-E pre-rRNAs observed in DMSO-treated cells could be the shorter version of 18S-E, created by exonucleases trimming. If the exonuclease trimming steps are affected after AZD1208 treatment, that would increase accumulation of longer 18S-E precursors (Figure 2.11a-b).

The fast migrating band (denoted by * in Figure 2.11a-b) might be an artifact. A similar band was also observed in ITS1 Northern blots for HeLa cells, and it was suggested to be an experimental artifact and not an alternatively processed 18S-E precursor (Preti et al., 2013). The ITS2 probe reveals a reduction in all the three pre-rRNA detected by this probe. Reduction in 45S/47S, 32S and 12S pre-rRNAs suggests a perturbation of the earliest processing steps of rRNAs of the 60S subunit.

Interestingly, KEGG pathway analysis of the genes affected by AZD1208-induced splicing changes pointed to the ribosome as the major target and gene ontology analysis pointed to RNA processing and ribosome biogenesis (Table 2.2 and Table 2.3). Modulation of alternative splicing could affect rRNA processing through snoRNAs. A number of snoRNAs (small nucleolar RNAs) are processed out of the introns from the pre-mRNAs of genes involved in protein synthesis (Hoeppner et al., 2010). These non-coding RNAs associate with various proteins to perform rRNA modification, and some snoRNAs are also required for rRNA processing (Peculis and Steitz, 1994). Thus, changes in splicing could have a direct impact on the abundance of snoRNAs and affect rRNA modification and processing. Over 68 snoRNA harboring genes were affected in AZD1208-treated MOLM-16 cells and splicing of 70 snoRNA harboring gene was affected by AZD1208 treatment in EOL-1 cells.

Initial understanding of rRNA processing came from experiments performed in yeast. It was only recently conclusively shown, that human pre-rRNA processing was much more complex than observed in yeast (Tafforeau et al., 2013). Using siRNA knockdown for 625 putative processing factors followed by Northern blot analysis for pre-rRNA processing, a study showed that 78 processing factors in humans did not have a yeast homolog (Tafforeau et al., 2013). These 625 proteins excluded ribosomal proteins previously known to affect rRNA processing (Robledo et al., 2008). Knockdown of protein expression of 286 factors (out of 625) caused rRNA processing defects in HeLa cells, revealing a higher level of complexity than previously anticipated (Tafforeau et al., 2013). Curiously, when we compared the list of Pim substrates with these 286 factors, we observed that 23 processing factors were also Pim kinase substrates (Table 2.4). Table 2.4 lists the pre-rRNA processing defects observed by Tafforeau et al., after siRNA knockdown of respective factors. We compared the pre-rRNA profile after Pim inhibition (ITS1: 41S down, 30S up, 26S down, 21S down, 18S-E up, ITS2:47S/45S down, 32S down, 12S down) with the known pre-rRNA profiles after siRNA knockdown of these proteins. The pre-rRNA perturbation profile of UTP20 knockdown is similar to the pre-rRNA profile observed after Pim inhibition as assayed by ITS1 Northern. Pim inhibition profile is also similar to the profile of NGDN knockdown (Table 2.4). In addition to 286 factors, there are 43 other processing factors identified by previous studies. Three of those 43 proteins are also Pim substrates (Table 2.4). As mentioned

before, loss of ribosomal proteins causes specific defects in rRNA processing (Robledo et al., 2008). Both small and large subunit proteins were identified as Pim kinase substrates (data not shown). Therefore, hypo-phosphorylation of ribosomal proteins could be causing these changes in pre-rRNA processing. Notably, loss of ribosomal protein rpS11 was shown to cause 30S accumulation (O'Donohue et al., 2010). rpS11 was also identified as a Pim substrate by RIKA. In conclusion, the effect of Pim kinase inhibition on pre-rRNA processing could be a cumulative effect of inhibition of various pre-rRNA processing factors and snoRNAs. Based on all the results discussed above, we demonstrate a substrate-guided approach to identify novel pathways regulated by a kinase and provide proofs of target pathway modulation in response to kinase inhibition.

The knowledge of novel kinase substrates not only improves our understanding of functions of kinases, but it can also guide putative co-therapy strategies. To test this idea for formulating combinations with Pim kinase inhibitors, we chose inhibitors to target ribosome biogenesis and pre-mRNA splicing. To target the spliceosome, we employed two spliceosome inhibitors- Sudemycin D6 (SD6) and Pladienolide B (PladB or PB). When combined with Pim inhibitor AZD1208, we observed synergistic cytotoxicity against MOLM-16 and EOL-1 cells. To target the ribosome, we employed two inhibitors, RNA pol I inhibitor- BMH21 and p70S6K inhibitor LY2584702.

Combinations of AZD1208 and BMH21 or AZD1208 with LY2584702 were also synergistic against MOLM-16 and EOL-1 cells (Table 2.5a).

OCI-M1 cells are resistant to AZD1208 treatment as seen by the low cytotoxic effect of AZD1208 treatment on these cells (Figure 2.15). Thus, instead of synergism, the cooperation of AZD1208 with other inhibitors is called 'potentiation'. We observe that AZD1208 potentiated BMH21 against OCI-M1 cells (Table 2.5b). Therefore, although Pim inhibition alone is not sufficient to efficiently inhibit OCI-M1 cell growth, in presence of RNA pol I inhibitor, Pim kinase deficiency created by AZD1208 becomes 'synthetic lethal'. We have also observed the potentiation of spliceosome inhibitor SD6 against OCI-M1 cells. However, the degree of potentiation is lower in AZD1208+SD6 than AZD1208+BMH21. At the highest concentration of both drugs, the cytotoxicity of combination is only slightly higher than SD6 alone (Figure 2.15b). One explanation for this observation is that a small population of cells resistant to inhibition by both AZD1208 and SD6 survives the treatment and causes the decrease in potentiation. Thus, OCI-M1 cells show higher CI values, signifying lower synergy/potentiation. Pladienolide B was able to inhibit OCI-M1 proliferation but did not synergize with AZD1208. LY2584702 alone was unable to inhibit growth or proliferation of OCI-M1 cells, and no potentiation was observed with AZD1208 (data not shown). These results underscore the importance of testing multiple drug combinations. As observed in OCI-M1 cells, inherent drug resistance to

kinase inhibitors is also reported in cancer patients (Busch et al., 2011; Wang et al., 2016). Thus, multiple drug combinations are needed, as patients have a variable response to the drug combinations and can benefit from having options.

The synergistic potential of each combination varied for individual cell lines, as seen by the CI-values (Table 2.5). AZD1208+BMH21 was most synergistic against OCI-M1 cells, while AZD1208+LY2584702 showed the strongest synergy against EOL-1 cells, and finally, all the four combinations showed similar synergism against MOLM-16 cells. These observations underscore the importance of identifying and testing multiple combinatorial strategies against malignant cells.

In conclusion, using Pim kinases as an example, we demonstrate the application of proteome-wide kinase substrate profiling to guide putative therapeutic combinations and putative pharmacodynamic biomarker discovery.

2.4 Materials and methods

Cell culture

The K562 cell line was procured from ATCC, MOLM-16, EOL-1 and OCI-M1 were purchased from DSMZ and maintained according to the recommended conditions at 5% CO₂ and 37°C. Antibiotics, antimycotics and antimycoplasma were added to the culture media to avoid any contamination.

PC3 cells were grown in RPMI 1640 (Corning Cellgro, #10-040-CV) with 10% fetal bovine serum (FBS). K562 cells were cultured in Iscove's modified Dulbecco's medium (IMDM) (Corning Cellgro, #10-016-CV) with 10% FBS. MOLM-16 and EOL-1 cells were grown in RPMI 1640 with 20% FBS. OCI-M1 cells were grown in IMDM (Corning Cellgro, #10-016-CV) with 20% FBS.

Inhibitor treatments

In this study, pharmacological inhibitors specifically targeting Pim kinases, p70S6 kinase, RNA Polymerase-I, and spliceosomes were used. For each experiment, indicated number of cells were seeded one day prior to the treatment. These cells were treated with indicated concentration of inhibitors for a particular duration as mentioned in the figure legends. Unless otherwise noted, complete medium with FBS and antibiotics was used to dilute the inhibitors. AZD1208 (pan-Pim inhibitor) (MedKoo Biosciences, #205763), LY2584702 (p70S6 kinase Inhibitor) (Selleck chemicals, #S7704), Pladienolide B (SF3B complex inhibitor) (Santacruz Biotechnology, #445493-23-2) were diluted in DMSO. BMH21 (RNA pol-I Inhibitor) was provided by our collaborator Dr. Marikki Laiho (Johns Hopkins University). BMH21 was provided as pre-solubilized in citrate buffer (pH 6). Sudemycin D6 (SD6) was provided by Dr. Thomas Webb (SRI biosciences). SD6 was provided pre-solubilized in DMSO. For vehicle (solvent) controls volume of DMSO or other vehicle added was equal to the volume of inhibitor stock made with the same vehicle.

RNA isolation and cDNA synthesis

8×10^5 - 1.5×10^6 cells were used for RNA extraction. Cells were washed with 1X PBS twice. RNA was extracted using Qiagen RNA miniprep kit (#74104). Total RNA was eluted in 30 μ L of RNase-free water. Fermentas DNase I (#EN0525) kit was used to remove any DNA contamination. RNA was stored at -80°C until further use. Total of 1-2 μ g of cleaned total RNA was used for cDNA synthesis using Thermo scientific maxima reverse transcription kit (#K1641) as per the manufacturer's protocol. cDNA was stored at -20°C , diluted 1:5 with nuclease-free water and used in RT-PCR and qRT-PCR reactions.

RT-PCR analysis

cDNA extracted from DMSO control-treated and inhibitor-treated AML cell lines were analyzed by RT-PCR to observe changes in CHAC1, NFYA and COG5 splicing. The primers were designed by comparing the mRNA sequences using NCBI nucleotide reference sequence database (RefSeq). The Primer blast feature of the NCBI blast was used to identify primers that recognized sequences on either side of the spliced exon. These primers can use the differentially spliced mRNAs as templates, and yield PCR products of distinct sizes that can be resolved using high density (2-2.5%) agarose gel electrophoresis. PCR reactions were standardized for each primer pair using the melting temperatures of primers and the final lengths of expected PCR

products based on the RefSeq information. The following primers were used to assess the spliced isoform abundance:

CHAC1 fwd: 5'-GCA GGG AGA CAC CTT CCA TC-3'

CHAC1 rev: 5'-AAA GAG AAG CCT CCA GCC AC-3'

NFYA fwd: 5'-CAG GCA GGA CAG ATT CAG CA-3'

NFYA rev: 5'-CCA AAC TGG CTG CTG GGA TA-3'

COG5 fwd: 5'-GGA CAG AGA AGA AAT GTG GCA G-3'

COG5 rev: 5'-GGG TTG CAC AGC ATT TTC CA-3'

β -Actin fwd: 5'-AGA GCT ACG AGC TGC CTG AC-3'

β -Actin rev: 5'-AGA ACT GTC TTG GCG TAC AG-3'

qRT-PCR analysis for MCL1 transcripts

MCL1 transcripts MCL-1L (assay name: Hs00172036_m1) and MCL-1s (assay name: Hs00766187_m1) were quantified using the Taqman assays (Thermo fisher Scientific). 30ng of total cDNA was used for each reaction. GAPDH (assay name: Hs99999905_m1) was used as a loading control. CFX96 Touch™ real-time PCR detection system was used for the reaction. Results were analyzed using the CFX manager software. Statistical analysis was also performed using the CFX manager software which used t-test to calculate p-values. Each sample was tested in triplicates, NO-RT (purified RNA instead of cDNA) controls were also tested in triplicate for each RNA samples with each probe reaction.

Microarray analysis

Microarray analysis was performed at Biopolymer laboratory, at University of Maryland Baltimore. RNA samples were checked for integrity using the Bioanalyzer (Agilent 6000). Only the samples with RIN number 10 were used for further analysis. The strategy used for microarray analysis is depicted in Figure 2.7. RNA samples extracted from AML cell lines with and without AZD1208 treatment were analyzed on Affymetrix GeneChip® human transcriptome analysis 2.0 (HTA 2.0). The signal intensity data was converted to CEL files. Resulting CEL files were converted to CHP files using the Affymetrix® Expression Console™ Software. Finally, microarray data was analyzed using Transcriptome Analysis Console (TAC) Software using CHP files from three biological replicates.

Analysis for comparison of MOLM-16 and EOL-1 microarray data

This analysis was performed using the data from TAC software and processing it with Microsoft Excel. The list of splicing changes between AZD1208 treated and DMSO treated samples were exported and converted to Excel files. The unique identifiers for probe selection region (PSR) IDs pertaining to a particular exon or junction and the associated splicing indices were used for analysis. Lists of PSRs for both cell lines were sorted, and then using the formula- IF (cell number=cell number,0,1), the lists were compared. If excel results turns out '0' then the PSR_IDs are identical. Next, using the 'IF' function again, the sign of splicing index associated with these PSR_IDs

were compared. Similar signs represent similar effect on exon inclusion or exclusion. Finally, using the 'Vlookup' function the PSR_IDs were traced back to the genes associated with these PSR_IDs.

Pathway analysis for splicing target genes

The common target genes identified by the procedure described above were analyzed using the gene set enrichment analysis method which uses the information from the Molecular Signature database (MSigDB) (Broad institute, UC San Diego) to identify enriched gene sets from the experimental data. The Pim inhibitor-induced splicing target genes were analyzed for KEGG gene set enrichment and GO biological process enrichment.

RNA electrophoresis

MOLM-16, EOL-1 and OCI-M1 cells were treated with Pim inhibitor (AZD1208) or S6 Kinase inhibitor (LY2584702) for indicated time. Total RNA was extracted using the Qiagen RNA miniprep kit (#74104) and then measured using a spectrophotometer for concentration and A260/280 ratio. A total of 5 µg RNA was mixed with 2X Glyoxal dye and incubated at 50°C for 30 min. RNA sample with dye were later resolved on 1% Agarose gel in 1X NorthernMax® Gly Gel prep/running buffer (Ambion: AM8678 10X diluted to 1X with MiliQ water) for 16 hours at 60V. After electrophoresis overnight, the RNA was transferred to Nytran membrane (GE Whatman™ 10416096) using Northern transfer buffer 3- 4 hours, using transfer buffer reservoir assembly.

Transferred RNA was crosslinked on membranes by UV irradiation in Spectrolink UV crosslinker at the optimal crosslink setting, and stored at -20°C.

Northern blot analysis for rRNA precursors

The probes used in this experiment were described previously (Tafforeau et al., 2013). The Northern blotting procedure was followed according to the Ambion NorthernMax-Gly Glyoxal based system (#AM1946). Before the hybridization reaction, membrane was soaked in water and incubated in hybridization buffer (Ultrasorb™, #AM8670) at 42°C for at least 3-4 hours. Oligonucleotides (Oligo) were synthesized by Invitrogen. Oligos were labeled $\gamma^{32}\text{P}$ ATP by Polynucleotide kinase reaction (PNK) using PNK (Fermentas) and buffer A (Fermentas) for 30 minutes at 37°C. The oligo to ATP ratio of 1:5 was used for each reaction. The unused probe was removed by passing the reaction mix through G-25 columns (GE healthcare: Illustra Microspin: 27-5325-01). The labeling was measured using scintillation counter and about 750,000 cpm/ml were added to the 12ml of Ultrasorb™. Each probe was hybridized in Ultrasorb™ solution at 42°C overnight (12-18 hours). After hybridization was complete, the unused probe was appropriately discarded and the membrane was washed twice with low and high stringency wash buffers respectively. Pre-rRNAs were detected using autoradiography. Membranes were stained with methylene blue (0.04% in methanol for 5-10

minutes) and destained (25% ethanol) to observed mature rRNAs. 18S was used as loading control for each Northern blot.

Sequences for probes used for Northern blot analysis:

ITS1- CCTCGCCCTCCGGGCTCCGGGCTCCGTTAATGATC

ITS2- CTGCGAGGGAACCCCCAGCCGCGCA

Northern quantitation was done by using ImageJ software to obtain values of band intensities (in terms of peak areas) which were normalized to 18S values. The fold change was calculated as ratio of AZD1208 treated value to DMSO treated value. Graphs were plotted using Prism software.

Western blotting

Cells were lysed in denaturing buffer containing urea (7M Urea, 2M thiourea, 20mM DTT, 1%C7BZ0, 20mM Tris pH 7.5) to retain the physiological phosphorylations on proteins. Total proteins were quantified using Bradford colorimetric analysis. 20-25 μ g total protein was used for each lysate. Western blotting analysis for total protein lysates was performed after LY2587402 treatment in MOLM-16 cells. Proteins were resolved in 12% SDS-PAGE gels at 150V for 60 mins. Resolved proteins were transferred to PVDF membranes (Immobilon® 0.45 μ m) at 100V for 60mins or 30V for 16 hours. Phospho-rpS^{235/236} antibody (Cell signaling technology #4858) and Beta actin loading control antibody (Thermo Scientific BA3R, #MA5-15739) were used to perform the Western blotting. Primary incubation was carried out at 4°C overnight followed by washes in 1X TBST (Tris based saline buffer with

Tween 20), followed by secondary antibody incubation at room temperature for 1 hour. Secondary antibodies used were Anti-rabbit IgG, HRP-linked antibody (Cell signaling #7074) and Anti-mouse IgG, HRP-linked antibody (Cell signaling technology, #7076). Chemiluminescent substrate ECL was used to detect HRP conjugated antibodies.

MTT assays

MTT stands for 3-(4,5-dimethylthiazol-2-yl)-2,5-diphenyltetrazolium bromide. For MTT assay, 5000 (OCI-M1), 10,000 (MOLM-16), or 20,000 (EOL-1) cells were seeded per well in 96-well plates and cultured overnight. Either DMSO or single drug, or combinations were diluted in media, and added in quadruplicates to the wells containing cells. Different ratios were tested for each combination for each cell line to identify the ratios at which maximum synergy is achieved. After 48 hours, the MTT metabolism indicative of number of live cells was measured by MTT assay (Promega, #G4000). MTT reagent was added for 4 hours at 37°C, followed by termination of reaction by adding neutralization solution, followed by incubation for 1 hour. The OD readings (570nm) were measured by Biotek synergy 2 plate reader. OD measurements for blank and OD at 650nm were subtracted from each value. The resulting values for inhibitor-treated versus control-treated samples were used to evaluate the FA (fraction affected) values. FA was calculated as $[1 - (\text{average OD for inhibitor-treated wells} / \text{average OD for control-treated wells})]$. The FA values were plugged into the CompuSyn

software (<http://www.combosyn.com>) to calculate the combination indices (CI values) at ED50, ED75, ED90 and ED95 (ED- Effective dose of combination). CI values represent the interaction between the drugs- $CI > 1$ shows antagonism, $CI = 1$ shows additive effect, $CI < 1$ shows synergy. A lower CI value shows the stronger synergy.

Chapter 3: Identification and validation of novel Pim kinase substrates hnRNPA1 and rpS6 as potential Pim combination therapy biomarkers

Contributions to the work

Dr. Xiang Li identified hnRNPA1 as Pim1 substrate, rpS6 as Pim2 substrate, and validated rpS6 as an *in vitro* Pim2 substrate (Figure 3.4b). Azim Raja helped in few cell culture and Western blot experiments. All other experiments were performed by Tejashree Anant Joglekar.

Abstract

Pro-growth kinase up-regulation is a common feature in cancer and a major target for intervention. Predictive and pharmacodynamic biomarkers are essential for identifying patients who will benefit from cancer therapy using kinase inhibitors. Given the established role of Pim kinases in various pro-cancer pathways, pharmacological inhibition of Pim kinases can potentially become an effective therapy against AML and other cancers. Pim inhibitors are in clinical trials for AML and other cancers. However, to date, very few substrates have been identified for Pim kinases. Using the kinase substrate profiling platform of reverse in-gel kinase assay (RIKA), we have identified numerous novel substrates of Pim kinases. Through *in vitro* kinase assays, we validated the phosphorylation on hnRNPA1 and rpS6. Pim1 phosphorylates hnRNPA1 at S¹⁹⁹ and shares the site with AKT. Pim2 phosphorylates S^{235/S236} of rpS6 *in vitro* and shares the target site with

p70S6K. These sites show dose-dependent decrease in phosphorylation after Pim inhibitor treatment in Pim inhibitor-responsive cells. Interestingly, rpS6 phosphorylation only decreases after combined inhibition by Pim and p70S6K inhibitors in Pim inhibitor resistant OCI-M1 cells. This research provides deeper insight into the pathways regulated by Pim kinases and validates two novel proteins as Pim kinase substrates. Moreover, both hnRNPA1 and rpS6 could function as biomarkers for combination therapy with Pim inhibitors.

3.1 Introduction

Numerous drugs specifically targeting kinases are being tested as cancer therapeutics in preclinical and clinical stages. However, a major hurdle in employing kinase inhibitors for therapy is the absence of reliable response markers for all the kinase targets (Dancey and Sausville, 2003). Unlike traditional chemotherapy, effective targeted therapy using kinase inhibitors would require an initial molecular screening to identify patients that will benefit from the treatment (Dancey and Sausville, 2003). For example, the selection of CML patients with the BCR-ABL translocation can be made by testing the mutation status at the BCR locus. However, in the absence of a driving mutation, surrogate markers or predictive biomarkers are required for identifying the patients who will benefit from kinase inhibitor therapy. Another concerning issue is acquired or innate drug resistance due to parallel compensatory signaling pathways. To this end, rational drug combination can be an effective solution. However, the lack of predictive and surrogate biomarkers may impede the development of these solutions. In addition, co-

targeting therapy may benefit from a novel set of biomarkers that respond to the effect on multiple molecular targets. A panel of proteins that respond to all the pathways targeted through combination therapy will provide an ideal predictive platform to test the effectiveness of drug combinations. In absence of phospho-specific antibodies, phosphorylation stoichiometry measurements before and after inhibitor treatments can be used.

Pim kinases are upregulated in various hematopoietic malignancies and solid tumors. With the aim of unraveling novel biomarkers for Pim kinase therapy, our lab has identified numerous Pim kinase substrates. This chapter includes the validation and significance of two Pim kinase substrates namely hnRNPA1 and rpS6 as novel biomarkers for Pim kinase inhibitors. Interestingly, as both proteins contain shared phosphorylation sites between Pim and other signaling pathways, we propose them to be ideal biomarkers for combination therapy between these pathways. The next section will introduce the role of each of the substrate proteins and the significance of phosphorylation in regulating their function.

3.1.1 hnRNPA1

hnRNPA1 is a member of the heterogeneous nuclear ribonucleoprotein (hnRNP) family of proteins. These proteins are present in the nucleus, bind nascent mRNAs and are involved in mRNA metabolism. There are approximately 20 hnRNPs identified to date and they are named from A to U. Some hnRNPs are retained in the nucleus while others are exported to the

cytoplasm as a complex with the mRNA during mRNA export. hnRNPA1 is the most abundant of all hnRNPs and is ubiquitously expressed (Kamma et al., 1995). hnRNPA1 is a factor that binds pre-mRNA, regulates alternative splicing of certain mRNAs and is exported out with the mature mRNA into the cytoplasm. Therefore, although mostly a nuclear protein, hnRNPA1 also shuttles in and out of the cytoplasm (Roy et al., 2014; Siomi and Dreyfuss, 1995).

The hnRNPA1 protein contains various domains that interact with RNA and other proteins. The N-terminus contains two RNA binding domains, RRM1 and RRM2 (RNA recognition motifs). These are involved in interaction with target mRNA. They have high sequence homology but function independently in RNA recognition (van der Houven van Oordt et al., 2000). The C-terminal region containing repeats of Arg-Gly-Gly (RGG) with aromatic residues in between is also involved in RNA and protein binding (Mayeda and Krainer, 1992). Another noteworthy structure in the C-terminus is the M9 sequence which contains multiple phosphorylatable serines and acts as a localization signal to direct shuttling in and out of the nucleus (Siomi and Dreyfuss, 1995).

Post-translational modification through phosphorylation is known to regulate the activity of hnRNPA1 (van der Houven van Oordt et al., 2000; Roy et al., 2014). It was shown that hnRNPA1 binding to RNA is regulated by

phosphorylation at S¹⁹⁹ *in vitro* and *in vivo* (Cobianchi et al., 1993; Jo et al., 2008). hnRNPA1 is a known IRES trans-acting factor (ITAF) involved in regulation of cap-independent translation of certain mRNAs. AKT phosphorylates hnRNPA1 at S¹⁹⁹ and abrogates its strand annealing ability making it ineffective in activating downstream internal ribosome entry site (IRES)-dependent translation of c-Myc and cyclin D1 mRNAs (Jo et al., 2008). Thus, hnRNPA1 phosphorylation causes a downregulation of c-Myc and cyclin D1 expression. However, hnRNPA1 is overexpressed in a variety of cancers (van der Houven van Oordt et al., 2000). A recent research study showed that hnRNPA1 is also phosphorylated at S^{4/6} by S6K2 in response to FGF2 signaling (Roy et al., 2014). hnRNPA1 phosphorylation at S^{4/6} regulates the export of anti-apoptotic mRNAs like BCLXL and XIAP into the cytoplasm. Once in the cytoplasm, phosphorylated S^{4/6} hnRNPA1 dissociates from the mRNAs, releasing their IRES repression. Dissociation of hnRNPA1 correlates with its sumoylation and interaction with 14-3-3 proteins followed by nuclear import. Thus, although hnRNPA1 represses the IRES-dependent expression when bound to the mRNAs, it in turn also causes an increase in mRNA expression by allowing export into the cytoplasm (Roy et al., 2014).

3.1.2 Ribosomal protein S6 (rpS6)

Ribosomal protein S6 (rpS6) is a 40S ribosomal small subunit protein. It is a part of the ribosomal complex and is important to the functioning of the ribosome. In normal conditions, the level of all ribosomal proteins is highly-

regulated in the cell (Warner and McIntosh, 2009; Zengel and Lindahl, 1994). However, cancer cells seem to rely heavily on an increased rate of translation (Dolfi et al., 2013). Thus, inhibition of ribosomal activity is a preferred strategy for cancer treatment (Bhat et al., 2015; Peltonen et al., 2014b). In addition to their classical roles in protein synthesis machinery, many ribosomal proteins also moonlight as regulators of other cellular functions. rpS6 is one of the most studied ribosomal proteins and is known to also regulate cell size, glucose homeostasis, and cell proliferation. rpS6 heterozygous deletion in mice leads to embryonic lethality during gastrulation at day 8.5. Homozygous deletion of $P53^{-/-}$ allows the embryos to survive until day 12.5 suggesting that a p53 mediated checkpoint is activated in response to rpS6 insufficiency (Panic et al., 2006). Thus, *rpS6* gene functions are important for proper development. *rpS6* knockout in hepatocytes halted their proliferation but not growth suggesting activation of a cell-cycle checkpoint in response to the loss of functional 40S subunits.

Phosphorylation plays a crucial role in the regulation of rpS6 functions. Five highly conserved serine residues in rpS6 at S²³⁵, S²³⁶, S²⁴⁰, S²⁴⁴, S²⁴⁷ are phosphorylated in response to different cellular stimuli (Meyuhas, 2008). The major kinase known to phosphorylate rpS6 is named p70S6K (also known as S6K1). rpS6 phosphorylation can be detected in the nucleus as well as in the cytoplasm (Pende et al., 2004a). The yeast homolog has only two phosphorylation sites (Ser²³² and Ser²³³) corresponding to the mammalian

sites S²³⁵ and S²³⁶. Predominantly, ribosomal protein S6 kinases (S6K1 and S6K2) phosphorylate rpS6. Ribosomal protein S6 Kinase (RSK) can also phosphorylate rpS6, albeit at a lower extent. Transgenic mice lacking both S6Ks still show the presence of phosphorylation at homologous sites, suggesting a role for other kinases in phosphorylation (Shima, 1998). rpS6 phosphorylation was present after rapamycin treatment of *S6K1^{-/-}/S6K2^{-/-}* mouse MEFs (Pende et al., 2004a). Thus, another unknown mTOR-independent pathway was thought to be regulating the phosphorylation of rpS6. This residual phosphorylation was sensitive to MAPK/ERK inhibition, thus a kinase regulated by the pathway seems to be regulating this phosphorylation on rpS6 (Pende et al., 2004b).

Since its discovery, rpS6 phosphorylation has been attributed various functions by some conflicting results. It was initially suggested that rpS6 phosphorylation regulates the rate of protein synthesis and phosphorylated rpS6 is mainly associated with polysomes (active ribosomes). However, these results were challenged by the lack of evidence of decreased protein synthesis in knock-in mice carrying alanine substitution mutations at all the 5 phosphorylation sites (Ruvinsky et al., 2005). Moreover, the MEFs from these mice show an increased rate of protein synthesis suggesting an inhibitory role of rpS6 phosphorylation (Ruvinsky et al., 2005). The next function attributed to rpS6 phosphorylation was regulation of 5'-Terminal OligoPyrimidine (5'-TOP) motif containing mRNAs (TOP-mRNAs). These transcripts encode

proteins in the translation machinery. In cellular stress conditions, these cis-regulatory motifs allow conservation of a cell's resources through transcriptional repression of TOP-mRNAs. However, subsequent research proved that regulation of TOP-mRNAs is not a function of phospho-rpS6 or p70S6K (Ruvinsky et al., 2005).

The next clues towards understanding functions of rpS6 phosphorylation also came from rpS6 phospho-null knock-in mice studies, showing a reduced cell size in various cell types (Ruvinsky et al., 2005). The pancreatic beta cells, IL7-dependent hepatic cells, and mouse embryonic fibroblasts derived from rpS6 phospho-null knock-in mice (rpS6^{P-/-}) showed reduced cell sizes compared to wild-type. This phenotype, however, does not manifest in other cell types like the acinar cells in the pancreas. Rapamycin treatment inhibits the mTOR pathway and induces a reduced cell size phenotype. rpS6^{P-/-} MEFs did not show further cell size reduction following rapamycin treatment. Thus, it was concluded that rpS6 phosphorylation is the driver of the cell size change after rapamycin treatment (Ruvinsky et al., 2005).

The following section describes the identification and validation of the proteins hnRNPA1 and rpS6 as Pim kinase substrates. We demonstrate Pim kinases as novel regulators of these proteins, in addition to previously known kinases. We also demonstrate that when a protein is a shared substrate of

two kinases, it can require inhibition of both the kinases to achieve significant dephosphorylation of the protein.

3.2 Results

3.2.1 Pim1 phosphorylates hnRNPA1 *in vitro*

hnRNPA1 was identified as a putative Pim1 substrate from 2D RIKA on total cell lysates of HeLa cells (Xiang Li, unpublished data not shown). To validate hnRNPA1 as a Pim kinase substrate, recombinant hnRNPA1 was purified from bacterial cells and hnRNPA1 phosphorylation was confirmed using purified recombinant hnRNPA1 protein in 1D RIKA for Pim1 (Figure 3.1a).

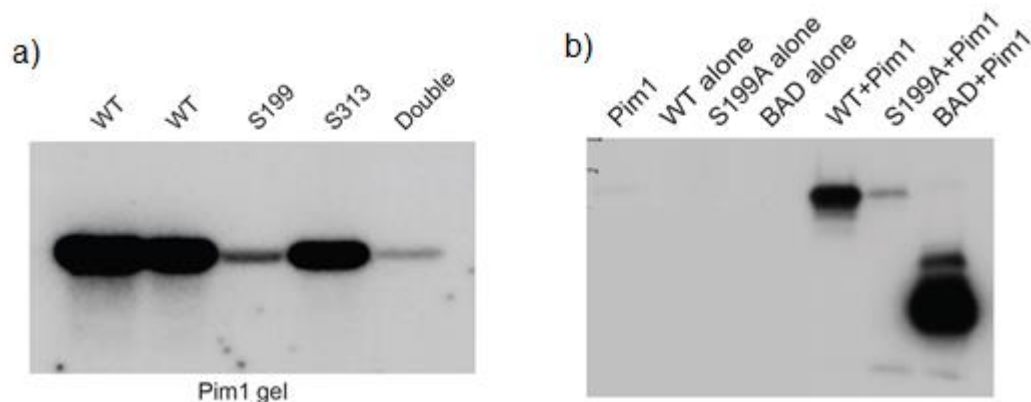


Figure 3.1 Validation of hnRNPA1 phosphorylation and identification of sites. a) Pim1 RIKA for hnRNPA1 WT, S¹⁹⁹A, S³¹³A, and S^{199_313}A double mutant. S¹⁹⁹A mutant shows loss of phosphorylation in RIKA. The two WT lanes have slightly different loading of protein. b) Pim1 *in vitro* kinase assay for hnRNPA1, S¹⁹⁹A, and protein BAD as a positive control.

This experiment was repeated with non-labeled ATP and then the hnRNPA1 band was excised and protein was extracted for LC-MS² analysis.

After trypsin digestion, the phospho-peptides were extracted and LC-MS² was performed. We identified serine 199 (S¹⁹⁹) and serine 313 (S³¹³) as the two possible phosphorylation sites. Both residues are known to be phosphorylated on human hnRNPA1 in cultured cells (Humphrey et al., 2013). Interestingly, a previous study chose to investigate AKT as the kinase phosphorylating hnRNPA1 based on the sequence around S¹⁹⁹. However, AKT (consensus sequence- R-X-R-X-X-S/T) and Pim kinases (consensus sequence- R-X-R-H-X-S) have highly similar consensus sequences and phosphorylate numerous common sites (Dan et al., 2004; Peng et al., 2007; Warfel and Kraft, 2015). The hnRNPA1 sequence N-terminal of S¹⁹⁹ is SQRGRSGS, and it is similar to the Pim consensus phosphorylation site RXRHXS.

To further verify the hnRNPA1 phosphorylation site, alanine substitution mutants were created at either or both sites and were cloned into bacterial expression vectors. Using the IPTG induced lac Z based expression system, recombinant proteins were expressed and 1D RIKA for Pim1 confirmed S¹⁹⁹ as the major phosphorylation site (Figure 3.1a). The phosphorylation due to Pim1 in the 1D Pim1 RIKA was reduced significantly when S¹⁹⁹ was mutated to alanine, but a negligible reduction was observed when S³¹³ was mutated to alanine (Figure 3.1a). The difference in WT hnRNPA1 phosphorylation between lane 1 and 2 is due to a difference in total protein loading (Figure 3.1a). We further validated this finding in an *in vitro*

kinase assay with Pim1 and hnRNPA1 incubated with $\gamma^{32}\text{P}$ -ATP. In agreement with the RIKA results, we found that the S¹⁹⁹A mutation abolishes most of the phosphorylation on hnRNPA1 (Figure 3.1b). Interestingly, *in vivo* AKT can also phosphorylate the site S¹⁹⁹ (Jo et al., 2008). This seems to be a common phenomenon that both of these kinases phosphorylate the same substrate, occasionally at the same site (Warfel and Kraft, 2015).

3.2.2 Confirmation of hnRNPA1 phosphorylation by Pim1 *in vivo*

In order to further validate hnRNPA1 as a physiological Pim1 substrate, we determined whether hnRNPA1 phosphorylation is reduced in response to pharmacological inhibition of Pim1. An antibody recognizing the phosphorylated S¹⁹⁹ epitope on hnRNPA1 was described previously (Jo et al., 2008; Martin et al., 2011). In addition to hnRNPA1 band, the antibody also recognizes a likely nonspecific band which does not respond to Pim inhibitor treatment. Three separate Pim inhibitors, CX6258, SGI1776 and AZD1208 affected hnRNPA1 phospho-status at S¹⁹⁹ as demonstrated by Western blotting for phospho-S¹⁹⁹ hnRNPA1 antibody (Figure 3.2a,b,c) in K562 human chronic myelogenous leukemia cells and MOLM-16 acute myeloid leukemia cells. SGI1776 (dual FLT3 and Pim inhibitor) and CX6258 (pan-Pim inhibitor) treatment induced a clear decrease in hnRNPA1 phospho-status at S¹⁹⁹ (Figure 3.2a,b). Previous study has shown that FBS may block SGI1776, thus we tested the effect of SGI1776 with 10% and 1% FBS. SGI1776 was able to reduce HnRNPA1 phosphorylation with either FBS concentrations. However, another pan-Pim inhibitor AZD1208 exerted a negligible effect on hnRNPA1

phosphorylation in K562 cells (Figure 3.2c lane 7-9). Next, we tested the effect of AZD1208 on hnRNPA1 S¹⁹⁹ phosphorylation in MOLM-16 cells. Indeed, treatment with AZD1208 induced a reduction in hnRNPA1 phosphorylation at S¹⁹⁹ in MOLM-16 cells (Figure 3.2c). However, these effects by Pim inhibitors were not seen in DU145 and PC3 prostate cancer cell lines with low levels of endogenous Pim1 (not shown). This suggests that level of responsiveness corresponds to endogenous Pim1 levels. These data provide strong support for the hypothesis that hnRNPA1 is a direct target of Pim1 in cells.

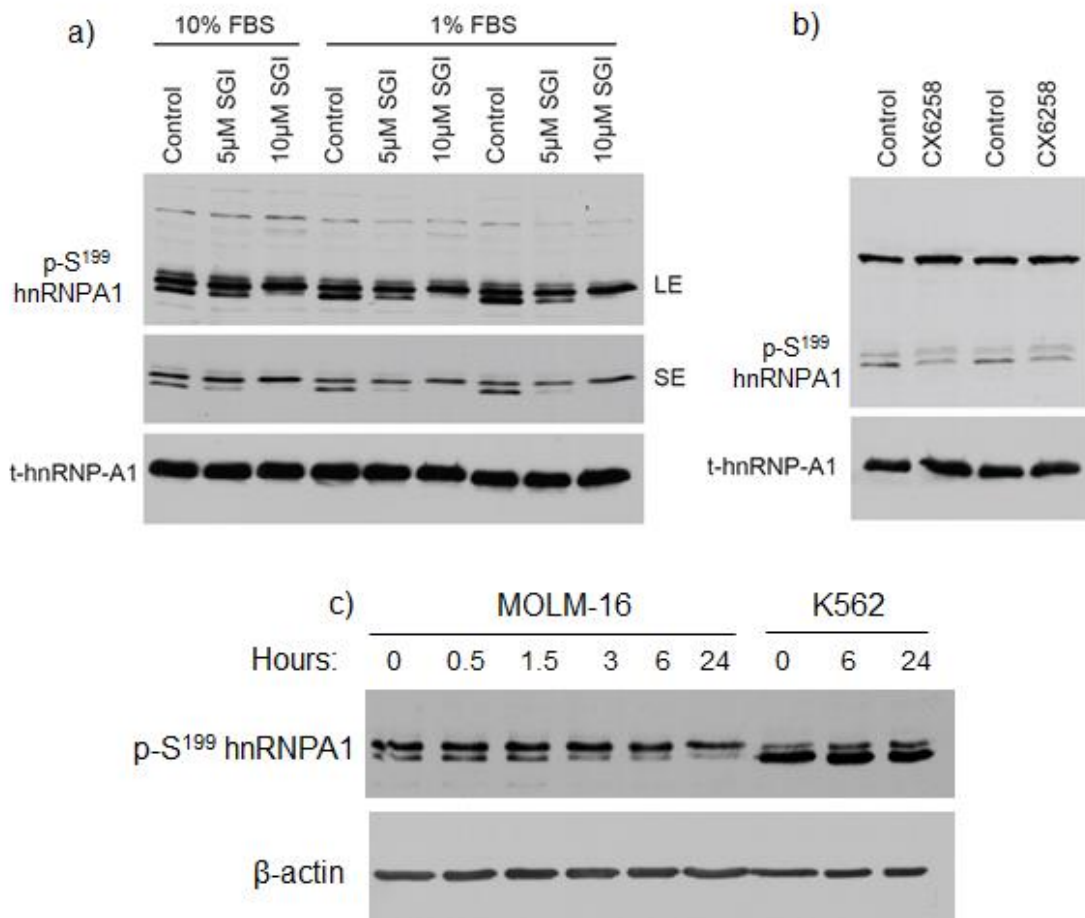


Figure 3.2 Validation of hnRNPA1 phosphorylation in cells. a) K562 cells were treated with indicated SGI1776 concentration for 24hr in presence of 10% or 1% FBS. Top panel shows the phospho S¹⁹⁹-hnRNPA1 blot (long exposure- LE), middle panel shows phospho-S¹⁹⁹ hnRNPA1 (short exposure- SE), and lower panel is total hnRNPA1. b) K562 cells were treated with 20 μM CX6258 for 4 hours. The top panel immunoblot for phospho-S¹⁹⁹-hnRNPA1, lower panel shows total hnRNPA1, c) MOLM-16 and K562 cells were treated with AZD1208 (1 μM) for indicated durations. The top panel shows phospho-S¹⁹⁹-hnRNPA1, lower panel shows immunoblot for β-actin used as a loading control.

3.2.3 Generation of stable cells expressing hnRNPA1 WT, S199A and S199E

hnRNPA1 is a multifunctional protein (Jean-Philippe et al., 2013). Phosphorylation at S¹⁹⁹ affects hnRNPA1's function as an IRES *trans*-acting factor, affecting IRES-dependent regulation of c-Myc and cyclin D1 (Jo et al., 2008). It is known that hnRNPA1 with phosphorylated S¹⁹⁹ can bind to the mRNA but cannot initiate the IRES-mediated expression (Jo et al., 2008). Thus, it is likely that presence of this modification may also affect other functions regulated by hnRNPA1. We transfected PC3 cells with PCDNA3-hnRNPA1 vectors to express wildtype hnRNPA1 and mutants S¹⁹⁹A and S¹⁹⁹E. Serine to alanine substitution in the S¹⁹⁹A hnRNPA1 created a condition of absence of phosphorylation, while a serine to glutamic acid mutation of the S¹⁹⁹E hnRNPA1 created a condition to mimic a negative charge at this site of the protein. Thus, we established PC3 stable lines expressing HA-tagged wild-type (WT), S¹⁹⁹A and S¹⁹⁹E hnRNPA1 (Figure 3.3a). The Western blot analysis for HA antibody showed the expression of HA-tagged protein in all the stably transfected PC3 cell lines. The relative

abundance of exogenous hnRNPA1 proteins observed by Western blot analysis for total protein showed a similar level among the transfected PC3 cell lines. This suggested that mutation of S¹⁹⁹ to alanine or glutamic acid does not cause a decrease in HnRNPA1 protein stability. Next, we tested if the mutations cause a change in localization of hnRNPA1. After performing immunofluorescence for the HA-tag, we observed that the expressed wildtype and mutant proteins predominantly localize to the nucleus. Thus, we did not observe a change in cellular localization upon S¹⁹⁹ mutation (Figure 3.3b). Using MTT assays we measured the growth rate of these transfected cell lines, with and without Pim inhibition (Figure 3.3c). Analysis of MTT data failed to reveal a significant difference in the proliferation of these cells. Thus, in conclusion, mutation of S¹⁹⁹ to alanine or glutamic acid did not affect the stability or localization of the hnRNPA1 protein, and exogenous expression of mutant hnRNPA1 did not affect the proliferation of PC3 cells.

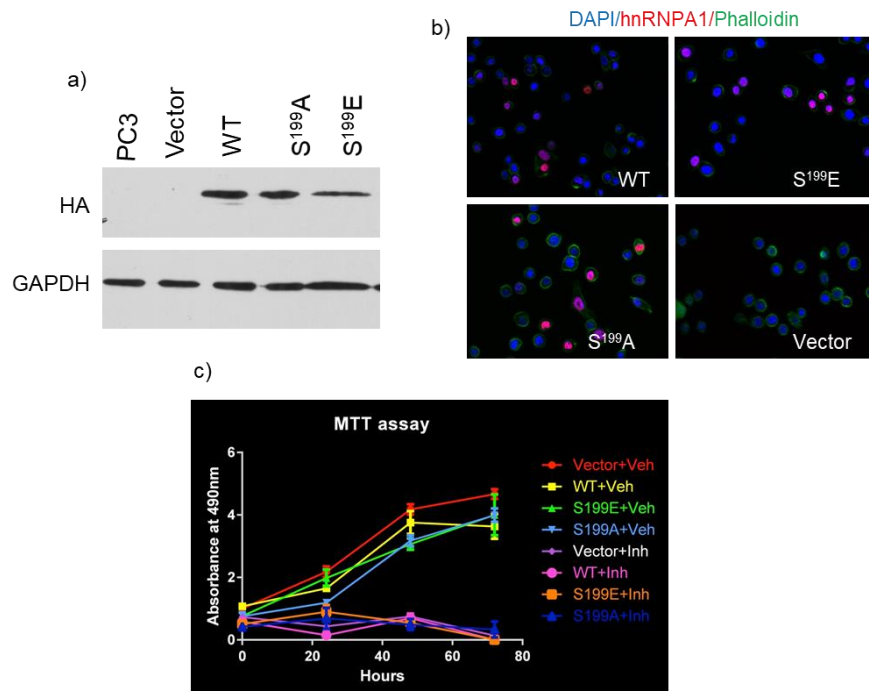
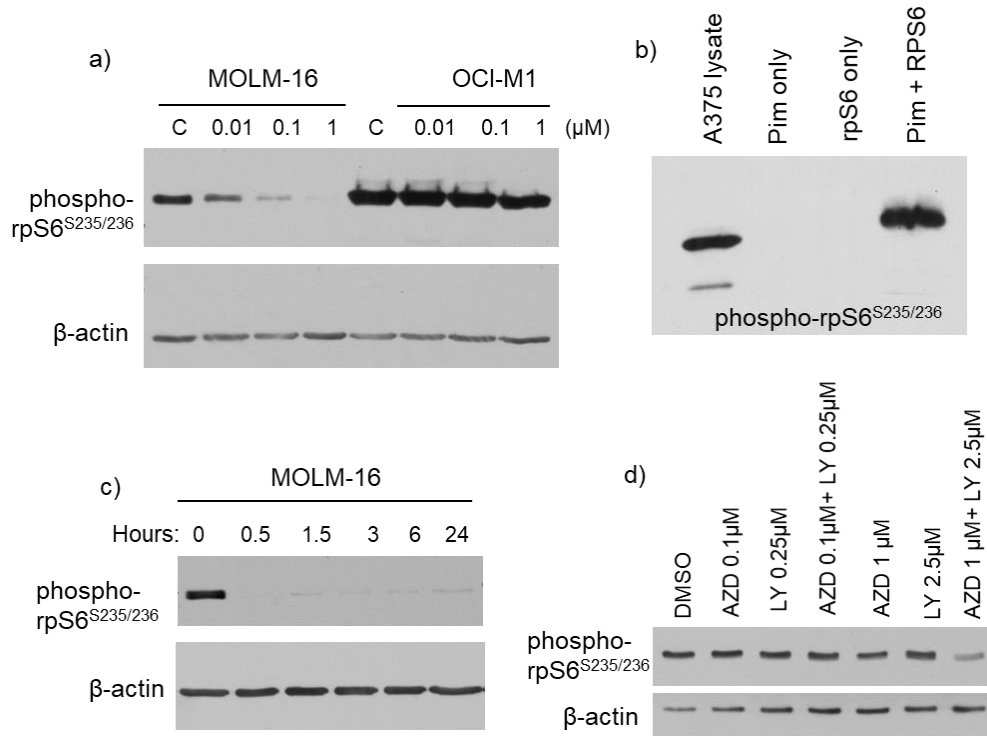


Figure 3.3 Characterization of HA-hnRNPA1 WT and mutant expressing stable cell lines. a) Western blot showing expression of the HA-tagged hnRNPA1 WT, S^{199A}, and S^{199E} in stably transfected PC3 cells. b) Immunofluorescence image for localization of overexpressed hnRNPA1 protein in these cells. c) Representative graph showing proliferation in MTT assay for all 4 cell lines with and without Pim1 inhibition by SGI1776 (10 μ M). (Veh-DMSO, Inh-Pim1 inhibitor).

3.2.4 Identification of rpS6 as a direct Pim kinase substrate

RpS6 was identified as a putative substrate of Pim2 in a Pim2 RIKA (Xiang Li, unpublished data, data not shown). We aimed to determine if rpS6 phosphorylation at S^{235/236} reduces after Pim kinase inhibition with AZD1208. We observed reduction in rpS6 phosphorylation after AZD1208 treatment in MOLM-16 cells but not in OCI-M1 cells (Figure 3.4a). However, this phenotype was previously described as an indirect effect of p70S6K inhibition due to the modulation of mTOR pathway caused by loss of Pim kinase activity (Keeton et al., 2014). Thus, we further analyzed whether Pim kinases can phosphorylate rpS6 *in vitro*. rpS6 was phosphorylated at residues S^{235/236} in a Pim2 *in vitro* kinase assay and validated by Western blotting with the phospho-rpS6 S^{235/236} antibody (Figure 3.4b, Xiang Li, unpublished data). These data suggest that rpS6 is a direct substrate for Pim2.

Figure 3.4 Validation of rpS6 phosphorylation by Pim kinases. a) AZD1208 treatment of MOLM-16 and OCI-M1 cells for 3 hours at denoted concentrations of AZD1208, (C-Control treated with DMSO). b) Western blot for phospho-rpS6^{S235/236} after *in vitro* kinase reaction by Pim2. The A375 cell lysate was used a positive control for phosphorylated rpS6. c) AZD1208 treatment on MOLM-16 cells at the various time points as denoted. Top panel shows immunoblot for phospho-rpS6 and lower blot for β -actin. d) Western blot for OCI-M1 cells treated with AZD1208, or LY2584702, or combination of both. Top panel shows immunoblot for phospho-rpS6 and lower blot for β -actin.



3.2.5 Dual inhibition of Pim kinases and p70S6K is required for effective inhibition of rpS6 phosphorylation in OCI-M1 cells

Pim kinases share overlapping functions and substrates with many other kinases. Thus, to verify whether rpS6 is also a shared substrate between Pim and p70S6K, we tested the effect of Pim inhibition on rpS6 in MOLM-16 cells and OCI-M1 cells. As previously described, Pim inhibition results in a

reduction in rpS6 phosphorylation at S^{235/236} in Pim inhibitor sensitive MOLM-16 cells. Within 30 minutes of treatment, rpS6 phosphorylation is significantly reduced in these cells (Figure 3.4c). However, no change in rpS6 phosphorylation was observed in Pim inhibitor resistant OCI-M1 cells (after 6 hours) (Figure 3.4d). p70S6K is known as a major kinase phosphorylating rpS6 (Bahrami-B et al., 2014). The small molecular inhibitor of p70S6K (LY2584702) has been described previously (Tolcher et al., 2014b). Surprisingly, the treatment of OCI-M1 cells with the p70S6K inhibitor (LY2584702) did not induce a reduction in rpS6 phosphorylation at S^{235/236}. However, only in presence of both the kinase inhibitors we observed a reduction in the level of rpS6 S^{235/236} phosphorylation (Figure 3.4d). Thus, we conclude that Pim kinases and p70S6K regulate compensatory mechanisms for rpS6 phosphorylation in OCI-M1 cells. The *in vitro* and *in vivo* results also support the direct phosphorylation of rpS6 by Pim2.

3.3 Discussion

When using kinase inhibitors for therapy, pharmacodynamic biomarkers are required for assessing response. Antibodies detecting the phosphoprotein substrates are generally used as biomarkers. However, if the protein is shared with other kinases, a change in phosphorylation may be compensated by the activity of the other kinase which may result in false negative observations. hnRNPA1 S¹⁹⁹ phosphorylation was suggested to be a biomarker for AKT inhibition (Martin et al., 2011). Based on our finding,

hnRNPA1 can also be phosphorylated by Pim kinases, thus, both kinase activities will affect the final phosphorylation stoichiometry of this protein and lack of hnRNPA1 response to AKT inhibitors may be due to Pim kinase activity.

Interestingly, hnRNPA1 may serve as a biomarker for AKT and Pim kinase co-therapy. A study using a combination of Pim and AKT inhibitors reported that the changes in phosphorylation of target proteins for either kinase did not correlate with the degree of cytotoxicity induced by the combination of both inhibitors (Meja et al., 2014). Thus, hnRNPA1 may serve as a shared biomarker that can correlate better to the cytotoxic response achieved by combining Pim and AKT inhibitors. Phosphorylation at S¹⁹⁹ is known to affect its function as IRES trans-acting factor for c-Myc and cyclin-D1 mRNAs. AKT also phosphorylates S¹⁹⁹ on hnRNPA1 (Jo et al., 2008). Thus, it is possible that Pim1 controls the activity of hnRNPA1 together with and in absence of AKT signaling. It will be interesting to inhibit both AKT and Pim1 together to see if it causes a greater reduction in the phosphorylation of cellular hnRNPA1 at S¹⁹⁹ and whether Pim inhibition can cause an hnRNPA1-dependent change in IRES-dependent c-Myc and cyclin D1 mRNAs. hnRNPA1 is a multifunctional protein, which regulates transcription, nuclear export and splicing of mRNAs (Jean-Philippe et al., 2013). Thus, other functions may also be regulated by Pim and AKT dependent phosphorylation of hnRNPA1.

rpS6 is another novel protein substrate of Pim kinases identified and validated in this study. Phosphorylation sites on rpS6 are also shared between Pim and p70S6K kinases. Our results from OCI-M1 cells demonstrate the compensatory effect from both kinases in the presence of a single inhibitor (Figure 3.4d). Thus, rpS6 can act as a biomarker for co-inhibition of p70S6K and Pim kinase pathways. Currently, rpS6 is used as an indirect biomarker for Pim responsiveness. As Pim kinases inhibit the PRAS40 (inactivator of mTOR pathway), Pim inhibition leads to inhibition of mTOR and subsequent inhibition of p70S6K leading to decreased rpS6 phosphorylation. However, the loss of rpS6 phosphorylation in OCI-M1 cells after the dual inhibition of p70S6K and Pim kinases did not correspond with a reduction in OCI-M1 cell proliferation. Inhibitors of either kinase did not induce inhibition of OCI-M1 cell proliferation and the combination also did not inhibit cell proliferation (data not shown). Thus, although the absence of rpS6 dephosphorylation can predict Pim inhibitor resistance, the rpS6 hypophosphorylation observed after inhibition may not correlate with reduced AML cell growth. Similar observations were reported in the clinical trial for AZD1208 using rpS6 as marker (Cortes et al., 2016)

As described earlier, rpS6 phosphorylation has been under intense investigation and various conflicting results have attributed different functions to phosphorylation of rpS6 (Meyuhas, 2008; Ruvinsky et al., 2005).

Transgenic mice with alanine substitution mutations (rpS6^{P-/-} mice) at all the five phosphorylation sites were created to validate the functions regulated by these phosphorylations (Ruvinsky et al., 2005). Several cell types in rpS6^{P-/-} showed reduced cell size. Also, mice lacking S6K isoforms showed reduced body size and reduced cell size in certain tissues (Shima, 1998). Interestingly, mice lacking all Pim kinase isoforms (triple knockout) also showed reduced body size and a slightly reduced cell size (Mikkers et al., 2004). The researchers attributed the reduced size of body to reduced cell number based on the studies in spleen and bone marrow cells. It will be interesting to compare the size of affected cell types in rpS6^{P-/-} mice, like the pancreatic β -cells, IL7-dependent fetal liver and mouse embryo fibroblast (MEF) to that of the triple knockout mice. Furthermore, triple Pim knockout and *S6K1*^{-/-}/*S6K2*^{-/-} mice have reduced body size and that phenotype could be a result of reduced phosphorylation of some of the shared substrates including 4EBP1 and rpS6 (Pende et al., 2004a; Shima et al., 1998).

Notably, the *S6K1*^{-/-}/*S6K2*^{-/-} mice show the presence of persistent rpS6 phosphorylation. This phosphorylation was rapamycin-resistant and caused by a mTOR independent kinase. p90RSK was identified as a possible candidate, and Pim kinases might also be responsible for this activity (Pende et al., 2004b). Given the role of Pim2 in driving mTOR independent signaling leading to chemoresistance, this function of rpS6 phosphorylation might also be shared between mTOR dependent S6Ks and independent p90RSK and

Pim kinases (Fox et al., 2005). In addition to the p90RSK activity regulated by MAPK-MEK-ERK pathway, Pim kinases can also be indirectly regulated by the MAPK pathway by regulating the NF κ B- dependent transcription of Pim kinases (Dhawan and Richmond, 2002). Notably, the effect of MAPK inhibition indirectly inhibiting p90RSK could only be observed in the absence of S6K activity (Pende et al., 2004b). On the contrary, we observed similar contributions between Pim kinase and S6K inhibition in reducing rpS6 phosphorylation in OCI-M1 cells (Figure 3.4c). Neither inhibitor alone was able to affect the phosphorylation of rpS6. Thus, Pim activity may be relevant for rpS6 phosphorylation at least in certain cell types.

In conclusion, we have identified novel substrates of Pim kinases shared with other kinases that are relevant for therapeutic intervention in cancer. Thus, these shared phosphorylation events on the substrates can function as biomarkers for combinatorial therapy targeting the kinases.

3.4 Materials and methods

Plasmid construction and cloning

Human hnRNPA1 cDNA was procured from Open Biosystems and cloned into PQE80L plasmid for bacterial expression, and into a mammalian expression vector pcDNA3 that includes a HA tag. The sites S199 and S313 were mutated to alanine using site directed mutagenesis by PCR. The site S199 was also mutated to glutamic acid to create a phosphomimetic mutation

and cloned in HA tag containing pcDNA3 vector. DH10 α cells were transformed with these vectors using electroporation and ampicillin-resistant transformed clones were selected, and validated by PCR and confirmed by DNA sequencing (Genewiz). DNA sequencing confirmed the integrity of the entire sequence and absence of random mutations. Confirmed PQE80L plasmids were transformed in BL21 cells for efficient protein expression. rpS6 was cloned in PQE80L plasmid by Dr. Xiang Li.

Recombinant protein production

BL21 cells transformed with PQE80L-hnRNPA1 plasmids were expanded into 2-liter culture and protein expression was induced by adding IPTG (5 mM). Cells were typically induced at 37°C for 4 hours. Induced cells were lysed under high pressure using a French press. Recombinant protein was pulled down using Ni²⁺-affinity chromatography and washed with either buffer containing urea (denatured protein purification: 20 mM Imidazole, 8 M urea, 100 mM Sodium phosphate), or buffer B (native protein purification: 300 mM NaCl, 100 mM Sodium phosphate, 20 mM Imidazole). Recombinant proteins were eluted using buffer containing high concentration of imidazole (250 mM Imidazole instead of 20 mM). Native elution buffer was supplemented with protease inhibitor cocktail. Using the procedure mentioned above, recombinant Pim1, hnRNPA1 WT, hnRNPA1 S¹⁹⁹A, and hnRNPA1 S³¹³A were expressed and isolated from bacterial BL21 cells. rpS6 was purified by

Dr. Xiang Li and protein BAD (used as positive control) was purified by previous graduate student Dr. Nicole Barkley.

In vitro kinase assay

In vitro kinase assays were previously described (Li et al., 2007). Briefly, to validate hnRNPA1 as a substrate of Pim1, recombinant hnRNPA1 (WT) and mutants S¹⁹⁹A and S¹⁹⁹E hnRNPA1 were incubated with recombinant Pim in buffer containing $\gamma^{32}\text{P}$ labeled ATP. After 1 hour incubation, the reaction was stopped by adding 2X Laemmli sample buffer. Proteins were resolved on 12% SDS-PAGE and transferred to a PVDF (Immobilon® 0.45 μm) membrane. Phosphorylation was detected by autoradiography.

Reverse in-gel Kinase assay (RIKA)

The technique of RIKA was previously established in our lab (Li et al., 2007). RIKA is a kinase substrate profiling technique that identifies direct substrates of kinases with high efficiency and a low false positive rate (Li et al., 2007). Use of radioisotope labeling and fractionated cellular extracts makes this method highly sensitive for identification of substrate in the pico molar range. For 1D RIKA, 20 $\mu\text{g/ml}$ of Pim1 in 8 M Urea, 50 mM NaH₂PO₄, 300 mM NaCl, 250 mM imidazole, 0.1% Tween was co-polymerized in SDS PAGE gel. Recombinant wildtype and mutant hnRNPA1 proteins were resolved by SDS-PAGE in gel containing recombinant Pim1 kinase. The RIKA protocol was

followed as previously described (Li et al., 2007). Following RIKA, the signals were visualized by autoradiography.

Identification of hnRNPA1 phosphorylation sites after Pim1 RIKA

Recombinant hnRNPA1 was resolved in gel with co-polymerized recombinant Pim1 and 1D RIKA was performed using non-radioactive ATP. The hnRNPA1 band was excised and peptides were isolated by in-gel trypsin digestion and purified. These samples were resolved by nano flow HPLC followed by peptide sequencing and identification of phosphorylation using Thermo fisher LTQ XL Mass spectrophotometer at the molecular characterization and analysis complex (MCAC) at UMBC.

Western blotting

Cells were lysed in denaturing buffer containing urea (7 M Urea, 2 M thiourea, 20 mM DTT, 1% C7BZ0, 20 mM Tris pH 7.5) to retain the physiological phosphorylations on proteins. Total proteins were quantified using Bradford colorimetric analysis. 20-25 µg total cell lysate was resolved on 12-14% acrylamide depending on the molecular weight of the protein of interest. Resolved proteins were transferred to PVDF membranes (Immobilon® 0.45µm) at 100V for 60 minutes or 30V for 16 hours. After protein transfer to PVDF membrane, the membranes were blocked in 5% BSA or 5% non-fat milk in TBST (1X). Primary antibody incubation was carried out at 4°C overnight, or at room temperature for 1 hour depending recommended

dilution and duration in manufacturer's guidelines. Secondary antibody incubation was carried out for 1 hour in 0.5% BSA diluted by 1:10000. The Table 3.1 provides list of antibodies used for this study. Secondary antibodies used- anti-rabbit IgG, HRP-linked antibody (Cell signaling technology, #7074) and anti-mouse IgG, HRP-linked antibody (Cell signaling technology, #7076). Chemiluminescent substrate ECL was used to detect HRP conjugated antibodies.

Antigen	Species	Dilution fold	Incubation	Vendor/Catalog
phospho-RPS6 (235/236)	Rabbit	2000-5000	4°C overnight	CST (#2211)
Actin (Beta)	Mouse	5000	RT 1 hour	Thermo (BA3R)
Human hnRNPA1 (Total)	Mouse	5000	4°C overnight	Sigma (R4528)
HA tag	Rat	5000	RT 1 hour	Roche (3F10)
Human Pim1	Mouse	500	4°C overnight	Santacruz (12H8)
phospho-HnRNPA1 S199	Rabbit	2000	4°C overnight	Gift from Dr. Joseph Gera's Lab (UCLA)
phospho-SR protein	Mouse	1000	4°C overnight	Life tech. Ref# 339400

Table 3.1 List of antibodies used

Cell culture

The cell lines PC3 and K562 were procured from ATCC, and MOLM-16, EOL-1 and OCI-M1 were purchased from DSMZ and maintained according to the recommended conditions at 5% CO₂ and 37°C. Antibiotics, antimycotics and

antimycoplasma were added to the culture media to avoid any contaminations. PC3 cells were grown in RPMI 1640 (Corning Cellgro, #10-040-CV) with 10% FBS. K562 cells were cultured in Iscove's modified Dulbecco's medium (IMDM) (Corning Cellgro, #10-016-CV) with 10% FBS. MOLM-16 and EOL-1 cells were grown in RPMI 1640 with 20% FBS. OCI-M1 cells were grown in IMDM with 20% FBS.

Inhibitor treatments

In this study pharmacological inhibitors of Pim kinases and p70S6 kinase were used. For each experiment, indicated number of cells was seeded, one day prior to the treatment. These cells were treated with indicated concentration of inhibitors for given duration as denoted in the figure legends. Unless otherwise noted, complete medium with FBS and antibiotics was used to dilute the inhibitors. AZD1208 (pan-Pim inhibitor) (MedKoo Biosciences: 205763), Ly2584702 (p70 S6 kinase Inhibitor) (Selleck chemicals: S7704), SGI1776 (pan-Pim inhibitor from AdooQ bioscience: A10838), CX-6258 (pan-Pim inhibitor) (Gift from Cylene pharmaceuticals) were diluted in DMSO.

Immunofluorescence

Attached cells were grown to ~70% confluency on cover slips placed in a 6-well plate. Cells were fixed in 4% PFA and treated with 0.2% Triton-X 100 and 1% newborn goat serum (NGS) in 1X PBS in humid chamber for 10 minutes to detect nuclear antigens. Blocking was done in 1% BSA in PBS (1X) and

primary antibody was diluted in 1% NGS in PBS (1X). Primary incubation was carried out by placing the cell coated cover slips in 6-well culture plates followed by adding anti-HA tag antibodies at 1:200 dilution and with gentle rocking at 4°C overnight. 1% NGS in PBS (1X) was used to wash the unbound antibody. Fluorescently tagged secondary antibodies (Cy3 tagged) were diluted in 1% NGS in PBS (1X) at 1:200 and incubated for 1 hour in dark. Nuclei were stained with DAPI as a counter stain. The Zeiss Axioimager Z1 microscope equipped with Apotome structural interface system at the lab of Dr. Michelle Starz-Gaiano (UMBC) was used to visualize and capture the images.

Transfection

HnRNPA1, either WT or mutant (S¹⁹⁹A, S¹⁹⁹E) was cloned into a modified pcDNA3 vector coding for an in-built HA tag on N-terminus and 6His-tag. The modified empty vector was used to transfect PC3 cells as a negative control. Cells stably expressing exogenous protein were selected by G418 (50 µg/ml-200 µg/ml) treatment for up to 6 weeks. The cell lines were maintained in G418 containing growth medium (100 µg/ml) and intermittently given a cycle through higher concentration of G418 to maintain stable transfection.

Chapter 4: Discussion and future directions

Intense investigation fueled by commercial and academic interest has brought us to the verge of a revolution in the field of personalized medicine for cancer treatment. The last two decades have seen an exponential increase in the number of inhibitors in the clinical pipeline, and kinase inhibitors already approved for cancer therapy (Wu et al., 2015). Thus, protein kinase inhibitors are positioned perfectly to play a pivotal role in this revolution. However, inherent and acquired inhibitor resistance, lack of predictive and pharmacodynamic biomarkers, and drug-related toxicity remain as major roadblocks. Therefore, there is an urgent need for identifying novel inhibitor responsive biomarkers and rational effective co-therapies, to identify patients who will benefit from these treatments, and to achieve a therapeutic response in more patients. We hypothesized that the knowledge of kinase substrates and pathways regulated by a kinase can be used to identify biomarkers and to rationalize synergistic combinations. To systematically test this hypothesis, using Pim kinases as an example, we have used the knowledge of novel substrates to identify putative inhibitor responsive biomarkers and synergistic drug combinations that show promise to treat AML. This chapter will dive deeper into the broad applications and significance of our findings, while also identifying goals for future research.

4.1 Pathways regulated by Pim kinases

To the best of our knowledge, this work provides the first insights into a previously unidentified role for Pim kinases in the regulation of two RNA processing mechanisms; pre-mRNA splicing and pre-rRNA processing.

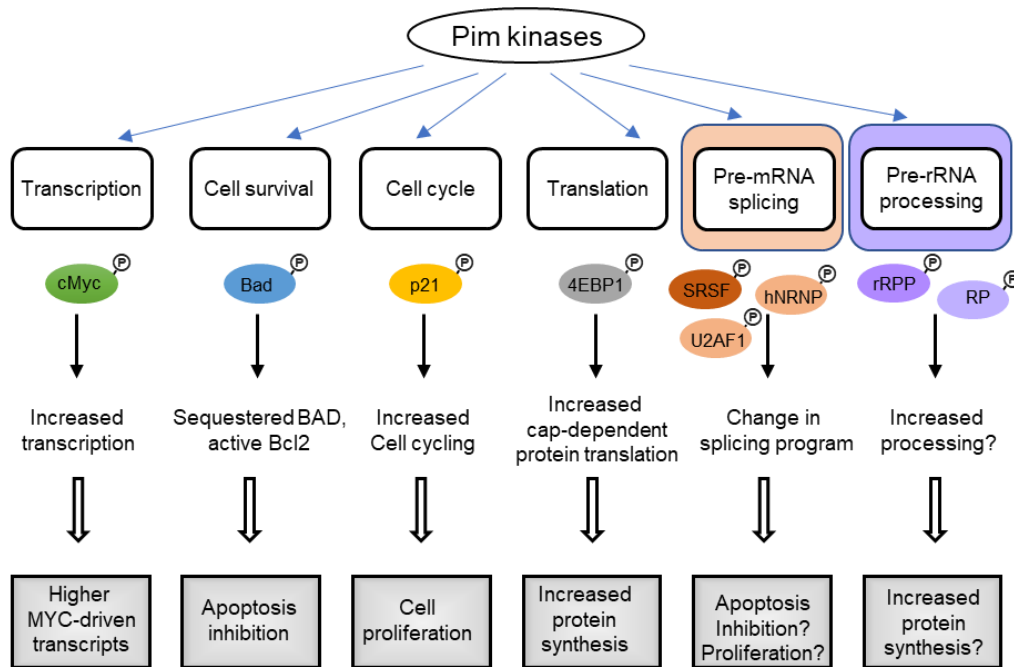


Figure 4.1 Novel and known pathways regulated by Pim kinases. Our work demonstrates that Pim kinases regulate novel RNA processing pathways: pre-mRNA splicing and pre-rRNA processing. These newly identified functions are depicted in the figure in addition to the known Pim functions. Our study shows that Pim kinases phosphorylate several splicing factors including SRSFs, hnRNPs and others. Through the regulation of pre-mRNA alternative splicing mediated by these substrates, Pim kinases could change the cellular splicing programs to evade apoptosis and increase proliferation in cells. Novel Pim kinase substrates also include rRNA processing factors and ribosomal proteins. Regulation of pre-rRNA processing by Pim kinase-dependent phosphorylation of these proteins, could contribute to the known Pim-dependent increase in protein synthesis (adapted from (Chen et al., 2011)).

The schematic Figure 4.1 depicts these new functions of Pim kinases in addition to the currently known functions. We speculate that the functions of the splicing factor substrates are regulated by Pim-dependent phosphorylation. These factors may regulate splicing of key players in survival and proliferation pathways. Thus, Pim activity can indirectly affect the relative abundance of these isoforms causing a modulation of their respective cellular functions. Pim inhibition is known to trigger apoptosis and cell cycle arrest causing inhibition of cell proliferation in various cancer cell lines (Chen et al., 2009; Keeton et al., 2014; Mumenthaler et al., 2009; Zemskova et al., 2008). The inhibitor-induced splicing changes may be contributing towards these cell fates. For example, Pim kinase inhibitors are known to activate several arms of the UPR pathway in prostate cancer cells (Song and Kraft, 2012). CHAC1 is induced by the ATF3 arm of the UPR pathway, and its over-expression induces apoptosis in human embryonic kidney cells (Mungrue et al., 2008). Pim inhibitor AZD1208 induces a switch in splicing between the two CHAC1 isoforms. These two CHAC1 isoforms might have different cellular functions. It will be extremely interesting to study the functional differences between CHAC1 isoforms and their roles in the regulation of ER-stress-induced apoptosis in the context of Pim activity.

Up-regulation of Pim kinases in cancer cells may change the profile of alternative pre-mRNA splicing, and contribute to the oncogenic functions of Pim kinases. Upon metformin treatment, ALL cells undergo ER stress/UPR

mediated apoptosis (Leclerc et al., 2013). Ironically, transcription of Pim2 is activated in response to metformin, which helps to protect ALL cells from metformin (Leclerc et al., 2013). Thus, protection from ER-stress-related apoptosis may be a function of Pim kinases in cancer. Thus, future research might focus on determining the effect of Pim over-expression on the switch in CHAC1 splicing and whether it contributes to the evasion of apoptosis.

The regulation of pre-rRNA processing by Pim kinases has broad implications to the functional relevance of Pim kinases in cancer. rRNA processing mainly takes place in the nucleoli. Enlargement of the nucleolus and increase in the number of nucleoli are key features of many aggressive cancers (Derenzini et al., 1998; Orsolich et al., 2016). The study of nucleolar proteins revealed that over 15 kinases are present in the nucleolus (Andersen et al., 2005). However, knowledge regarding the role of protein kinases in the regulation of pre-rRNA processing is lacking. Since Pim inhibition affects multiple pre-rRNA processing steps in AML cells, and causes accumulation of precursors, it most likely decreases the rate of rRNA maturation. Thus, it remains to be investigated whether over-expression of Pim kinases can cause an increase in the rate of rRNA maturation. Pim kinase-dependent regulation of pre-rRNA processing may result in an increased rate of processing to match the demands in proliferating cells. Protein translation has been identified as a major target for Pim inhibitors, and we hypothesize that

inhibition of rRNA processing contributes to this previous observation (Keeton et al., 2014; Yang et al., 2012).

hRIO kinases are among the few kinases implicated in regulations of pre-rRNA processing. hRIO1 regulates the processing of 18S-E, and co-sediments with the ribosome 40S subunit (Widmann et al., 2012). Interestingly, Pim1 also co-sediments with the 80S subunits, and to a lesser extent with free 40S subunits (Chiocchetti et al., 2005). Analogous to the role of hRIO1, we have observed processing changes in rRNAs of both small and large sub-units after inhibition of Pim activity. However, it also remains to be decided if Pim kinase interaction with ribosome is necessary for any of these processing steps. Small molecular inhibitors that target Rio1 have been developed and were shown to inhibit *Archeoglobus fulgidus* (AfRio1) (Mielecki et al., 2013). Specific inhibitors may be developed to target hRIO in future. Co-inhibition of Pim and hRIO kinases may be another putative avenue to future investigation for cancer treatment.

Recently, Tor1 (yeast mTOR) and CK2 were shown to control a processing switch between two rRNA maturation pathways in yeast (Kos-Braun et al., 2017). It remains to be investigated whether mTOR and CK2 mediate pre-rRNA processing switch in human cells. However, this function of Tor1 was independent of Sch9 (yeast homolog of S6K) (Kos-Braun et al., 2017). Interestingly, S6 kinase has been implicated in the transcriptional

regulation of ribosome biogenesis factors in human cells (Chauvin et al., 2014). We demonstrate that the inhibition of p70S6K did not induce processing defects similar to those observed after Pim inhibition. This observation has two implications- first, the recent discovery in yeast supports our finding that S6K activity does not regulate pre-rRNA processing, and second, it provides evidence that an indirect effect of deregulation of ribosome biogenesis did not cause pre-rRNA processing defects. Thus, the effect of Pim kinase inhibition is likely a direct effect of phosphorylation of rRNA processing factors.

Mice having genetic deletions of all the three Pim kinases are viable and fertile. However, these triple knockouts (TKO) have small body size and impaired hematopoiesis (An et al., 2013) MEFs from Pim TKO mice show reduced rates of protein synthesis and growth (Beharry et al., 2011). Perturbation of rRNA processing may be partly responsible for the slower rate of protein synthesis. Thus, using Northern blot analysis, the pre-rRNA abundance can be compared to wild type MEFs.

Another approach to studying Pim-dependent RNA processing mechanisms can involve CRISPR-mediated mutations to create alanine substitution of Pim kinase phosphorylation sites on the substrates, followed by reporter assay for splicing defects, or Northern blot analysis for rRNA processing. Using this method, the individual functional significance of Pim-

dependent phosphorylation can be revealed. Through comparative analysis of pre-rRNA profiles, after Pim inhibition to the known pre-rRNA profiles of Pim substrate-rRNA processing factors, (presented in Table 2.5), we have identified two putative substrates UTP20 and NGDN, which could be further investigated for their roles in the Pim-dependent regulation of rRNA maturation.

4.2 Biomarkers for Pim kinase inhibitor responsiveness

Our work has identified two types of biomarkers for kinase inhibitors. The first type of putative biomarkers is alternative splicing changes caused by Pim inhibition. Previous studies on breast and ovarian cancer tissues found alternative splicing events (ASEs) that were solely associated with the respective cancers, and a set of overlapping ASEs from both cancers (Klinck et al., 2008; Venables et al., 2008). By measuring these ASEs, the researchers were able to distinguish between normal and cancer tissues, and also classify the tumors further by grade (Venables et al., 2008). We speculate that the Pim inhibitor-induced AS changes can be applied to distinguish between Pim inhibitor responsive and non-responsive patients. We demonstrated that the responsiveness of AML cell lines to Pim inhibitor correspond with the occurrence of alternative splicing changes after inhibitor treatment. To identify a panel of Pim-dependent alternative splicing changes, the analysis presented here can be repeated for other known responsive and nonresponsive cell lines (Meja et al., 2014). Comparing the results for all cell

lines, the top 15 most robust and consistent AS changes can be identified as alternative splicing markers. After *in vitro* Pim inhibition in patient samples, the modulation of these alternative splicing markers can then be tested in addition to growth assay to observe the correlation between inhibitor responsiveness and alternative splicing changes. The second type of putative biomarkers identified by this study is rRNA processing defects induced by Pim kinase inhibition. The changes in pre-rRNA abundance were observed in Pim inhibitor responsive AML cell lines and not in OCI-M1 cells. Similar to the changes in alternative splicing, we could also test the pre-rRNA processing defects in other cell lines and patient samples to test the correlation between inhibitor responsiveness and change in pre-rRNA abundance.

We have also shown the regulation of hnRNPA1 and rpS6 phosphorylation by Pim kinases in AML cell lines. We identified phosphorylation sites on both of these proteins. We show by creating alanine substitution mutations, or by use of phospho-site-specific antibodies that S199 on hnRNPA1 is phosphorylated by Pim1, and S²³⁵/S²³⁶ of rpS6 are phosphorylated by Pim2. However, the fact that phosphorylation sites on both of these proteins are shared substrates with other kinases, provides an opportunity to test them as biomarkers for combined inhibition. AKT is known to phosphorylate S199 of hnRNPA1 (Jo et al., 2008). Also, Pim and AKT co-inhibition were shown to be an effective strategy to overcome inhibitor resistance in AML cell lines and primary patient samples (Meja et al., 2014).

Thus, hnRNPA1 may serve as a good biomarker for observing the effect of Pim and AKT co-inhibition.

4.3 Putative therapeutic drug combinations for AML treatment

The Pharmacological audit trail (PhAT) provides guidelines for the development of anticancer drugs and identifies clear milestones for a successful therapeutic agent. Some of the aspects of PhAT are; 1) identification of patient population that will benefit from the treatment, 2) establishing proof of pathway modulation by use of biomarkers, 3) identifying strategies to overcome resistance by combination or sequential therapy (Banerji and Workman, 2016). These guidelines are recommendations for researcher and some of these have been implemented in cancer therapeutics development (Chapman et al., 2011; Kwak et al., 2010). In order to apply these parameters to kinase inhibitor oncotherapy, responsive biomarkers and effective therapeutic combinations are required for all the targeted kinases. In this study, we have described a substrate-guided approach to identify synergistic combinations with kinase inhibitors. These combinations have a high propensity of success because they target crucial cellular mechanisms driven by the kinase in question. Thus, using this method, researchers can make informed decisions to test inhibitor combinations for other kinases. An example of such a kinase is the NPM-ALK fusion protein kinase found in lymphoma and lung cancers (Pearson et al., 2012). ALK inhibitors have been approved for therapy in non-small cell lung cancer NSCLC (Awad and Shaw,

2014). High-throughput RIKA technology can be applied to profile new substrates of NPM-ALK. The substrate-profile can guide future therapeutic combinations that can be tested against NSCLC.

We have identified four synergistic inhibitor combinations that can be used to target AML cells. Notably, the combination of AZD1208 and BMH21 was effective against all AML cell lines and showed highest synergistic potential against OCI-M1 cells. Thus, this combination may be used to overcome the resistance to Pim inhibitors similar to that observed in OCI-M1 cells. rRNA biogenesis and maturation have emerged as important targets for cancer therapy (Brighenti et al., 2015). BMH21 inhibits the synthesis of rRNA by RNA pol I (Peltonen et al., 2014a). Recently, another RNA pol I inhibitor CX5461 was shown to inhibit AML tumor growth in patient-derived xenograft (PDX) models for AML (Hein et al., 2017). The combination of CX5461 with Pim inhibitor CX-6258 showed improved efficacy, reduced proliferation, and increased cell death of PDX model of prostate cancer. Thus, the combination of AZD1208 and BMH21 may also be effective against other cancers that are addicted to Pim activity.

Another effective strategy for putative AML therapy identified by this study is the combination of Pim inhibitors with spliceosome inhibitors. A subset of AML patients show a high incidence of splicing factor mutations (Scott and Rebel, 2013). These mutations may cause deregulated splicing

and drive the disease pathogenesis. Thus, inhibition of spliceosome may be an effective strategy against these subtypes of AML. However, the clinical trial for spliceosome inhibitor E7107 for solid malignancies had to be terminated due to treatment-related vision impairment in two patients, despite showing a dose-dependent inhibition of splicing in peripheral monocytes from the patients (Dehm, 2013; Eskens et al., 2013). Use of synergistic combinations may also allow the reduction of individual drug dosage without reducing the efficacy. Thus, the synergistic combination of Pim inhibitors with spliceosome inhibitors may be needed in the future to reduce dose-limiting toxicities observed with spliceosome inhibition.

In conclusion, we describe a method to translate the knowledge of broad kinase-substrate profiles into testable hypotheses driving discovery of therapeutic synergies for oncology treatment.

References

- Adamia, S., Haibe-Kains, B., Pilarski, P.M., Bar-Natan, M., Pevzner, S., Avet-Loiseau, H., Lode, L., Verselis, S., Fox, E.A., Burke, J., et al. (2014). A Genome-Wide Aberrant RNA Splicing in Patients with Acute Myeloid Leukemia Identifies Novel Potential Disease Markers and Therapeutic Targets. *Clin. Cancer Res.* *20*, 1135–1145.
- Agrawal, A.A., Salsi, E., Chatrikhi, R., Henderson, S., Jenkins, J.L., Green, M.R., Ermolenko, D.N., and Kielkopf, C.L. (2016). An extended U2AF(65)-RNA-binding domain recognizes the 3' splice site signal. *Nat. Commun.* *7*, 10950.
- Aho, T.L.T., Sandholm, J., Peltola, K.J., Mankonen, H.P., Lilly, M., and Koskinen, P.J. (2004). Pim-1 kinase promotes inactivation of the pro-apoptotic Bad protein by phosphorylating it on the Ser112 gatekeeper site. *FEBS Lett.* *571*, 43–49.
- Alvarado, Y., Kantarjian, H.M., Luthra, R., Ravandi, F., Borthakur, G., Garcia-Manero, G., Konopleva, M., Estrov, Z., Andreeff, M., and Cortes, J.E. (2014). Treatment with FLT3 inhibitor in patients with *FLT3*-mutated acute myeloid leukemia is associated with development of secondary *FLT3*-tyrosine kinase domain mutations. *Cancer* *120*, 2142–2149.
- Amaravadi, R., and Thompson, C.B. (2005). The survival kinases Akt and Pim as potential pharmacological targets. *J. Clin. Invest.* *115*, 2618–2624.
- Amin, E.M., Oltean, S., Hua, J., Gammons, M.V.R., Hamdollah-Zadeh, M., Welsh, G.I., Cheung, M.K., Ni, L., Kase, S., Rennel, E.S., et al. (2011). WT1 Mutants Reveal SRPK1 to Be a Downstream Angiogenesis Target by Altering

VEGF Splicing. *Cancer Cell* 20, 768–780.

An, N., Kraft, A.S., and Kang, Y. (2013). Abnormal hematopoietic phenotypes in Pim kinase triple knockout mice. *J. Hematol. Oncol.* 6, 12.

Andersen, J.S., Lam, Y.W., Leung, A.K.L., Ong, S.-E., Lyon, C.E., Lamond, A.I., and Mann, M. (2005). Nucleolar proteome dynamics. *Nature* 433, 77–83.

Aravantinos, G., and Pectasides, D. (2014). Bevacizumab in combination with chemotherapy for the treatment of advanced ovarian cancer: a systematic review. *J. Ovarian Res.* 7, 57.

Awad, M.M., and Shaw, A.T. (2014). ALK inhibitors in non-small cell lung cancer: crizotinib and beyond. *Clin. Adv. Hematol. Oncol.* 12, 429–439.

Back, S.H., Schröder, M., Lee, K., Zhang, K., and Kaufman, R.J. (2005). ER stress signaling by regulated splicing: IRE1/HAC1/XBP1. *Methods* 35, 395–416.

Bae, J., Leo, C.P., Yu Hsu, S., and W Hsueh, A.J. (2000). MCL-1S, a Splicing Variant of the Antiapoptotic BCL-2 Family Member MCL-1, Encodes a Proapoptotic Protein Possessing Only the BH3 Domain*.

Bahrami-B, F., Ataie-Kachoie, P., Pourgholami, M.H., and Morris, D.L. (2014). p70 Ribosomal protein S6 kinase (*Rps6kb1*): an update. *J. Clin. Pathol.* 67, 1019–1025.

Bain, J., Plater, L., Elliott, M., Shpiro, N., Hastie, C.J., Mclauchlan, H., Klevernic, I., Arthur, J.S.C., Alessi, D.R., and Cohen, P. (2007). The selectivity of protein kinase inhibitors: a further update. *Biochem. J.* 408, 297–315.

- Banerji, U., and Workman, P. (2016). Critical parameters in targeted drug development: the pharmacological audit trail. *Semin. Oncol.* 43, 436–445 .
- Baselga, J., Cortés, J., and Kim, S. (2012). Pertuzumab plus Trastuzumab plus Docetaxel for Metstatic Breast Cancer. *N. Engl. J. Med.* 7, 109–119.
- Beharry, Z., Mahajan, S., Zemskova, M., Lin, Y.-W., Tholanikunnel, B.G., Xia, Z., Smith, C.D., and Kraft, A.S. (2011). The Pim protein kinases regulate energy metabolism and cell growth. *Proc. Natl. Acad. Sci.* 108, 528–533.
- Bennett, J.M., Young, M.L., Andersen, J.W., Cassileth, P.A., Tallman, M.S., Paietta, E., Wiernik, P.H., and Rowe, J.M. (1997). Long-term survival in acute myeloid leukemia: the Eastern Cooperative Oncology Group experience. *Cancer* 80, 2205–2209.
- Berglund, J.A., Abovich, N., and Rosbash, M. (1998). A cooperative interaction between U2AF65 and mBBP/SF1 facilitates branchpoint region recognition. *Genes Dev.* 12, 858–867.
- Bertwistle, D., Sugimoto, M., and Sherr, C.J. (2004). Physical and functional interactions of the Arf tumor suppressor protein with nucleophosmin/B23. *Mol. Cell. Biol.* 24, 985–996.
- Bhat, M., Robichaud, N., Hulea, L., Sonenberg, N., Pelletier, J., and Topisirovic, I. (2015). Targeting the translation machinery in cancer. *Nat. Rev. Drug Discov.* 14, 261–278.
- Biankin, A. V., Waddell, N., Kassahn, K.S., Gingras, M.-C., Muthuswamy, L.B., Johns, A.L., Miller, D.K., Wilson, P.J., Patch, A.-M., Wu, J., et al. (2012). Pancreatic cancer genomes reveal aberrations in axon guidance pathway genes. *Nature* 491, 399–405.

Blethrow, J.D., Glavy, J.S., Morgan, D.O., and Shokat, K.M. (2008). Covalent capture of kinase-specific phosphopeptides reveals Cdk1-cyclin B substrates. *Proc. Natl. Acad. Sci.* *105*, 1442–1447.

Brighenti, E., Treré, D., and Derenzini, M. (2015). Targeted cancer therapy with ribosome biogenesis inhibitors: a real possibility? *Oncotarget* *6*, 38617–38627.

Brunen, D., García-Barchino, M.J., Malani, D., Basheer, N.J., Lieftink, C., Beijersbergen, R.L., Murumägi, A., Porkka, K., Wolf, M., Zwaan, C.M., et al. (2016). Intrinsic resistance to PIM kinase inhibition in AML through p38 α -mediated feedback activation of mTOR signaling. *Oncotarget* *7*, 37407–37419.

Burger, K., Mühl, B., Harasim, T., Rohmoser, M., Malamoussi, A., Orban, M., Kellner, M., Gruber-Eber, A., Kremmer, E., Hölzel, M., et al. (2010). Chemotherapeutic Drugs Inhibit Ribosome Biogenesis at Various Levels. *J. Biol. Chem.* *285*, 12416–12425.

Burger, K., Mühl, B., Rohmoser, M., Coordes, B., Heidemann, M., Kellner, M., Gruber-Eber, A., Heissmeyer, V., Strässer, K., and Eick, D. (2013). Cyclin-dependent Kinase 9 Links RNA Polymerase II Transcription to Processing of Ribosomal RNA. *J. Biol. Chem.* *288*, 21173–21183.

Busch, J., Seidel, C., Weikert, S., Wolff, I., Kempkensteffen, C., Weinkauff, L., Hinz, S., Magheli, A., Miller, K., and Grünwald, V. (2011). Intrinsic resistance to tyrosine kinase inhibitors is associated with poor clinical outcome in metastatic renal cell carcinoma. *BMC Cancer* *11*, 295.

Campagnoli, M.F., Ramenghi, U., Armiraglio, M., Quarello, P., Garelli, E., Carando, A., Avondo, F., Pavesi, E., Fribourg, S., Gleizes, P.E., et al. (2008).

RPS19 mutations in patients with Diamond-Blackfan anemia. *Hum. Mutat.* 29, 911–920.

Chapman, P.B., Hauschild, A., Robert, C., Haanen, J.B., Ascierto, P., Larkin, J., Dummer, R., Garbe, C., Testori, A., Maio, M., et al. (2011). Improved Survival with Vemurafenib in Melanoma with BRAF V600E Mutation. *N. Engl. J. Med.* 364, 2507–2516.

Chauvin, C., Koka, V., Nouschi, A., Mieulet, V., Hoareau-Aveilla, C., Dreazen, A., Cagnard, N., Carpentier, W., Kiss, T., Meyuhas, O., et al. (2014). Ribosomal protein S6 kinase activity controls the ribosome biogenesis transcriptional program. *Oncogene* 33, 474–483.

Chen, L.S., Redkar, S., Bearss, D., Wierda, W.G., and Gandhi, V. (2009). Pim kinase inhibitor, SGI-1776, induces apoptosis in chronic lymphocytic leukemia cells. *Blood* 114, 4150–4157.

Chen, L.S., Redkar, S., Taverna, P., Cortes, J.E., and Gandhi, V. (2011). Mechanisms of cytotoxicity to Pim kinase inhibitor, SGI-1776, in acute myeloid leukemia. *Blood* 118, 693–702.

Chen, W.W., Chan, D.C., Donald, C., Lilly, M.B., and Kraft, A.S. (2005). Pim family kinases enhance tumor growth of prostate cancer cells. *Mol. Cancer Res.* 3, 443–451.

Chiocchetti, A., Gibello, L., Carando, A., Aspesi, A., Secco, P., Garelli, E., Loreni, F., Angelini, M., Biava, A., Dahl, N., et al. (2005). Interactions between RPS19, mutated in Diamond-Blackfan anemia, and the PIM-1 oncoprotein. *Haematologica* 90, 1453–1462.

Chou, T.-C. (2010). *Drug Combination Studies and Their Synergy*

Quantification Using the Chou-Talalay Method. *Cancer Res.* 70, 440–446.
Cobianchi, F., Calvio, C., Stoppini, M., Buvoli, M., and Riva, S. (1993).
Phosphorylation of human hnRNP protein A1 abrogates in vitro strand
annealing activity. *Nucleic Acids Res.* 21, 949–955.

Cobleigh, M.A., Vogel, C.L., Tripathy, D., Robert, N.J., Scholl, S.,
Fehrenbacher, L., Wolter, J.M., Paton, V., Shak, S., Lieberman, G., et al.
(1999). Multinational study of the efficacy and safety of humanized anti-HER2
monoclonal antibody in women who have HER2-overexpressing metastatic
breast cancer that has progressed after chemotherapy for metastatic disease.
J. Clin. Oncol. 17, 2639–2648.

Cohen, P., and Knebel, A. (2006). KESTREL: a powerful method for
identifying the physiological substrates of protein kinases. *Biochem. J.* 393,
1–6.

Collins, M.O., Yu, L., and Choudhary, J.S. (2007). Analysis of protein
phosphorylation on a proteome-scale. *Proteomics* 7, 2751–2768.

Colwill, K., Feng, L.L., Yeakley, J.M., Gish, G.D., Cácereso, J.F., Pawson, T.,
and Fu, X.D. (1996). SRPK1 and Clk/Sty protein kinases show distinct
substrate specificities for serine/arginine-rich splicing factors. *J. Biol. Chem.*
271, 24569–24575.

Cortes, J., Tamura, K., DeAngelo, D.J., de Bono, J., Lorente, D., Minden, M.,
Uy, G.L., Kantarjian, H., Keating, K., McEachern, K., et al. (2016). Abstract
CT147: Phase I studies of AZD1208, a PIM kinase inhibitor, in patients with
recurrent or refractory acute myelogenous leukemia or advanced solid
tumors. *Cancer Res.* 76.

Crews, L.A., Zipeto, M., Anna, K., Ball, E.D., Burkart, M.D., and Jamieson,

C.H. (2013). A Highly Selective SF3B1-Targeted Splicing Inhibitor Reduces Human CD34+ Cell Survival and Self-Renewal In Acute Myeloid Leukemia. *Blood* 122.

Crews, L.A., Balaian, L., Delos Santos, N.P., Leu, H.S., Court, A.C., Lazzari, E., Sadarangani, A., Zipeto, M.A., La Clair, J.J., Villa, R., et al. (2016). RNA Splicing Modulation Selectively Impairs Leukemia Stem Cell Maintenance in Secondary Human AML. *Cell Stem Cell* 19, 599–612.

Cuyper, H.T., Selten, G., Quint, W., Zijlstra, M., Maandag, E.R., Boelens, W., van Wezenbeek, P., Melief, C., and Berns, A. (1984). Murine leukemia virus-induced T-cell lymphomagenesis: integration of proviruses in a distinct chromosomal region. *Cell* 37, 141–150.

Daley, G., Van Etten, R., and Baltimore, D. (1990). Induction of chronic myelogenous leukemia in mice by the P210bcr/abl gene of the Philadelphia chromosome. *Science* (80-.). 247.

Dalla-Favera, R., Bregni, M., Erikson, J., Patterson, D., Gallo, R.C., and Croce, C.M. (1982). Human c-myc onc Gene is Located on the Region of Chromosome 8 that is Translocated in Burkitt Lymphoma Cells. *Proc. Natl. Acad. Sci.* 79, 7824–7827.

Dan, H.C., Sun, M., Kaneko, S., Feldman, R.I., Nicosia, S. V, Wang, H.G., Tsang, B.K., and Cheng, J.Q. (2004). Akt Phosphorylation and Stabilization of X-linked Inhibitor of Apoptosis Protein (XIAP). *J. Biol. Chem.* 279, 5405–5412.

Dancey, J., and Sausville, E.A. (2003). Issues and progress with protein kinase inhibitors for cancer treatment. *Nat Rev Drug Discov* 2, 296–313.

Decker, S., Finter, J., Forde, A.J., Kissel, S., Schwaller, J., Mack, T.S., Kuhn,

A., Gray, N., Follo, M., Jumaa, H., et al. (2014). PIM Kinases Are Essential for Chronic Lymphocytic Leukemia Cell Survival (PIM2/3) and CXCR4-Mediated Microenvironmental Interactions (PIM1). *Mol. Cancer Ther.* 13, 1231–1245.

Dehm, S.M. (2013). Test-firing ammunition for spliceosome inhibition in cancer. *Clin. Cancer Res.* 19, 6064–6066.

Delom, F., and Chevet, E. (2006). Phosphoprotein analysis: from proteins to proteomes. *Proteome Sci.* 4, 15.

Deneen, B., Welford, S.M., Ho, T., Hernandez, F., Kurland, I., and Denny, C.T. (2003). PIM3 proto-oncogene kinase is a common transcriptional target of divergent EWS/ETS oncoproteins. *Mol. Cell. Biol.* 23, 3897–3908.

Derenzini, M., Trerè, D., Pession, A., Montanaro, L., Sirri, V., and Ochs, R.L. (1998). Nucleolar function and size in cancer cells. *Am. J. Pathol.* 152, 1291–1297.

DeVita, V.T., and Rosenberg, S.A. (2012). Two Hundred Years of Cancer Research. *N. Engl. J. Med.* 366, 2207–2214.

Dhawan, P., and Richmond, A. (2002). A novel NF-kappa B-inducing kinase-MAPK signaling pathway up-regulates NF-kappa B activity in melanoma cells. *J. Biol. Chem.* 277, 7920–7928.

Dolfi, S.C., Chan, L.L.-Y., Qiu, J., Tedeschi, P.M., Bertino, J.R., Hirshfield, K.M., Oltvai, Z.N., and Vazquez, A. (2013). The metabolic demands of cancer cells are coupled to their size and protein synthesis rates. *Cancer Metab.* 1, 20.

Druker, B.J., Guilhot, F., O'Brien, S.G., Gathmann, I., Kantarjian, H.,

Gattermann, N., Deininger, M.W.N., Silver, R.T., Goldman, J.M., Stone, R.M., et al. (2006). Five-Year Follow-up of Patients Receiving Imatinib for Chronic Myeloid Leukemia. *N. Engl. J. Med.* 355, 2408–2417.

Drygin, D., Lin, A., Bliesath, J., Ho, C.B., O'Brien, S.E., Proffitt, C., Omori, M., Haddach, M., Schwaebe, M.K., Siddiqui-Jain, A., et al. (2011). Targeting RNA polymerase I with an oral small molecule CX-5461 inhibits ribosomal RNA synthesis and solid tumor growth. *Cancer Res.* 71, 1418–1430.

DuRose, J.B., Scheuner, D., Kaufman, R.J., Rothblum, L.I., and Niwa, M. (2009). Phosphorylation of eukaryotic translation initiation factor 2 α coordinates rRNA transcription and translation inhibition during endoplasmic reticulum stress. *Mol. Cell. Biol.* 29, 4295–4307.

Dutca, L.M., Gallagher, J.E.G., and Baserga, S.J. (2011). The initial U3 snoRNA:pre-rRNA base pairing interaction required for pre-18S rRNA folding revealed by in vivo chemical probing. *Nucleic Acids Res.* 39, 5164–5180.

Eichler, D.C., and Craig, N. (1994). Processing of eukaryotic ribosomal RNA. *Prog. Nucleic Acid Res. Mol. Biol.* 49, 197–239.

Eskens, F.A.L.M., Ramos, F.J., Burger, H., O'Brien, J.P., Piera, A., de Jonge, M.J.A., Mizui, Y., Wiemer, E.A.C., Carreras, M.J., Baselga, J., et al. (2013). Phase I Pharmacokinetic and Pharmacodynamic Study of the First-in-Class Spliceosome Inhibitor E7107 in Patients with Advanced Solid Tumors. *Clin. Cancer Res.* 19, 6296–6304.

Falini, B., Mecucci, C., Tiacci, E., Alcalay, M., Rosati, R., Pasqualucci, L., La Starza, R., Diverio, D., Colombo, E., Santucci, A., et al. (2005). Cytoplasmic Nucleophosmin in Acute Myelogenous Leukemia with a Normal Karyotype. *N. Engl. J. Med.* 352, 254–266.

Farrar, J.E., Quarello, P., Fisher, R., O'Brien, K.A., Aspesi, A., Parrella, S., Henson, A.L., Seidel, N.E., Atsidaftos, E., Prakash, S., et al. (2014).

Exploiting pre-rRNA processing in Diamond Blackfan anemia gene discovery and diagnosis. *Am. J. Hematol.* 89, 985–991.

Feldman, J.D., Vician, L., Crispino, M., Tocco, G., Marcheselli, V.L., Bazan, N.G., Baudry, M., and Herschman, H.R. (1998). KID-1, a protein kinase induced by depolarization in brain. *J. Biol. Chem.* 273, 16535–16543.

Ferreira-Cerca, S., Pöll, G., Gleizes, P.E., Tschochner, H., and Milkereit, P. (2005). Roles of eukaryotic ribosomal proteins in maturation and transport of pre-18S rRNA and ribosome function. *Mol. Cell* 20, 263–275.

Fischer, T., Stone, R.M., DeAngelo, D.J., Galinsky, I., Estey, E., Lanza, C., Fox, E., Ehninger, G., Feldman, E.J., Schiller, G.J., et al. (2010). Phase IIB Trial of Oral Midostaurin (PKC412), the FMS-Like Tyrosine Kinase 3 Receptor (FLT3) and Multi-Targeted Kinase Inhibitor, in Patients With Acute Myeloid Leukemia and High-Risk Myelodysplastic Syndrome With Either Wild-Type or Mutated FLT3. *J. Clin. Oncol.* 28, 4339–4345.

Flaherty, K.T., Infante, J.R., Daud, A., Gonzalez, R., Kefford, R.F., Sosman, J., Hamid, O., Schuchter, L., Cebon, J., Ibrahim, N., et al. (2012). Combined BRAF and MEK inhibition in melanoma with BRAF V600 mutations. *N. Engl. J. Med.* 367, 1694–1703.

Fox, C.J., Hammerman, P.S., and Thompson, C.B. (2005). The Pim kinases control rapamycin-resistant T cell survival and activation. *J. Exp. Med.* 201, 259–266.

Fukuhara, T., Hosoya, T., Shimizu, S., Sumi, K., Oshiro, T., Yoshinaka, Y., Suzuki, M., Yamamoto, N., Herzenberg, L.A., Herzenberg, L.A., et al. (2006).

Utilization of host SR protein kinases and RNA-splicing machinery during viral replication. *Proc. Natl. Acad. Sci.* *103*, 11329–11333.

Gammons, M. V, Lucas, R., Dean, R., Coupland, S.E., Oltean, S., and Bates, D.O. (2014). Targeting SRPK1 to control VEGF-mediated tumour angiogenesis in metastatic melanoma. *Br. J. Cancer* *111*, 477–485.

Garcia, P.D., Langowski, J.L., Wang, Y., Chen, M., Castillo, J., Fanton, C., Ison, M., Zavorotinskaya, T., Dai, Y., Lu, J., et al. (2014). Pan-PIM Kinase Inhibition Provides a Novel Therapy for Treating Hematologic Cancers. *Clin. Cancer Res.* *20*, 1834–1845.

Goebel, G., Berger, R., Strasak, A.M., Egle, D., Müller-Holzner, E., Schmidt, S., Rainer, J., Presul, E., Parson, W., Lang, S., et al. (2012). Elevated mRNA expression of CHAC1 splicing variants is associated with poor outcome for breast and ovarian cancer patients. *Br. J. Cancer* *106*, 189–198.

Granneman, S., and Baserga, S.J. (2005). Crosstalk in gene expression: coupling and co-regulation of rDNA transcription, pre-ribosome assembly and pre-rRNA processing. *Curr. Opin. Cell Biol.* *17*, 281–286.

Green, A.S., Maciel, T.T., Hospital, M.-A., Yin, C., Mazed, F., Townsend, E.C., Pilorge, S., Lambert, M., Paubelle, E., Jacquelin, A., et al. (2015). Pim kinases modulate resistance to FLT3 tyrosine kinase inhibitors in FLT3-ITD acute myeloid leukemia. *Sci. Adv.* *1*, e1500221.

Grimwade, D., and Hills, R.K. (2009). Independent prognostic factors for AML outcome. *ASH Educ. Progr. B.* *2009*, 385–395.

Grisolano, J.L., O’Neal, J., Cain, J., and Tomasson, M.H. (2003). An activated receptor tyrosine kinase, TEL/PDGFBetaR, cooperates with AML1/ETO to

induce acute myeloid leukemia in mice. *Proc. Natl. Acad. Sci. U. S. A.* *100*, 9506–9511.

Haddach, M., Michaux, J., Schwaebe, M.K., Pierre, F., O'Brien, S.E., Borsan, C., Tran, J., Raffaele, N., Ravula, S., Drygin, D., et al. (2012). Discovery of CX-6258. A Potent, Selective, and Orally Efficacious pan-Pim Kinases Inhibitor. *ACS Med. Chem. Lett.* *3*, 135–139.

Harada, M., Benito, J., Yamamoto, S., Kaur, S., Arslan, D., Ramirez, S., Jacamo, R., Plataniias, L., Matsushita, H., Fujimura, T., et al. (2015). The novel combination of dual mTOR inhibitor AZD2014 and pan-PIM inhibitor AZD1208 inhibits growth in acute myeloid leukemia via HSF pathway suppression. *Oncotarget* *6*, 37930–37947.

Harbour, J.W., Roberson, E.D.O., Anbunathan, H., Onken, M.D., Worley, L.A., and Bowcock, A.M. (2013). Recurrent mutations at codon 625 of the splicing factor SF3B1 in uveal melanoma. *Nat. Genet.* *45*, 133–135.

Hein, N., Cameron, D.P., Hannan, K.M., Nguyen, N.-Y.N., Fong, C.Y., Sornkom, J., Wall, M., Pavy, M., Cullinane, C., Diesch, J., et al. (2017a). Inhibition of Pol I transcription treats murine and human AML by targeting the leukemia-initiating cell population. *Blood* *129*, 2882–2895.

Henras, A.K., Plisson-Chastang, C., O'Donohue, M.-F., Chakraborty, A., and Gleizes, P.-E. (2015). An overview of pre-ribosomal RNA processing in eukaryotes. *Wiley Interdiscip. Rev. RNA* *6*, 225–242.

Henry, Y., Wood, H., Morrissey, J.P., Petfalski, E., Kearsey, S., and Tollervey, D. (1994). The 5' end of yeast 5.8S rRNA is generated by exonucleases from an upstream cleavage site. *EMBO J.* *13*, 2452–2463.

Hernandez, N. (2001). Small nuclear RNA genes: a model system to study fundamental mechanisms of transcription. *J. Biol. Chem.* 276, 26733–26736.

Hodgkin, J. (2001). What does a worm want with 20,000 genes? *Genome Biol.* 2, COMMENT2008.

Hoepfner, M.P., White, S., Jeffares, D.C., and Poole, A.M. (2010). Evolutionarily Stable Association of Intronic snoRNAs and microRNAs with Their Host Genes. *Genome Biol. Evol.* 1, 420–428.

Hogan, C., Hutchison, C., Marcar, L., Milne, D., Saville, M., Goodlad, J., Kernohan, N., and Meek, D. (2008). Elevated levels of oncogenic protein kinase Pim-1 induce the p53 pathway in cultured cells and correlate with increased Mdm2 in mantle cell lymphoma. *J. Biol. Chem.* 283, 18012–18023.

Holohan, C., Van Schaeybroeck, S., Longley, D.B., and Johnston, P.G. (2013). Cancer drug resistance: an evolving paradigm. *Nat. Rev. Cancer* 13, 714–726.

Hoover, D.S., Wingett, D.G., Zhang, J., Reeves, R., and Magnuson, N.S. (1997). Pim-1 protein expression is regulated by its 5'-untranslated region and translation initiation factor eIF-4E. *Cell Growth Differ.* 8, 1371–1380.

Hospital, M.-A., Green, A.S., Lacombe, C., Mayeux, P., Bouscary, D., and Tamburini, J. (2012). The FLT3 and Pim kinases inhibitor SGI-1776 preferentially target FLT3-ITD AML cells. *Blood* 119, 1791–1792.

van der Houven van Oordt, W., Diaz-Meco, M.T., Lozano, J., Krainer, a R., Moscat, J., and Cáceres, J.F. (2000). The MKK(3/6)-p38-signaling cascade alters the subcellular distribution of hnRNP A1 and modulates alternative splicing regulation. *J. Cell Biol.* 149, 307–316.

Hu, X.F., Li, J., Vandervalk, S., Wang, Z., Magnuson, N.S., and Xing, P.X. (2009). PIM-1-specific mAb suppresses human and mouse tumor growth by decreasing PIM-1 levels, reducing Akt phosphorylation, and activating apoptosis. *J. Clin. Invest.* 119, 362–375.

Huang, S., and Spector, D.L. (1992). U1 and U2 small nuclear RNAs are present in nuclear speckles. *Proc. Natl. Acad. Sci. U. S. A.* 89, 305–308.

Huang, S.-M.A., Wang, A., Greco, R., Li, Z., Barberis, C., Tabart, M., Patel, V., Schio, L., Hurley, R., Chen, B., et al. (2014). Combination of PIM and JAK2 inhibitors synergistically suppresses MPN cell proliferation and overcomes drug resistance. *Oncotarget* 5, 3362–3374.

Huang, Y., Yario, T.A., and Steitz, J.A. (2004). A molecular link between SR protein dephosphorylation and mRNA export. *Proc. Natl. Acad. Sci.* 101, 9666–9670.

Humphrey, S.J., Yang, G., Yang, P., Fazakerley, D.J., Stöckli, J., Yang, J.Y., and James, D.E. (2013). Dynamic Adipocyte Phosphoproteome Reveals that Akt Directly Regulates mTORC2. *Cell Metab.* 17, 1009–1020.

Iadevaia, V., Caldarola, S., Biondini, L., Gismondi, a, Karlsson, S., Dianzani, I., and Loreni, F. (2010). PIM1 kinase is destabilized by ribosomal stress causing inhibition of cell cycle progression. *Oncogene* 29, 5490–5499.

Jády, B.E., Darzacq, X., Tucker, K.E., Matera, A.G., Bertrand, E., and Kiss, T. (2003). Modification of Sm small nuclear RNAs occurs in the nucleoplasmic Cajal body following import from the cytoplasm. *EMBO J.* 22, 1878–1888.

James, M.J., and Zomerdijk, J.C.B.M. (2004). Phosphatidylinositol 3-kinase and mTOR signaling pathways regulate RNA polymerase I transcription in

response to IGF-1 and nutrients. *J. Biol. Chem.* 279, 8911–8918.

Jean-Philippe, J., Paz, S., and Caputi, M. (2013). hnRNP A1: The Swiss Army Knife of gene expression. *Int. J. Mol. Sci.* 14, 18999–19024.

Jo, O.D., Martin, J., Bernath, A., Masri, J., Lichtenstein, A., and Gera, J. (2008). Heterogeneous nuclear ribonucleoprotein A1 regulates cyclin D1 and c-myc internal ribosome entry site function through Akt signaling. *J. Biol. Chem.* 283, 23274–23287.

Johnson, J.M., Castle, J., Garrett-Engele, P., Kan, Z., Loerch, P.M., Armour, C.D., Santos, R., Schadt, E.E., Stoughton, R., and Shoemaker, D.D. (2003). Genome-Wide Survey of Human Alternative Pre-mRNA Splicing with Exon Junction Microarrays. *Science* (80-.). 302, 2141–2144.

Kamma, H., Portman, D.S., and Dreyfuss, G. (1995). Cell Type-Specific Expression of hnRNP Proteins. *Exp. Cell Res.* 221, 187–196.

Karni, R., de Stanchina, E., Lowe, S.W., Sinha, R., Mu, D., and Krainer, A.R. (2007). The gene encoding the splicing factor SF2/ASF is a proto-oncogene. *Nat. Struct. Mol. Biol.* 14, 185–193.

Kawasome, H., Papst, P., Webb, S., Keller, G.M., Johnson, G.L., Gelfand, E.W., and Terada, N. (1998). Targeted disruption of p70(s6k) defines its role in protein synthesis and rapamycin sensitivity. *Proc. Natl. Acad. Sci. U. S. A.* 95, 5033–5038.

Keeton, E.K., McEachern, K., Dillman, K.S., Palakurthi, S., Cao, Y., Grondine, M.R., Kaur, S., Wang, S., Chen, Y., Wu, A., et al. (2014). AZD1208, a potent and selective pan-Pim kinase inhibitor, demonstrates efficacy in preclinical models of acute myeloid leukemia. *Blood* 123, 905–913.

Kelly, K.R., Espitia, C.M., Taverna, P., Choy, G., Padmanabhan, S., Nawrocki, S.T., Giles, F.J., and Carew, J.S. (2012). Targeting PIM kinase activity significantly augments the efficacy of cytarabine. *Br. J. Haematol.* 156, 129–132.

Kerbel, R.S. (2008). Tumor Angiogenesis. *N. Engl. J. Med.* 358, 2039–2049.
Keren, H., Lev-Maor, G., and Ast, G. (2010). Alternative splicing and evolution: diversification, exon definition and function. *Nat. Rev. Genet.* 11, 345–355.

Khwaja, A., Bjorkholm, M., Gale, R.E., Levine, R.L., Jordan, C.T., Ehninger, G., Bloomfield, C.D., Estey, E., Burnett, A., Cornelissen, J.J., et al. (2016). Acute myeloid leukaemia. *Nat. Rev. Dis. Prim.* 2, 16010.

Kim, E., Du, L., Bregman, D.B., and Warren, S.L. (1997). Splicing factors associate with hyperphosphorylated RNA polymerase II in the absence of pre-mRNA. *J. Cell Biol.* 136, 19–28.

Klinck, R., Bramard, A., Inkel, L., Dufresne-Martin, G., Gervais-Bird, J., Madden, R., Paquet, E.R., Koh, C., Venables, J.P., Prinos, P., et al. (2008). Multiple alternative splicing markers for ovarian cancer. *Cancer Res.* 68, 657–663.

Knighton, D.R., Zheng, J.H., Ten Eyck, L.F., Ashford, V.A., Xuong, N.H., Taylor, S.S., and Sowadski, J.M. (1991). Crystal structure of the catalytic subunit of cyclic adenosine monophosphate-dependent protein kinase. *Science* 253, 407–414.

Koblish, H., Shin, N., Hall, L., O'Connor, S., Wang, Q., Wang, K., Leffet, L., Covington, M., Burke, K., Boer, J., et al. (2015). Abstract 5416: Activity of the

pan-PIM kinase inhibitor INCB053914 in models of acute myelogenous leukemia. *Cancer Res.* 75.

Koboldt, D.C., Fulton, R.S., McLellan, M.D., Schmidt, H., Kalicki-Veizer, J., McMichael, J.F., Fulton, L.L., Dooling, D.J., Ding, L., Mardis, E.R., et al. (2012). Comprehensive molecular portraits of human breast tumours. *Nature* 490, 61–70.

Kornblihtt, A.R., Schor, I.E., Alló, M., Dujardin, G., Petrillo, E., and Muñoz, M.J. (2013). Alternative splicing: a pivotal step between eukaryotic transcription and translation. *Nat. Rev. Mol. Cell Biol.* 14, 153–165.

Kos-Braun, I.C., Jung, I., and Koš, M. (2017). Tor1 and CK2 kinases control a switch between alternative ribosome biogenesis pathways in a growth-dependent manner. *PLOS Biol.* 15, e2000245.

Krebs, J.E., Lewin, B., Kilpatrick, S.T., and Goldstein, E.S. (2014). *Lewin's genes XI.* (Jones & Bartlett Learning).

Kwak, E.L., Bang, Y.-J., Camidge, D.R., Shaw, A.T., Solomon, B., Maki, R.G., Ou, S.-H.I., Dezube, B.J., Jänne, P.A., Costa, D.B., et al. (2010). Anaplastic lymphoma kinase inhibition in non-small-cell lung cancer. *N. Engl. J. Med.* 363, 1693–1703.

Lafontaine, D.L.J. (2015). Noncoding RNAs in eukaryotic ribosome biogenesis and function. *Nat. Struct. & Mol. Biol.* 22, 11–19.

Lagiseti, C., Palacios, G., Goronga, T., Freeman, B., Caufield, W., and Webb, T.R. (2013). Optimization of Antitumor Modulators of Pre-mRNA Splicing. *J. Med. Chem.* 56, 10033–10044.

Lai, M.C., Lin, R.I., Huang, S.Y., Tsai, C.W., and Tarn, W.Y. (2000). A human importin-beta family protein, transportin-SR2, interacts with the

phosphorylated RS domain of SR proteins. *J. Biol. Chem.* 275, 7950–7957.

Landau, D.A., Carter, S.L., Stojanov, P., McKenna, A., Stevenson, K., Lawrence, M.S., Sougnez, C., Stewart, C., Sivachenko, A., Wang, L., et al. (2013). Evolution and Impact of Subclonal Mutations in Chronic Lymphocytic Leukemia. *Cell* 152, 714–726.

Lazaris-Karatzas, A., Montine, K.S., and Sonenberg, N. (1990). Malignant transformation by a eukaryotic initiation factor subunit that binds to mRNA 5' cap. *Nature* 345, 544–547.

Leclerc, G.M., Leclerc, G.J., Kuznetsov, J.N., DeSalvo, J., and Barredo, J.C. (2013). Metformin Induces Apoptosis through AMPK-Dependent Inhibition of UPR Signaling in ALL Lymphoblasts. *PLoS One* 8, e74420.

Li, J., Hu, X.F., Loveland, B.E., and Xing, P.X. (2009). Pim-1 expression and monoclonal antibody targeting in human leukemia cell lines. *Exp. Hematol.* 37, 1284–1294.

Li, X., Guan, B., Srivastava, M.K., Padmanabhan, A., Hampton, B.S., and Bieberich, C.J. (2007). The reverse in-gel kinase assay to profile physiological kinase substrates. *Nat. Methods* 4, 957–962.

Li, X., Cox, J.T., Huang, W., Kane, M., Tang, K., and Bieberich, C.J. (2016). Quantifying Kinase-Specific Phosphorylation Stoichiometry Using Stable Isotope Labeling In a Reverse In-Gel Kinase Assay. *Anal. Chem.* 88, 11468–11475.

Li, Z., Van Calcar, S., Qu, C., Cavenee, W.K., Zhang, M.Q., and Ren, B. (2003). A global transcriptional regulatory role for c-Myc in Burkitt's lymphoma cells. *Proc. Natl. Acad. Sci. U. S. A.* 100, 8164–8169.

- Lin, J., Xie, Z., Zhu, H., and Qian, J. (2010a). Understanding protein phosphorylation on a systems level. *Brief. Funct. Genomics* 9, 32–42.
- Lin, Y.W., Beharry, Z.M., Hill, E.G., Song, J.H., Wang, W., Xia, Z., Zhang, Z., Aplan, P.D., Aster, J.C., Smith, C.D., et al. (2010b). A small molecule inhibitor of Pim protein kinases blocks the growth of precursor T-cell lymphoblastic leukemia/lymphoma. *Blood* 115, 824–833.
- Long, G. V, Stroyakovskiy, D., Gogas, H., Levchenko, E., de Braud, F., Larkin, J., Garbe, C., Jouary, T., Hauschild, A., Grob, J.-J., et al. (2015). Dabrafenib and trametinib versus dabrafenib and placebo for Val600 BRAF-mutant melanoma: a multicentre, double-blind, phase 3 randomised controlled trial. *Lancet (London, England)* 386, 444–451.
- Lowenberg, B., Downing, J.R., and Burnett, A. (1999). Acute Myeloid Leukemia. *N. Engl. J. Med.* 341, 1051–1062.
- Luque-Cabal, M., García-Tejido, P., Fernández-Pérez, Y., Sánchez-Lorenzo, L., and Palacio-Vázquez, I. (2016). Mechanisms Behind the Resistance to Trastuzumab in HER2-Amplified Breast Cancer and Strategies to Overcome It. *Clin. Med. Insights. Oncol.* 10, 21–30.
- Macdonald, A., Campbell, D.G., Toth, R., McLauchlan, H., Hastie, C.J., and Arthur, J.S.C. (2006). Pim kinases phosphorylate multiple sites on Bad and promote 14-3-3 binding and dissociation from Bcl-XL. *BMC Cell Biol.* 7, 1.
- Malumbres, M., and Barbacid, M. (2007). Cell cycle kinases in cancer. *Curr. Opin. Genet. Dev.* 17, 60–65.
- Manning, G. (2002). The Protein Kinase Complement of the Human Genome.

Science (80-.). 298, 1912–1934.

Martin, J., Masri, J., Cloninger, C., Holmes, B., Artinian, N., Funk, A., Ruegg, T., Anderson, L., Bashir, T., Bernath, A., et al. (2011). Phosphomimetic Substitution of Heterogeneous Nuclear Ribonucleoprotein A1 at Serine 199 Abolishes AKT-dependent Internal Ribosome Entry Site-transacting Factor (ITAF) Function via Effects on Strand Annealing and Results in Mammalian Target of Rapamycin Complex 1 (mTORC1) Inhibitor Sensitivity. *J. Biol. Chem.* 286, 16402–16413.

Matera, A.G., and Wang, Z. (2014). A day in the life of the spliceosome. *Nat. Rev. Mol. Cell Biol.* 15, 108–121.

Matikainen, S., Sareneva, T., Ronni, T., Lehtonen, A., Koskinen, P.J., and Julkunen, I. (1999). Interferon-alpha activates multiple STAT proteins and upregulates proliferation-associated IL-2Ralpha, c-myc, and pim-1 genes in human T cells. *Blood* 93, 1980–1991.

Matlin, A.J., Clark, F., and Smith, C.W.J. (2005). Understanding alternative splicing: towards a cellular code. *Nat. Rev. Mol. Cell Biol.* 6, 386–398.

Mayeda, A., and Krainer, A.R. (1992). Regulation of alternative pre-mRNA splicing by hnRNP A1 and splicing factor SF2. *Cell* 68, 365–375.

Meja, K., Stengel, C., Sellar, R., Huszar, D., Davies, B.R., Gale, R.E., Linch, D.C., and Khwaja, A. (2014). PIM and AKT kinase inhibitors show synergistic cytotoxicity in acute myeloid leukaemia that is associated with convergence on mTOR and MCL1 pathways. *Br. J. Haematol.* 167, 69–79.

Meyuhas, O. (2008). Chapter 1 Physiological Roles of Ribosomal Protein S6: One of Its Kind. pp. 1–37.

Mielecki, M., Krawiec, K., Kiburu, I., Grzelak, K., Zagórski, W., Kierdaszuk, B., Kowa, K., Fokt, I., Szymanski, S., Swierk, P., et al. (2013). Development of novel molecular probes of the Rio1 atypical protein kinase. *Biochim. Biophys. Acta* 1834, 1292–1301.

Mikkers, H., Nawijn, M., Allen, J., Brouwers, C., Verhoeven, E., Jonkers, J., and Berns, A. (2004). Mice Deficient for All PIM Kinases Display Reduced Body Size and Impaired Responses to Hematopoietic Growth Factors. *Mol. Cell. Biol.* 24, 6104–6115.

Miller, K.D., Siegel, R.L., Lin, C.C., Mariotto, A.B., Kramer, J.L., Rowland, J.H., Stein, K.D., Alteri, R., and Jemal, A. (2016). Cancer treatment and survivorship statistics, 2016. *CA. Cancer J. Clin.* 66, 271–289.

Misteli, T., and Spector, D.L. (1996). Serine/threonine phosphatase 1 modulates the subnuclear distribution of pre-mRNA splicing factors. *Mol. Biol. Cell* 7, 1559–1572.

Misteli, T., and Spector, D.L. (1997). Protein phosphorylation and the nuclear organization of pre-mRNA splicing. *Trends Cell Biol.* 7, 135–138.

Misteli, T., Cáceres, J.F., Clement, J.Q., Krainer, A.R., Wilkinson, M.F., and Spector, D.L. (1998). Serine phosphorylation of SR proteins is required for their recruitment to sites of transcription in vivo. *J. Cell Biol.* 143, 297–307.

Mizuno, K., Shirogane, T., Shinohara, A., Iwamatsu, A., Hibi, M., and Hirano, T. (2001). Regulation of Pim-1 by Hsp90. *Biochem Biophys Res Commun* 281, 663–669.

Mumenthaler, S.M., Ng, P.Y.B., Hodge, A., Bearss, D., Berk, G., Kanekal, S.,

- Redkar, S., Taverna, P., Agus, D.B., and Jain, A. (2009). Pharmacologic inhibition of Pim kinases alters prostate cancer cell growth and resensitizes chemoresistant cells to taxanes. *Mol. Cancer Ther.* 8, 2882–2893.
- Mungrue, I.N., Pagnon, J., Kohanim, O., Gargalovic, P.S., and Lusic, A.J. (2008). CHAC1/MGC4504 Is a Novel Proapoptotic Component of the Unfolded Protein Response, Downstream of the ATF4-ATF3-CHOP Cascade. *J. Immunol.* 182, 466–476.
- Nagarajan, L., Louie, E., Tsujimoto, Y., ar-Rushdi, A., Huebner, K., and Croce, C.M. (1986). Localization of the human pim oncogene (PIM) to a region of chromosome 6 involved in translocations in acute leukemias. *Proc. Natl. Acad. Sci. U. S. A.* 83, 2556–2560.
- Natarajan, K., Bhullar, J., Shukla, S., Burcu, M., Chen, Z.-S., Ambudkar, S. V, and Baer, M.R. (2013). The Pim kinase inhibitor SGI-1776 decreases cell surface expression of P-glycoprotein (ABCB1) and breast cancer resistance protein (ABCG2) and drug transport by Pim-1-dependent and -independent mechanisms. *Biochem. Pharmacol.* 85, 514–524.
- Nawijn, M.C., Alendar, A., and Berns, A. (2011). For better or for worse: the role of Pim oncogenes in tumorigenesis. *Nat. Rev. Cancer* 11, 23–34.
- O'Donohue, M.-F., Choesmel, V., Faubladiere, M., Fichant, G., and Gleizes, P.-E. (2010). Functional dichotomy of ribosomal proteins during the synthesis of mammalian 40S ribosomal subunits. *J. Cell Biol.* 190, 853–866.
- Oeffinger, M., Zenklusen, D., Ferguson, A., Wei, K.E., El Hage, A., Tollervey, D., Chait, B.T., Singer, R.H., and Rout, M.P. (2009). Rrp17p Is a Eukaryotic Exonuclease Required for 5' End Processing of Pre-60S Ribosomal RNA. *Mol. Cell* 36, 768–781.

Ohno, M., Segref, A., Bachi, A., Wilm, M., and Mattaj, I.W. (2000). PHAX, a Mediator of U snRNA Nuclear Export Whose Activity Is Regulated by Phosphorylation. *Cell* 101, 187–198.

Oltean, S., and Bates, D.O. (2014). Hallmarks of alternative splicing in cancer. *Oncogene* 33, 5311–5318.

Orsolich, I., Jurada, D., Pullen, N., Oren, M., Eliopoulos, A.G., and Volarevic, S. (2016). The relationship between the nucleolus and cancer: Current evidence and emerging paradigms. *Semin. Cancer Biol.* 37–38, 36–50.

Osowski, C.M., and Urano, F. (2010). The binary switch between life and death of endoplasmic reticulum-stressed beta cells. *Curr. Opin. Endocrinol. Diabetes. Obes.* 17, 107–112.

Panic, L., Tamarut, S., Sticker-jantscheff, M., Barkic, M., Solter, D., Uzelac, M., and Grabus, K. (2006). Ribosomal Protein S6 Gene Haploinsufficiency Is Associated with Activation of a p53-Dependent Checkpoint during Gastrulation □ †. 26, 8880–8891.

Parenteau, J., Durand, M., Véronneau, S., Lacombe, A.-A., Morin, G., Guérin, V., Cecez, B., Gervais-Bird, J., Koh, C.-S., Brunelle, D., et al. (2008). Deletion of many yeast introns reveals a minority of genes that require splicing for function. *Mol. Biol. Cell* 19, 1932–1941.

Pearson, J.D., Lee, J.K.H., Bacani, J.T.C., Lai, R., and Ingham, R.J. (2012). NPM-ALK: The Prototypic Member of a Family of Oncogenic Fusion Tyrosine Kinases. *J. Signal Transduct.* 2012, 123253.

Peculis, B.A. (1997). The sequence of the 5' end of the U8 small nucleolar

RNA is critical for 5.8S and 28S rRNA maturation. *Mol. Cell. Biol.* 17, 3702–3713.

Peculis, B.A., and Steitz, J.A. (1994). Sequence and structural elements critical for U8 snRNP function in *Xenopus* oocytes are evolutionarily conserved. *Genes Dev.* 8, 2241–2255.

Peltonen, K., Colis, L., Liu, H., Jaamaa, S., Zhang, Z., af Hallstrom, T., Moore, H.M., Sirajuddin, P., and Laiho, M. (2014a). Small Molecule BMH-Compounds That Inhibit RNA Polymerase I and Cause Nucleolar Stress. *Mol. Cancer Ther.* 13, 2537–2546.

Peltonen, K., Colis, L., Liu, H., Trivedi, R., Moubarek, M.S., Moore, H.M., Bai, B., Rudek, M.A., Bieberich, C.J., and Laiho, M. (2014b). A targeting modality for destruction of RNA polymerase I that possesses anticancer activity. *Cancer Cell* 25, 77–90.

Pende, M., Um, S.H., Mieulet, V., Sticker, M., Goss, V.L., Mestan, J., Mueller, M., Fumagalli, S., Kozma, S.C., and Thomas, G. (2004a). S6K1(-)/S6K2(-) mice exhibit perinatal lethality and rapamycin-sensitive 5'-terminal oligopyrimidine mRNA translation and reveal a mitogen-activated protein kinase-dependent S6 kinase pathway. *Mol. Cell. Biol.* 24, 3112–3124.

Pende, M., Um, S.H., Mieulet, V., Sticker, M., Goss, V.L., Mestan, J., Mueller, M., Fumagalli, S., Kozma, S.C., and Thomas, G. (2004b). S6K1(-)/S6K2(-) mice exhibit perinatal lethality and rapamycin-sensitive 5'-terminal oligopyrimidine mRNA translation and reveal a mitogen-activated protein kinase-dependent S6 kinase pathway. *Mol. Cell. Biol.* 24, 3112–3124.

Peng, C., Knebel, A., Morrice, N.A., Li, X., Barringer, K., Li, J., Jakes, S., Werneburg, B., and Wang, L. (2007). Pim kinase substrate identification and

specificity. *J. Biochem.* 141, 353–362.

Pogacic, V., Bullock, A.N., Fedorov, O., Filippakopoulos, P., Gasser, C., Biondi, A., Meyer-Monard, S., Knapp, S., and Schwaller, J. (2007). Structural Analysis Identifies Imidazo[1,2-b]Pyridazines as PIM Kinase Inhibitors with In vitro Antileukemic Activity. *Cancer Res.* 67.

Popivanova, B.K., Li, Y.Y., Zheng, H., Omura, K., Fujii, C., Tsuneyama, K., and Mukaida, N. (2007). Proto-oncogene, Pim-3 with serine/threonine kinase activity, is aberrantly expressed in human colon cancer cells and can prevent Bad-mediated apoptosis. *Cancer Sci.* 98, 321–328.

Preti, M., O'Donohue, M.-F., Montel-Lehry, N., Bortolin-Cavaillé, M.-L., Choismel, V., and Gleizes, P.-E. (2013). Gradual processing of the ITS1 from the nucleolus to the cytoplasm during synthesis of the human 18S rRNA. *Nucleic Acids Res.* 41, 4709–4723.

Qian, K.C., Wang, L., Hickey, E.R., Studts, J., Barringer, K., Peng, C., Kronkaitis, A., Li, J., White, A., Mische, S., et al. (2005). Structural Basis of Constitutive Activity and a Unique Nucleotide Binding Mode of Human Pim-1 Kinase. *J. Biol. Chem.* 280, 6130–6137.

Rau, R., and Brown, P. (2009). Nucleophosmin (NPM1) mutations in adult and childhood acute myeloid leukaemia: towards definition of a new leukaemia entity. *Hematol. Oncol.* 27, 171–181.

Rebello, R.J., Kusnadi, E., Cameron, D.P., Pearson, H.B., Lesmana, A., Devlin, J.R., Drygin, D., Clark, A.K., Porter, L., Pedersen, J., et al. (2016). The Dual Inhibition of RNA Pol I Transcription and PIM Kinase as a New Therapeutic Approach to Treat Advanced Prostate Cancer. *Clin. Cancer Res.* 22, 5539–5552.

Reed, J.C. (1999). Dysregulation of Apoptosis in Cancer. *J. Clin. Oncol.* *17*, 2941–2941.

Renneville, A., Roumier, C., Biggio, V., Nibourel, O., Boissel, N., Fenaux, P., and Preudhomme, C. (2008). REVIEW Cooperating gene mutations in acute myeloid leukemia: a review of the literature. *Leukemia* *22*, 915–931.

Robledo, S., Idol, R.A., Crimmins, D.L., Ladenson, J.H., Mason, P.J., and Bessler, M. (2008). The role of human ribosomal proteins in the maturation of rRNA and ribosome production. *RNA* *14*, 1918–1929.

Röllig, C., Bornhäuser, M., Thiede, C., Taube, F., Kramer, M., Mohr, B., Aulitzky, W., Bodenstein, H., Tischler, H.-J., Stuhlmann, R., et al. (2011). Long-term prognosis of acute myeloid leukemia according to the new genetic risk classification of the European LeukemiaNet recommendations: evaluation of the proposed reporting system. *J. Clin. Oncol.* *29*, 2758–2765.

Roy, R., Durie, D., Li, H., Liu, B.-Q., Skehel, J.M., Mauri, F., Cuorvo, L. V., Barbareschi, M., Guo, L., Holcik, M., et al. (2014). hnRNPA1 couples nuclear export and translation of specific mRNAs downstream of FGF-2/S6K2 signalling. *Nucleic Acids Res.* *42*, 12483–12497.

Roy, R., Huang, Y., Seckl, M.J., and Pardo, O.E. (2017). Emerging roles of hnRNPA1 in modulating malignant transformation. *Wiley Interdiscip. Rev. RNA* e1431.

Ruvinsky, I., Sharon, N., Lerer, T., Cohen, H., Stolovich-Rain, M., Nir, T., Dor, Y., Zisman, P., and Meyuhas, O. (2005a). Ribosomal protein S6 phosphorylation is a determinant of cell size and glucose homeostasis. *Genes Dev.* *19*, 2199–2211.

Sakharkar, M.K., Chow, V.T.K., and Kanguane, P. (2004). Distributions of exons and introns in the human genome. *In Silico Biol.* 4, 387–393.

Saris, C.J., Domen, J., and Berns, A. (1991). The pim-1 oncogene encodes two related protein-serine/threonine kinases by alternative initiation at AUG and CUG. *EMBO J.* 10, 655–664.

Saurabh, K., Scherzer, M.T., Shah, P.P., Mims, A.S., Lockwood, W.W., Kraft, A.S., and Beverly, L.J. (2014). The PIM family of oncoproteins: Small kinases with huge implications in myeloid leukemogenesis and as therapeutic targets. *Oncotarget* 5, 8503.

Schäfer, T., Maco, B., Petfalski, E., Tollervey, D., Böttcher, B., Aebi, U., and Hurt, E. (2006). Hrr25-dependent phosphorylation state regulates organization of the pre-40S subunit. *Nature* 441, 651–655.

Schessl, C., Rawat, V.P.S., Cusan, M., Deshpande, A., Kohl, T.M., Rosten, P.M., Spiekermann, K., Humphries, R.K., Schnittger, S., Kern, W., et al. (2005). The AML1-ETO fusion gene and the FLT3 length mutation collaborate in inducing acute leukemia in mice. *J. Clin. Invest.* 115, 2159–2168.

Schillewaert, S., Wacheul, L., Lhomme, F., and Lafontaine, D.L.J. (2012). The evolutionarily conserved protein Las1 is required for pre-rRNA processing at both ends of ITS2. *Mol. Cell. Biol.* 32, 430–444.

Schmucker, D., and Flanagan, J.G. (2004). Generation of Recognition Diversity in the Nervous System. *Neuron* 44, 219–222.

Scott, L.M., and Rebel, V.I. (2013). Acquired Mutations That Affect Pre-mRNA Splicing in Hematologic Malignancies and Solid Tumors. *JNCI J. Natl. Cancer Inst.* 105, 1540–1549.

Serrano, M., Lin, A.W., McCurrach, M.E., Beach, D., and Lowe, S.W. (1997). Oncogenic ras provokes premature cell senescence associated with accumulation of p53 and p16INK4a. *Cell* 88, 593–602.

Shah, K., Liu, Y., Deirmengian, C., and Shokat, K.M. (1997). Engineering unnatural nucleotide specificity for Rous sarcoma virus tyrosine kinase to uniquely label its direct substrates. *Proc. Natl. Acad. Sci. U. S. A.* 94, 3565–3570.

Shah, N.P., Tran, C., Lee, F.Y., Chen, P., Norris, D., and Sawyers, C.L. (2004). Overriding Imatinib Resistance with a Novel ABL Kinase Inhibitor. *Science* (80-.). 305, 399–401.

Shen, H., and Green, M.R. RS domains contact splicing signals and promote splicing by a common mechanism in yeast through humans.

Shi, Y. (2017). The Spliceosome: A Protein-Directed Metalloribozyme. *J. Mol. Biol.* 429, 2640–2653.

Shima, H. (1998). Disruption of the p70s6k/p85s6k gene reveals a small mouse phenotype and a new functional S6 kinase. *EMBO J.* 17, 6649–6659.

Shima, H., Pende, M., Chen, Y., Fumagalli, S., Thomas, G., and Kozma, S.C. (1998). Disruption of the p70 s6k /p85 s6k gene reveals a small mouse phenotype and a new functional S6 kinase. *EMBO J.* 17, 6649–6659.

Shukron, O., Vainstein, V., Kündgen, A., Germing, U., and Agur, Z. (2012). Analyzing transformation of myelodysplastic syndrome to secondary acute myeloid leukemia using a large patient database. *Am. J. Hematol.* 87, 853–860.

Siomi, H., and Dreyfuss, G. (1995). A nuclear localization domain in the

hnRNP A1 protein. *J. Cell Biol.* 129, 551–560.

Sleeman, J.E., and Lamond, A.I. (1999). Newly assembled snRNPs associate with coiled bodies before speckles, suggesting a nuclear snRNP maturation pathway. *Curr. Biol.* 9, 1065–1074.

Sloan, K.E., Bohnsack, M.T., Schneider, C., and Watkins, N.J. (2014). The roles of SSU processome components and surveillance factors in the initial processing of human ribosomal RNA. *RNA* 20, 540–550.

Song, J.H., and Kraft, A.S. (2012). Pim Kinase Inhibitors Sensitize Prostate Cancer Cells to Apoptosis Triggered by Bcl-2 Family Inhibitor ABT-737. *Cancer Res.* 72.

Sportoletti, P., Grisendi, S., Majid, S.M., Cheng, K., Clohessy, J.G., Viale, A., Teruya-Feldstein, J., and Pandolfi, P.P. (2008). Npm1 is a haploinsufficient suppressor of myeloid and lymphoid malignancies in the mouse. *Blood* 111, 3859–3862.

Srivastava, L., Lapik, Y.R., Wang, M., and Pestov, D.G. (2010). Mammalian DEAD box protein Ddx51 acts in 3' end maturation of 28S rRNA by promoting the release of U8 snoRNA. *Mol. Cell. Biol.* 30, 2947–2956.

Szotkowski, T., Muzik, J., Maaloufova, J., Kozak, T., Jarosova, M., Michalova, K., Sreinerova, K., Vydra, J., Lanska, M., Katrincsakova, B., et al. Prognostic factors and treatment outcome in 1,516 adult patients with de novo and secondary acute myeloid leukemia in 1999–2009 in 5 hematology intensive care centers in the Czech Republic.

Tafforeau, L., Zorbas, C., Langhendries, J.-L., Mullineux, S.-T., Stamatopoulou, V., Mullier, R., Wacheul, L., and Lafontaine, D.L.J. (2013).

The Complexity of Human Ribosome Biogenesis Revealed by Systematic Nucleolar Screening of Pre-rRNA Processing Factors. *Mol. Cell* 51, 539–551.

Tallman, M.S., Gilliland, D.G., and Rowe, J.M. (2005). Drug therapy for acute myeloid leukemia. *Blood* 106, 1154–1163.

Tao, T., Sondalle, S.B., Shi, H., Zhu, S., Perez-Atayde, A.R., Peng, J., Baserga, S.J., and Look, A.T. (2017). The pre-rRNA processing factor DEF is rate limiting for the pathogenesis of MYCN-driven neuroblastoma. *Oncogene* 36, 3852–3867.

Taub, R., Kirsch, I., Morton, C., Lenoir, G., Swan, D., Tronick, S., Aaronson, S., and Leder, P. (1982). Translocation of the c-myc gene into the immunoglobulin heavy chain locus in human Burkitt lymphoma and murine plasmacytoma cells. *Proc. Natl. Acad. Sci. U. S. A.* 79, 7837–7841.

Thiede, C., Steudel, C., Mohr, B., Schaich, M., Schäkel, U., Platzbecker, U., Wermke, M., Bornhäuser, M., Ritter, M., Neubauer, A., et al. (2002). Analysis of FLT3-activating mutations in 979 patients with acute myelogenous leukemia: association with FAB subtypes and identification of subgroups with poor prognosis. *Blood* 99, 4326–4335.

Thomson, E., and Tollervey, D. (2010). The final step in 5.8S rRNA processing is cytoplasmic in *Saccharomyces cerevisiae*. *Mol. Cell. Biol.* 30, 976–984.

Tolcher, A., Goldman, J., Patnaik, A., Papadopoulos, K.P., Westwood, P., Kelly, C.S., Bumgardner, W., Sams, L., Geeganage, S., Wang, T., et al. (2014a). A phase I trial of LY2584702 tosylate, a p70 S6 kinase inhibitor, in patients with advanced solid tumours. *Eur. J. Cancer* 50, 867–875.

Tolcher, A., Goldman, J., Patnaik, A., Papadopoulos, K.P., Westwood, P.,

- Kelly, C.S., Bumgardner, W., Sams, L., Geeganage, S., Wang, T., et al. (2014b). A phase I trial of LY2584702 tosylate, a p70 S6 kinase inhibitor, in patients with advanced solid tumours. *Eur. J. Cancer* *50*, 867–875.
- Tron, A.E., Keeton, E.K., Ye, M., Casas-Selves, M., Chen, H., Dillman, K.S., Gale, R.E., Stengel, C., Zinda, M., Linch, D.C., et al. (2016). Next-generation sequencing identifies a novel *ELAVL1–TYK2* fusion gene in MOLM-16, an AML cell line highly sensitive to the PIM kinase inhibitor AZD1208. *Leuk. Lymphoma* *57*, 2927–2929.
- Tseng, C.-K., and Cheng, S.-C. (2008). Both Catalytic Steps of Nuclear Pre-mRNA Splicing Are Reversible. *Science* (80-.). *320*, 1782–1784.
- Venables, J.P., Klinck, R., Bramard, A., Inkel, L., Dufresne-Martin, G., Koh, C., Gervais-Bird, J., Lapointe, E., Froehlich, U., Durand, M., et al. (2008). Identification of Alternative Splicing Markers for Breast Cancer. *Cancer Res.* *68*, 9525–9531.
- Verbeek, S., van Lohuizen, M., van der Valk, M., Domen, J., Kraal, G., and Berns, A. (1991). Mice bearing the E mu-myc and E mu-pim-1 transgenes develop pre-B-cell leukemia prenatally. *Mol. Cell. Biol.* *11*, 1176–1179.
- Verma, D., Kantarjian, H., Faderl, S., O'Brien, S., Pierce, S., Vu, K., Freireich, E., Keating, M., Cortes, J., and Ravandi, F. (2010). Late relapses in acute myeloid leukemia: analysis of characteristics and outcome. *Leuk. Lymphoma* *51*, 778–782.
- Wang, G.-S., and Cooper, T.A. (2007). Splicing in disease: disruption of the splicing code and the decoding machinery. *Nat. Rev. Genet.* *8*, 749–761.
- Wang, M., and Kaufman, R.J. (2014). The impact of the endoplasmic reticulum protein-folding environment on cancer development. *Nat. Rev.*

Cancer 14, 581–597.

Wang, E.T., Sandberg, R., Luo, S., Khrebtkova, I., Zhang, L., Mayr, C., Kingsmore, S.F., Schroth, G.P., and Burge, C.B. (2008). Alternative isoform regulation in human tissue transcriptomes. *Nature* 456, 470–476.

Wang, J., Wang, B., Chu, H., and Yao, Y. (2016). Intrinsic resistance to EGFR tyrosine kinase inhibitors in advanced non-small-cell lung cancer with activating EGFR mutations. *Onco. Targets. Ther.* 9, 3711–3726.

Wang, L., Lawrence, M.S., Wan, Y., Stojanov, P., Sougnez, C., Stevenson, K., Werner, L., Sivachenko, A., DeLuca, D.S., Zhang, L., et al. (2011a). SF3B1 and other novel cancer genes in chronic lymphocytic leukemia. *N. Engl. J. Med.* 365, 2497–2506.

Wang, L.-L., Gao, C., and Chen, B.-A. (2011b). [Research progress on mechanism of MDS transformation into AML]. *Zhongguo Shi Yan Xue Ye Xue Za Zhi* 19, 254–259.

Wansink, D., Schul, W., van der Kraan, I., van Steensel, B., van Driel, R., and de Jong, L. (1993). Fluorescent labeling of nascent RNA reveals transcription by RNA polymerase II in domains scattered throughout the nucleus. *J. Cell Biol.* 122.

Warfel, N.A., and Kraft, A.S. (2015). PIM kinase (and Akt) biology and signaling in tumors. *Pharmacol. Ther.* 151, 41–49.

Warner, J.R., and McIntosh, K.B. (2009). How common are extraribosomal functions of ribosomal proteins? *Mol. Cell* 34, 3–11.

Weirauch, U., Beckmann, N., Thomas, M., Grünweller, A., Huber, K., Bracher,

F., Hartmann, R.K., and Aigner, A. (2013). Functional role and therapeutic potential of the pim-1 kinase in colon carcinoma. *Neoplasia* 15, 783–794.

Welch, J.S., Ley, T.J., Link, D.C., Miller, C.A., Larson, D.E., Koboldt, D.C., Wartman, L.D., Lamprecht, T.L., Liu, F., Xia, J., et al. (2012). The origin and evolution of mutations in acute myeloid leukemia. *Cell* 150, 264–278.

Widmann, B., Wandrey, F., Badertscher, L., Wyler, E., Pfannstiel, J., Zemp, I., and Kutay, U. (2012). The kinase activity of human Rio1 is required for final steps of cytoplasmic maturation of 40S subunits. *Mol. Biol. Cell* 23, 22–35.

Wilhelm, M., Schlegl, J., Hahne, H., Gholami, A.M., Lieberenz, M., Savitski, M.M., Ziegler, E., Butzmann, L., Gessulat, S., Marx, H., et al. (2014). Mass-spectrometry-based draft of the human proteome. *Nature* 509, 582–587.

Woolard, J., Wang, W.-Y., Bevan, H.S., Qiu, Y., Morbidelli, L., Pritchard-Jones, R.O., Cui, T.-G., Sugiono, M., Waive, E., Perrin, R., et al. (2004). VEGF_{165b}, an Inhibitory Vascular Endothelial Growth Factor Splice Variant. *Cancer Res.* 64, 7822–7835.

Wozniak, M.B., Villuendas, R., Bischoff, J.R., Aparicio, C.B., Martínez Leal, J.F., de La Cueva, P., Rodriguez, M.E., Herreros, B., Martin-Perez, D., Longo, M.I., et al. (2010). Vorinostat interferes with the signaling transduction pathway of T-cell receptor and synergizes with phosphoinositide-3 kinase inhibitors in cutaneous T-cell lymphoma. *Haematologica* 95, 613–621.

Wu, P., Nielsen, T.E., and Clausen, M.H. (2015). FDA-approved small-molecule kinase inhibitors. *Trends Pharmacol. Sci.* 36, 422–439.

Xiao, S.H., and Manley, J.L. (1997). Phosphorylation of the ASF/SF2 RS domain affects both protein-protein and protein-RNA interactions and is necessary for splicing. *Genes Dev.* 11, 334–344.

Xie, Y., Xu, K., Dai, B., Guo, Z., Jiang, T., Chen, H., and Qiu, Y. (2005). The 44 kDa Pim-1 kinase directly interacts with tyrosine kinase Etk/BMX and protects human prostate cancer cells from apoptosis induced by chemotherapeutic drugs. *Oncogene* 25, 70–78.

Yang, Q., Chen, L.S., Neelapu, S.S., Miranda, R.N., Medeiros, L.J., and Gandhi, V. (2012). Transcription and translation are primary targets of Pim kinase inhibitor SGI-1776 in mantle cell lymphoma. *Blood* 120, 3491–3500.

Yang, Q., Chen, L.S., and Gandhi, V. (2014). Mechanism-based combinations with Pim kinase inhibitors in cancer treatments. *Curr. Pharm. Des.* 20, 6670–6681.

Yap, T.A., Omlin, A., and de Bono, J.S. (2013). Development of Therapeutic Combinations Targeting Major Cancer Signaling Pathways. *J. Clin. Oncol.* 31, 1592–1605.

Yip-Schneider, M.T., Horie, M., and Broxmeyer, H.E. (1995). Transcriptional induction of pim-1 protein kinase gene expression by interferon gamma and posttranscriptional effects on costimulation with steel factor. *Blood* 85, 3494–3502.

Yokoi, A., Kotake, Y., Takahashi, K., Kadowaki, T., Matsumoto, Y., Minoshima, Y., Sugi, N.H., Sagane, K., Hamaguchi, M., Iwata, M., et al. (2011). Biological validation that SF3b is a target of the antitumor macrolide pladienolide. *FEBS J.* 278, 4870–4880.

Yoshida, K., and Ogawa, S. (2014). Splicing factor mutations and cancer. *Wiley Interdiscip. Rev. RNA* 5, 445–459.

Yoshida, K., Sanada, M., Shiraishi, Y., Nowak, D., Nagata, Y., Yamamoto, R.,

Sato, Y., Sato-Otsubo, A., Kon, A., Nagasaki, M., et al. (2011). Frequent pathway mutations of splicing machinery in myelodysplasia. *Nature* 478, 64–69.

Zemskova, M., Sahakian, E., Bashkirova, S., and Lilly, M. (2008). The PIM1 kinase is a critical component of a survival pathway activated by docetaxel and promotes survival of docetaxel-treated prostate cancer cells. *J. Biol. Chem.* 283, 20635–20644.

Zengel, J.M., and Lindahl, L. (1994). Diverse mechanisms for regulating ribosomal protein synthesis in *Escherichia coli*. *Prog. Nucleic Acid Res. Mol. Biol.* 47, 331–370.

Zhang, J., Yang, P.L., and Gray, N.S. (2008). Targeting cancer with small molecule kinase inhibitors. *Nat. Rev. Cancer* 9, 28–39.

Zhao, M., Pan, X., Layman, R., Lustberg, M.B., Mrozek, E., Macrae, E.R., Wesolowski, R., Carothers, S., Puhalla, S., Shapiro, C.L., et al. (2014). A Phase II study of bevacizumab in combination with trastuzumab and docetaxel in HER2 positive metastatic breast cancer. *Invest. New Drugs* 32, 1285–1294.

Zhong, X.-Y., Ding, J.-H., Adams, J.A., Ghosh, G., and Fu, X.-D. (2009). Regulation of SR protein phosphorylation and alternative splicing by modulating kinetic interactions of SRPK1 with molecular chaperones. *Genes Dev.* 23, 482–495.

Zhou, Z., Qiu, J., Liu, W., Zhou, Y., Plocinik, R.M., Li, H., Hu, Q., Ghosh, G., Adams, J.A., Rosenfeld, M.G., et al. (2012). The Akt-SRPK-SR Axis Constitutes a Major Pathway in Transducing EGF Signaling to Regulate Alternative Splicing in the Nucleus. *Mol. Cell* 47, 422–433.

Zhukova, Y.N., Alekseeva, M.G., Zakharevich, N. V, Shtil, A.A., and Danilenko, V.N. (2011). Pim family of protein kinases: Structure, functions, and roles in hematopoietic malignancies. *Mol. Biol.* 45, 695–703.

Zindy, F., Eischen, C.M., Randle, D.H., Kamijo, T., Cleveland, J.L., Sherr, C.J., and Roussel, M.F. (1998). Myc signaling via the ARF tumor suppressor regulates p53-dependent apoptosis and immortalization. *Genes Dev.* 12, 2424–2433.

Zorio, D.A.R., and Blumenthal, T. (1999). Both subunits of U2AF recognize the 3' splice site in *Caenorhabditis elegans*. *Nature* 402, 835–838.

